

**MODELING THE EFFECTS OF CLIMATE CHANGE ON GLACIERS
IN THE UPPER NORTH SASKATCHEWAN RIVER BASIN**

EVAN L. J. BOOTH

B.A.Sc., University of Lethbridge 2009.

A Thesis
Submitted to the School of Graduate Studies
of the University of Lethbridge
in Partial Fulfillment of the
Requirements for the Degree

MASTER OF SCIENCE

Department of Geography
University of Lethbridge
LETHBRIDGE, ALBERTA, CANADA

© Evan Leslie James Booth, 2011

ABSTRACT

This thesis is focused on determining the rate at which the climate of western North America (WNA) has changed in recent history, and looks at the impact that projected future climatic changes will have on a large glaciated watershed in the Canadian Rocky Mountains. The rate of change over WNA is quantified for 485 climate stations for the period 1950-2005 using indicators developed by the World Meteorological Organization (WMO). Results of the analysis show statistically significant historical trends across the study area. To gauge the effect of climate change on glaciers, a mass balance model was developed and integrated with the University of Lethbridge GENESYS hydrometeorological model. GCM future climate scenarios were used to model change in the Upper North Saskatchewan River Basin through 2100. Results forecast dramatic declines (> 80%) in total glacier area, ice volume, and streamflow contribution by 2100.

ACKNOWLEDGEMENTS

I would like to thank everyone who has helped me to complete this research over the past two years. My first and deepest gratitude is extended to my wife Meg and my family who have supported me both emotionally and financially throughout my University education.

I am grateful to Dr Jim Byrne for giving me the opportunity to pursue my graduate studies under his direction. The emotional, professional, and financial support you have provided me over the past two years will never be forgotten. Thank you for pushing me to accomplish goals that at the outset of this research seemed unattainable. I am also grateful for the direction provided by my Co-Supervisor Dr Hester Jiskoot. Without your guidance, patience, and devotion to my cause I do not think that this work would have been completed. I would like to thank Dr Stefan Kienzle who served as a mentor throughout my undergraduate and graduate studies. Thanks for always having an open door. A special thanks to Dr Adriana Predoi-Cross, Dr Joel Harper, and Dr Karl Staenz for being part of my examination committee.

I am also grateful to all my fellow students, colleagues, and friends who have helped me along the way. Mark Mueller, Ryan MacDonald, Sarah Dalla Vicenza, Mike Nemeth, and Dez Tessler deserve special mention. Without your work and support I would not have made it.

TABLE OF CONTENTS

ABSTRACT	iii
ACKNOWLEDGEMENTS	iv
TABLE OF CONTENTS	v
LIST OF TABLES	vii
LIST OF FIGURES.....	viii
CHAPTER 1: INTRODUCTION	1
1.1 Introduction	1
1.2 Research Objectives	3
1.3 Thesis Structure.....	4
CHAPTER 2: CLIMATIC CHANGES IN WESTERN NORTH AMERICA	5
2.1 Introduction	5
2.1.2 Previous Research	7
2.2 Study Area Regions	11
2.3 Data	15
2.4 Climate Change Indices	17
2.5 Methods	20
2.6 Results and Discussion	25
2.6.1 Pacific Northwest	25
2.6.2 Northwest Plains	34
2.6.3 Humid Continental Plains	37
2.6.4 Gulf	40
2.6.5 American Southwest	43
2.6.6 California-Nevada	47
2.7 Summary and Conclusions	50
CHAPTER 3: MODELING THE EFFECTS OF CLIMATE CHANGE ON GLACIATED ALPINE RIVER BASINS	52
3.1 Introduction	52
3.2 Climate Change in Alpine Environments.....	53
3.3 Glacier Mass Balance: Response to Climate Change.....	56
3.4 Simulating Mountain Hydrometeorology.....	59
3.4.1 Simulating Micrometeorology	61
3.4.2 Simulating SWE and Mountain Hydrology	64

3.5 Modeling Glacier Mass Balance	67
3.5.1 Static Response: Temperature Index Models	68
3.5.2 Static Response: Energy Balance Method.....	70
3.5.3 Dynamic Response of Glaciers	72
3.5.4 Estimating Glacier Volume	73
3.5.5 Glacier Runoff.....	75
3.6 Summary and Conclusions.....	76
CHAPTER 4: DEVELOPMENT AND APPLICATION OF A GLACIER MASS BALANCE MODEL IN THE UPPER NORTH SASKATCHEWAN RIVER BASIN.....	78
4.1 Introduction	78
4.2 Study Area.....	79
4.3 Methods: Meteorological Data.....	83
4.4 Methods: Spatial Data	87
4.5 Methods: Modeling	89
4.5.1 GENGRID	91
4.5.2 GENESYS	98
4.5.3 ICEGEN	103
4.5.3.1 ICEGEN v1: Volume-based Redistribution	108
4.5.3.2 ICEGEN v2: Flow Approximation Redistribution.....	109
4.5.4 GCM Future Climate Scenarios	110
4.6 Results and Discussion.....	112
4.6.1 Peyto Glacier	112
4.6.2 UNSRB Glacier Modeling	115
4.7 Summary and Conclusions.....	122
CHAPTER 5: CONCLUSIONS.....	123
5.1 Thesis Summary	123
5.2 Recommendations	126
REFERENCES.....	127

LIST OF TABLES

Table 2.1: Summary Definitions of selected ETCCDMI climate indices used.....	18
Table 2.2: Summary of station specific trends by region for all indices.	24
Table 2.3: Regional analysis statistics.....	25
Table 3.1: Melt factors for snow (k_s) and ice (k_i) determined for a number of glaciers in western Canada (Source: Shea <i>et al.</i> , 2009).....	70
Table 4.1: Correlation analysis results comparing observed winter mass balance at Peyto Glacier with stations in proximity to the UNSRB.....	86
Table 4.2: Correlation analysis results comparing observed ~May 1 SWE totals at snow surveys with stations in proximity to the UNSRB	87
Table 4.3: Glacier volume (IWE) estimations for the UNSRB	107

LIST OF FIGURES

Figure 2.1: Study area map showing regional classification system and locations of climate stations.....	12
Figure 2.2: Frequency histograms of weather station trend slopes for the period 1950- 2005, for each climate indicator over WNA	21
Figure 2.3: Frequency histograms of weather station trend slopes for the period 1950- 2005, for selected climate indicator over each region in WNA	22
Figure 2.4: PNW regional mean time series for GSL index.....	26
Figure 2.5: 100 year GSL time series for Agassiz, BC	27
Figure 2.6: Calculated trends in temperature indices across WNA by station	30
Figure 2.7: Spatial interpolation of calculated trends in temperature indices across WNA....	31
Figure 2.8: Calculated trends in precipitation indices across WNA by station	32
Figure 2.9: Spatial interpolation of calculated trends in precipitation indices across WNA...	33
Figure 2.10: NWP regional mean time series for PRCPT index	35
Figure 2.11: 100 year TX90p time series for Kalispell, MT	35
Figure 2.12: HCP regional mean time series for SDII index	38
Figure 2.13: 100 year SDII time series for Neosho, MO	38
Figure 2.14: GLF regional mean time series for R95p index.....	41
Figure 2.15: 100 year R95p time series for Brenham, TX	41
Figure 2.16: ASW regional mean time series for FD0 index	45
Figure 2.17: 100 year FD0 time series for Fort Collins, CO	45
Figure 2.18: CNV regional mean time series for TN90P index	48
Figure 2.19: 100 year TN90P time series for Ukiah, CA.....	48
Figure 3.1: Large-scale mean length variations of glaciers across a number of global regions. (Source: Oerlemans, 2005).....	54
Figure 3.2: Five year moving averages of Peyto Glacier seasonal and net mass balance (Source: Demuth and Keller, 2006)	56
Figure 3.3: Mean monthly changes in precipitation as a function of elevation and season (Source: MacDonald <i>et al.</i> 2009)	66
Figure 3.4: Upper North Saskatchewan River watershed elevation-area distribution and associated historical average of simulated maximum SWE (Source: MacDonald <i>et al.</i> , (in review)).....	67
Figure 3.5: Surface area vs. glacier volume for 144 glaciers world-wide, plotted on a log-log scale. (Bahr <i>et al.</i> 1997)	74
Figure 4.1: Study Area Map for the North Saskatchewan River Basin above Edmonton, Alberta.....	80

Figure 4.2: Study Area Map for the UNSRB	82
Figure 4.3: Area-elevation distribution of glaciers in the UNSRB	83
Figure 4.4: Driver station average monthly precipitation (1971-2000).....	85
Figure 4.5: Digital elevation model for the UNSRB	88
Figure 4.6: GENESYS glacier modeling routine flowchart	90
Figure 4.7: Air temperature lapse rate comparison	94
Figure 4.8: Winter precipitation totals by elevation for Peyto Glacier and PRISM datasets	95
Figure 4.9: Winter precipitation correction applied within GENGRID	96
Figure 4.10: Glaciers for which winter precipitation correction was applied (green).....	97
Figure 4.11: Sensitivity analysis on TREQ cold-storage and mass balance	99
Figure 4.12: Elevation based temperature index melt factors	101
Figure 4.13: Conceptual flow chart of ICEGEN module	104
Figure 4.14: Estimated average glacier depth profile per elevation bin for Peyto Glacier	107
Figure 4.15: Amount of change expected in 2050 for future GCM scenarios selected for use in GENESYS ice modeling routine.....	111
Figure 4.16: Observed vs. simulated mass balance for Peyto Glacier	113
Figure 4.17: Simulated 1966-2010 mass balance and total IWE volume for Peyto Glacier for ICEGEN v1	114
Figure 4.18: Simulated 1990-2100 UNSRB IWE volume using ICEGEN v1 (A) and ICEGEN v2 (B).....	116
Figure 4.19: Simulated 1990-2100 UNSRB glacier area-elevation relationships using ICEGEN v1 (A) and ICEGEN v2 (B)	117
Figure 4.20: Simulated future Columbia Icefield glacier areal extent for 1900, 2020, 2050, and 2080	119
Figure 4.21: Simulated 1990-2100 UNSRB glacier melt runoff using ICEGEN v1 (A) and ICEGEN v2 (B).....	121

CHAPTER 1

INTRODUCTION

1.1. Introduction

Over the past two decades, the International Panel on Climate Change (IPCC) has systematically mapped out the challenges facing the human species due to the radical impact we have had on the climate of the Earth. Thousands of renowned and accomplished scientists have contributed to advancing the science of climate research, making incredible advancements towards understanding of the natural systems of the planet we inhabit. The evidence supporting the fact that anthropogenic industrial output has caused irreversible harm to the atmosphere is now overwhelming (Solomon *et al.*, 2007). The damage caused to the planet since the industrial revolution of the mid 19th century represents an unprecedented threat to humanity (Gleick *et al.*, 2010). Despite the overwhelming scientific evidence, “Climate Change” remains a very heated debate in post-modern Western society. Governments and corporations are unwilling to take the steps necessary to reduce the amount of harmful emissions being released into the atmosphere, and the public is being misinformed about the reality of the problem. This is especially true in Alberta, where our chief export is petroleum, a product whose production and use directly contributes to the problems outlined by the IPCC.

However, based on the results of this study and others completed at the University of Lethbridge (Lapp *et al.*, 2005; MacDonald *et al.*, 2009; Larson *et al.*, 2010; Kienzle *et al.*, 2011; etc.), the province of Alberta will not be immune to the effects of a rapidly changing climate. One of the areas that is most susceptible to changes in climate is the

Western Cordillera that forms the backbone of the North America and serves as the headwaters for rivers that are used by millions of people downstream. Warming temperatures over the past 50 years have already begun to radically change the climate of western North America, causing an earlier onset of spring (Easterling, 2002), an increased risk of pest invasion in our forests (Kurz *et al.*, 2008), a higher likelihood of catastrophic wildfire (Westerling *et al.*, 2006), and a dramatic decline in glaciers (Bolch *et al.*, 2010). If government and industry are unwilling to change their practices in the hope of reducing the rate of anthropogenic climate change, then society as a whole must adapt to the new climatic conditions created by man's negligence. This thesis seeks to determine the rate at which our continent has already been altered by climate change, and the future changes we can expect in an important glaciated basin on the eastern slopes of the Canadian Rocky Mountains.

1.2. Research Objectives

The work presented in this thesis builds on the current body of knowledge pertaining to how climate change has affected western North America in the recent past, and gauges the impact that projected changes to the climate will have on the region in the future. Two general objectives were set forth to guide the direction of this research:

1. Construct a historical database of meteorological data from across western North America and use it to statistically analyze the extent to which the climatology of the continent has changed over the past 50 years.
2. Develop a new glacier mass balance model for integration with the GENESYS modeling routine to determine the historical and potential future effects that changes in the climate will have on the glaciers in the Upper North Saskatchewan River Basin.

1.3. Thesis Structure

This thesis is organized in 5 chapters. Chapter 1 introduces the general objectives of this research. Chapter 2 is focused on determining the extent to which western North America has already been altered by recent climatic changes. The chapter serves as a stand-alone paper and has been submitted and accepted for publication in the International Journal of Climatology. Chapter 3 serves as an introduction and literature review of the concepts related to the development of a mass balance glacier model for use in determining the effects of climate change on alpine glaciers. Chapter 4 is focused on accomplishing the second research objective and details the development, application, and results of the new glacier mass balance model in the Upper North Saskatchewan River Basin. Like chapter 2, chapter 4 is designed to be a stand-alone paper to be submitted for publication in an academic journal. As such, there is some overlap from the literature review done in Chapter 3. Chapter 5 concludes the thesis, summarizing the findings contained herein, and makes recommendations for future work in this area.

CHAPTER 2

CLIMATIC CHANGES IN WESTERN NORTH AMERICA, 1950 - 2005

2.1. Introduction

Water resources are coming under increasing pressure from societal demands related in large part to the growing population of Western North America (WNA). Global climate change is expected to alter the hydrologic cycle and place additional stress on water supplies and demands (Gleick *et al.*, 2010). The last two decades of research into the subject of climate change have confirmed that surface air temperatures have been significantly increasing over the period of record. It is now well established that human activities are contributing to modern climate change by altering the natural composition of the atmosphere (Karl and Trenberth, 2003; Solomon *et al.*, 2007). Although global average surface air temperature is projected to continue to increase, climate change will affect different regions of the globe in different ways (Portman *et al.*, 2009). This is expected, as changes in surface temperatures are related to changes in atmospheric circulation and precipitation patterns (Dore, 2005).

Temperature and precipitation variability in WNA is driven primarily by ocean currents in the Pacific, and to a lesser extent the Atlantic. Strong links have been established between precipitation patterns over WNA and Sea Surface Temperatures (SST), primarily the Pacific Decadal Oscillation (PDO) which is generally accompanied by different phases of the El Niño Southern Oscillation (ENSO) (Lapp *et al.*, 2002; Hoerling *et al.*, 2010; St. Jacques *et al.*, 2010). The PDO is generally considered to have shifted to a warmer El Niño dominated phase in 1976-77, and may have shifted

back to a cooler La Nina dominated phase in 1997-98 (Seager and Vecchi, 2010). Due to their influence over the climate of WNA, shifts in the PDO naturally influence any trends calculated in temperature and precipitation. The length of this study (55 years) was determined to be long enough to capture both phases, therefore minimizing their influence on the trends. It is important to note, however, the role that natural variability plays in the changing climate of the continent, and the extent to which it may be masking anthropogenic forcing (Seager *et al.*, 2007; Hoerling *et al.*, 2010).

Changing precipitation patterns and intensity, coupled with rising temperatures, could potentially spell disaster for many societal sectors by increasing the risk of both drought and flooding in sensitive environments. The goal of this research was to analyze daily historical climate data to determine the extent to which the climatology of WNA has been altered over the period 1950 to 2005. Daily temperature and precipitation data from 490 stations across western Canada and the western United States were obtained, summarized and analyzed to assess changes in climate. Previously established climate change indicators were applied to the data to evaluate historical change, and compare change between different regions. Trends are calculated for eight indicators focusing on station specific temperate and precipitation thresholds that are important in defining regional climatology. Additional analysis was carried out for the period 1906-2005 to gauge the amount of change and place the larger study in context. A regional analysis based on large, generalized geographic divisions was used to compare climatic change over different areas of the continent. Station-specific statistical output was then integrated in a Geographic Information System (GIS) to aid

in identification of spatially coherent trends in temperature and precipitation indices across western North America.

2.1.1. Previous Research

Different regions will vary in their long term trends, towards more or less precipitation with warmer or cooler temperatures. A number of studies have addressed trends in extreme temperature and precipitation events across different geographic regions and timescales. Syntheses of the work that has been done on trends in the historical precipitation record showed increased annual variance during the latter half of the twentieth century in nearly all regions with sufficient records for analysis (Dore, 2005; Portman *et al.*, 2009). As anthropogenic atmospheric change intensifies the hydrologic cycle it is expected that there will be a change in the frequency of so-called “extreme” climatic events, where daily precipitation and temperature exceed their normal thresholds (Groisman *et al.*, 1999). Many studies have modeled the potential changes in climate expected over the next century as a result of human activities. The 2007 IPCC report summarizes model projections for North America, identifying an expected dramatic rise in air temperatures across WNA. Future trends in precipitation are much more difficult to model given their link to SSTs and the uncertainty towards the response of ocean oscillations to climate change. Results differ between regions and models but mean trends indicate an increase in precipitation over most of WNA, with decreases in the southwest portion of the continent (Christensen *et al.*, 2007).

Studies focusing on historical Canadian climate trends have returned mixed results. Akinremi *et al.* (1999) carried out a precipitation trend analysis for the

Canadian Prairies in order to test the hypothesis that an intensification of the hydrologic cycle has accompanied global warming. The authors analyzed data from 37 climate stations from 1920 to 1995 by classifying precipitation events based on intensity. The study found significant trends for total annual precipitation but no trend for heavy precipitation events. Results were similar for Mekis and Hogg (1999) who analyzed a precipitation time series for all of Canada, based on homogeneous geographic regions. Zhang *et al.* (2000) analyzed Canadian trends in maximum, minimum, and mean temperature, diurnal temperature range, total precipitation, and snowfall ratio for the period of 1900-1998. The study found significant positive trends in annual precipitation across the country, except on the Canadian Prairies, an area which also showed the greatest amount of warming. Zhang *et al.* (2001) found few statistically significant trends in the frequency of heavy precipitation events over the twentieth century, concluding that a generalized increase in extreme precipitation over Canada has not accompanied increases in the concentration of greenhouse gases. Vincent and Mekis (2006) analyzed air temperature and precipitation for Canada using indices that describe the type, frequency, and intensity of precipitation. A set of ten indices were developed using the annual average for each station for the period of 1961-90. The study found that in the south of the country there are generally more days with precipitation, a decrease in daily intensity, and a decrease in the snowfall to total precipitation ratio. Overall, studies of extreme climatic events in Canada have shown that an intensification of the hydrologic cycle in the Canadian west has not yet accompanied the increasing air temperatures associated with climate change.

Studies focusing on the United States have shown larger and more significant results for precipitation- and temperature-based climate indices. Kunkel (2003) examined trends in North American extreme precipitation for the period 1895 to 2000 using an Extreme Precipitation Index to measure the frequency of events. The results of the study showed a large increase in the frequency of extreme precipitation events over the U.S. as a whole during the latter twentieth century, while the results for Canada were more mixed. Groisman *et al.* (2004) analyzed historical trends in temperature and precipitation over the conterminous U.S. using area weighted averages for a number of geographic regions. The study found warming trends, especially in northern regions, and a nationwide increase in intense precipitation, attributing the increase in 'very heavy' precipitation to an earlier onset of spring and summer-like conditions which creates more opportunity for the formation of convective systems. This earlier onset of spring is supported by Easterling (2002), who notes significant changes in the date of the last spring frost in all regions of the United States. Meehl *et al.* (2009) found that high temperature records in the U.S. since January 2000 outnumber extreme low temperature records by a ratio of two to one. Pryor *et al.* (2009) found strong significant trends in extreme precipitation events across the U.S., especially in the Great Plains region.

Similar studies have been done focusing on the European and global picture. Frich *et al.* (2002) analyzed a newly created global dataset in order to determine if there has been a change in the frequency or severity of climatic extremes during the period 1946 to 1999. The data were analyzed using ten extreme climate indices, selected from a set of 27 core climate change indicators developed by the World Meteorological

Organization (WMO) and the World Climate Research Program's Expert Team on Climate Change Detection, Monitoring and Indices (ETCCDMI) in order to coordinate global studies evaluating historical change. Global trends in extremes were analyzed by calculating a simple global average of all the valid stations, with a density of one or two stations per 250,000 km². As expected, the results of the study for precipitation-based indicators show different patterns of change throughout the globe, although many areas show statistically significant increases in the extreme precipitation indicators. Frich *et al.* (2002) concluded that during the latter half of the twentieth century, on average the global climate has become wetter and warmer, as expected under enhanced greenhouse conditions. Klein Tank and Können (2003) analyzed trends in temperature and precipitation extremes in Europe for the period 1946 to 1999. Using the same core WMO indices mentioned above, the study found pronounced warming trends throughout Europe. Stations reporting significant increases in annual precipitation were often accompanied by an increasing intensity of the heaviest events. Alexander *et al.* (2006) studied changes in daily climatic extremes using a global gridded dataset. The WMO indices were applied to a newly created global dataset to assess the magnitude of change over the period 1951-2003. Using calculated global averages, the study found large significant warming trends in temperature based indices and significant increases in precipitation towards wetter conditions in the late twentieth century.

2.2. Study Area Regions

The area of concern for this research was Western North America (WNA), a region that produces a substantial proportion of the world food supply through irrigation-based agriculture, and is home to an increasingly large population. The study area covers a large geographical range that includes many diverse ecological zones. The 485 climate stations used here are spread over an area of more than 8 million km² that includes 22 states west of the Mississippi River and four Canadian provinces west of the Great Lakes. The climatology varies widely, from the hot deserts of southern Arizona to the temperate rainforests of the Pacific Northwest. Previous studies have found some of the largest positive trends for extreme precipitation are in North America's central Great Plains, while negative trends are most common in the interior western states (Groisman *et al.*, 2004; Pryor *et al.*, 2009). Focusing on WNA, as opposed to the entire continent or globe, allows for more detailed investigation regarding the potential causes and regional implications of the results, while still maintaining a broad focus.

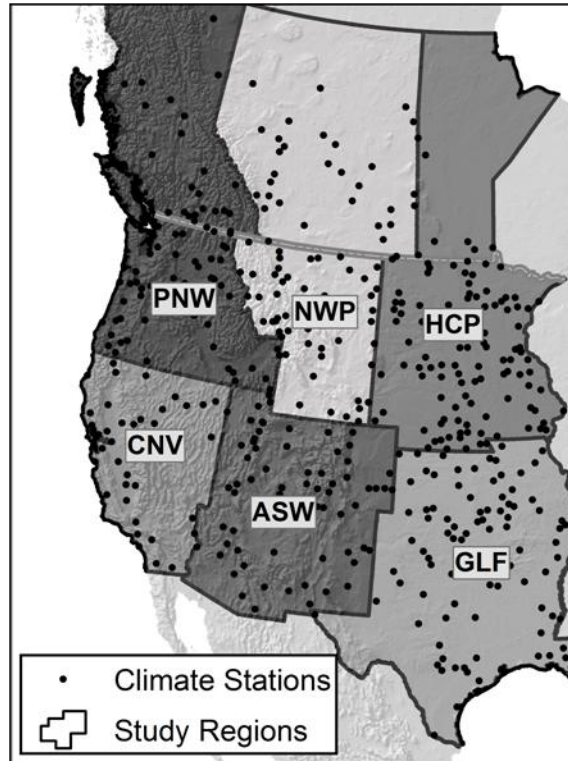


Figure 2.1: Study area map showing regional classification system and locations of climate stations. Regions (clockwise from top left): Pacific Northwest (PNW), Northwest Plains (NWP), Humid-Continetal Plains (HCP), Gulf (GLF), American Southwest (ASW), California-Nevada (CNV).

For the purposes of this study, Western North America was divided into 6 general geographic regions (Figure 2.1). Political boundaries were used to delineate the regions to simplify the process and aid in identification of regional trends. Due to the diverse climate and terrain in WNA these regions should not be regarded as cohesive ecological units, as all units encompass a number of different climatic regimes. Regions were defined based on similarities according to the Köppen-Geiger Classification System (Peel *et al.*, 2007), on the regions used by Groisman *et al.* (2004) and Karl and Koss (1984), as well as by the air masses that control their climate (Ahrens, 2008). The six regions used here are as follows (Figure 2.1):

- **The Pacific Northwest Region (PNW)**

The PNW region is centered on Washington State and also includes Oregon, Idaho, and British Columbia. The geography of the region is dominated by mountainous terrain, encompassing the Coast Range, the Cascades, and the northwestern portion of the Rocky Mountains. The climate is largely controlled by the maritime air mass of the northern Pacific. The highly varied topography results in a region made up of a wide spectrum of climatic zones, due primarily to the effects of orographic precipitation and temperature lapse rates. The climate is so varied that it includes eight different climatic types according to the Köppen-Geiger classification that vary from the warm and dry northern Mediterranean zone in Oregon to the snow-dominated sub-polar regions of the northern Cordillera.

- **The Northwest Plains Region (NWP)**

The NWP region is comprised of the northern states of Montana and Wyoming, and the Canadian provinces Alberta and Saskatchewan to the north. The area includes the eastern slopes of the northern Rocky Mountains, as well as the arid foothills and plains located in their rain shadow. The climate is primarily driven by the continental polar air mass and its interactions with the maritime Pacific air mass from the west. The region is dominated by dry semi-arid steppe and highland plateaus. Much of the landscape in the region has been given over to agricultural development, with cereal grains, oilseeds, pasture, and hay, as the primary crops being cultivated.

- **The Humid Continental Plains Region (HCP)**

The HCP region includes the states of North Dakota, South Dakota, Nebraska, Minnesota, and Iowa, as well as the Canadian province of Manitoba. The climate is driven primarily by interactions between the dry continental polar air mass originating in the Canadian Arctic and the warm moist maritime tropical air masses that originate in the Gulf of Mexico and the Pacific. The region's climatology is dominated by the humid-continental zone, with northern regions experiencing more severe winters than those in the southern half of the region.

- **The Gulf Region (GLF)**

The GLF region is made up of states whose climate is mostly driven by the maritime tropical air mass that originates over the Gulf of Mexico and includes Texas, Oklahoma, Kansas, Missouri, Arkansas, and Louisiana. This area falls mostly within the humid-subtropical zone, and as such it is a moist climate with usually mild winters. The Gulf Region is the most likely to be affected by tropical storms, and includes the southern portions of 'tornado alley' located on the southern Great Plains.

- **The American Southwest Region (ASW)**

The ASW region includes the 'Four Corner' states of Utah, Colorado, Arizona, and New Mexico. The geography of this area is dominated by the Colorado Plateau and the southern Rocky Mountains, and although it is almost semi-arid throughout, areas of higher elevation act as the crucial water tower of the Colorado River which provides water and hydro-electric power to millions of people in the American southwest (Barnett and Pierce, 2008). The climatology of the region in the summer is driven

primarily by the hot and dry continental tropic air mass that originates over central Mexico. In the winter, interactions between various air masses contribute to heavy snowfall in some areas. It is classified mostly as arid desert and semi-arid steppe, although the relief of the southern Rocky Mountains and the Colorado Plateau provide great variability in some areas.

- **The California-Nevada Region (CNV)**

The CNV region simply encompasses the states of California and Nevada. The region's climatology is driven by the Pacific maritime polar air mass in the north, and the tropical maritime air mass in the south. Most of the area is classified as a warm-dry Mediterranean-type climate, with central California producing much of North America's commercial vegetable production through intensive irrigation. The region also includes the hot deserts of south-eastern California and southern Nevada, as well as the snow-dominated alpine regions that make up the Sierra-Nevada Mountains.

2.3. Data

Daily historical air temperature and precipitation data for the United States were obtained from the Historical Climatology Network (HCN), a database compiled by the National Climate Data Center and comprised of a subset of stations from the US Cooperative Observers Network (COOP). This database offers historical climate records from over 1200 stations across the continental United States. Stations included in the HCN database were selected to minimize inhomogeneities associated with observation times, station relocation, and the potential for heat island bias (Williams *et al.*, 2006). Daily historical data for Canada were downloaded from Environment

Canada's National Climate Data and Information Archive, with preference given to those stations with the most complete records of observation.

A common problem when analyzing historical climate records is missing weather data. Programs were developed to quantify the amount of missing data present in each record and flag those stations with a substantial amount of missing daily values. Following the general procedure of Frich *et al.* (2002), annual records were considered to be missing if more than 10% of daily values were missing, or if more than 3 months contained more than 20% missing days. Stations were excluded that did not have at least 75% of years reporting. No effort was made to replace missing days with estimated daily values taken from nearby stations as this would compromise the analysis of the daily records. The final database for the analysis included 485 climate stations in WNA (Figure 2.1).

Programs were developed to extract the required elements from the different formats used by the two countries, convert U.S. temperature and precipitation data into degrees Celsius and millimeters, and place all the data into a single format for use in analysis. Although some station records in North America date back over a century, in order to run this analysis with as many stations as possible it was determined to begin at 1950 and end at 2005. This time frame is similar to that used in other recent studies (Alexander *et al.* 2006; Portman *et al.* 2009) and allowed for inclusion of more stations, as a far greater number have good historical records post 1950. Extending the time frame into decades prior to 1950 presents many difficulties with regard to data availability. Many records are very sparse or non-existent in the 1930s and 40s due to the stresses associated with the Great Depression and World War Two. While it is true

that some stations have quality records dating back to the turn of the century, the majority unfortunately do not. Data downloaded from the US HCN V2 database at the time of analysis extended through 2008 for some stations. However, data availability was not uniform across all states and stations. Data downloaded from Environment Canada was also sparse for recent years, especially in British Columbia, where online database reports for most stations only extended through the end of 2004. Further complicating the issue is the fact that many stations in the historical database have undergone a transition to an automated system over the last decade, often moving locations at the same time. This prohibits the use of some recent data in our study, since due to homogeneity concerns, no station joining or data infilling was attempted for this project. To provide some comparison with longer-term trends, the analysis was also completed for the period 1906-2005 for six high quality stations, one from each region, testing all indices for trends for a 100 year period. It is important to note that while a single station cannot necessarily capture trends over a whole region, a longer analysis provides a valuable tool for comparing trends calculated over different time scales. In some cases, the time period sampled can have an impact on the calculated trends.

2.4. Climate Change Indices

In an effort to harmonize climate investigations and facilitate easier comparisons between studies, a single set of indicators was proposed by a WMO Commission. A set of 27 core climate change indices were developed by the WMO and the ETCCDMI in order to coordinate global studies evaluating historical change (Frich *et al.*, 2002;

Peterson, 2005; Alexander *et al.*, 2006). The climate change indicators focus primarily on daily precipitation and temperature events that have a return period ranging from weeks to months, rather than years. While this means that the events may not be ‘extreme’ in the classic sense, the lower thresholds allow for better trend detection and calculation over longer time periods. The 27 WMO core climate indices were calculated for all stations that met the data requirements of the study. A full list of the 27 core indices and their descriptions can be found in Zhang and Yang (2004). Eight indicators were selected for further analysis and interpretation, summarized in Table 2.1. Four indices were chosen to quantify change in temperature, and four indices quantify changes in precipitation over WNA.

Table 2.1: Summary Definitions of selected ETCCDMI climate indices

Temperature Indices		Definition
Frost Days	FD0	number of days where $T_{min} < 0^{\circ}C$
Growing Season	GSL	period when $T_{mean} > 5^{\circ}C$ for > 5 days and when $T_{mean} < 5^{\circ}C$ for > 5 days
Warm Nights	TN90P	percentage of days where $T_{min} > 90$ th percentile
Warm Days	TX90P	percentage of days where $T_{max} > 90$ th percentile
Precipitation Indices		Definition
Daily Intensity	SDII	total annual precip/number of events greater than 1mm
Wet Days	R5MM	number of days where precip > 5 mm
Very Wet Days	R95P	annual total precipitation from events > 95 th percentile
Total Annual	PRCPT	total annual precipitation from events greater than 1mm

The temperature indices chosen were among the most representative of changes that would likely have a direct impact on the environment and population of the study regions, as opposed to being the most ‘extreme’ indices:

- **Frost Days (FD0)** is the annual count of days when the minimum temperature is below $0^{\circ}C$, representing the amount of time during the year that frost is possible.

This index was chosen over the similar Ice Days index (when $T_{\max} < 0^{\circ}\text{C}$) because it is capable of detecting trends in southern regions where the maximum daily temperature rarely falls below freezing.

- **Growing Season Length (GSL)** is defined as the annual count of days between the first occurrence of six consecutive days with a daily mean temperature $\geq 5^{\circ}\text{C}$, and the first occurrence after July 1 of six consecutive days with a daily mean temperature $\leq 5^{\circ}\text{C}$. This annual count roughly represents the amount of time that a region can be agriculturally productive. Any changes in the GSL (as well as the FD0) could have profound implications in regions where late or early frosts have the potential to devastate entire crops.
- **Warm Days (TX90p)** is the annual percentage of days when the maximum temperature is greater than the station-specific 90th percentile, defined based on a 1961 to 1990 base period. This index was chosen to be most suited to determine whether maximum temperatures increased during the study period.
- **Warm Nights (TN90p)** is the annual percentage of days when the minimum temperature is greater than the station-specific 90th percentile, defined based on a 1961 to 1990 base period. This index further quantifies the amount that the climate is warming through an increase in minimum temperatures.

The precipitation-based indices used in this study were also chosen from the 27 core indices on the basis of importance to the environment and population of western North America:

- The **Simple Daily Intensity Index (SDII)** is calculated by dividing PRCPT by the annual number of precipitation events ($> 1 \text{ mm}$). This simple measure

provides an indication of whether an intensification of the hydrologic cycle has accompanied any temperature changes in western North America.

- **Significantly Wet Days (R5mm)** is defined as the annual count of precipitation events greater than 5 mm. R5mm events represent days where the amount of precipitation received is enough to potentially have an effect on arid and semi-arid ecosystems where heavy precipitation events are rare.
- **Very Wet Days (R95p)** are defined as the annual total precipitation that is received from events that are greater than the station-specific 95th percentile, defined based on a 1961 to 1990 base period. The R95p index provides a measure of the extent to which an increase in PRCPT is driven by extreme events.
- **Total Annual Precipitation (PRCPT)** is the annual sum of all recorded precipitation events greater than 1 mm. The 1 mm threshold removes the effects that trace measurement recording efficiency can have on trend calculations.

2.5. Methods

Indices were calculated on an annual basis for each station for the period 1950-2005, and for one station from each region for the period 1906-2005, utilizing the RClimDex software developed at the Climate Research Branch of Meteorological Service of Canada, in conjunction with the ETCCDMI (Zhang and Yang, 2004).

Trends were calculated using linear regression and significance levels were determined using a non-parametric Mann-Kendall test to determine whether the slopes differed significantly from zero. A number of programs were developed and used to aid in processing the vast amount of output data generated by the individual analyses done on

all climate stations. Trends calculated for each climate indicator were combined in a single database file for further analysis. Regional and 100yr station time-series have been presented for a unique index for each region.

Linear trends for each station were used to calculate mean trends over the whole study area and by region for each index. The distributions of slopes were examined and found to be normally distributed in the vast majority of cases (Figures 2.2 and 2.3). The regional mean slope of the trend of each index distribution was then tested to determine if they were significantly different from zero. Slope of the regression line was used as an indication of a detectable increasing or decreasing trend in each index, over the time period specified.

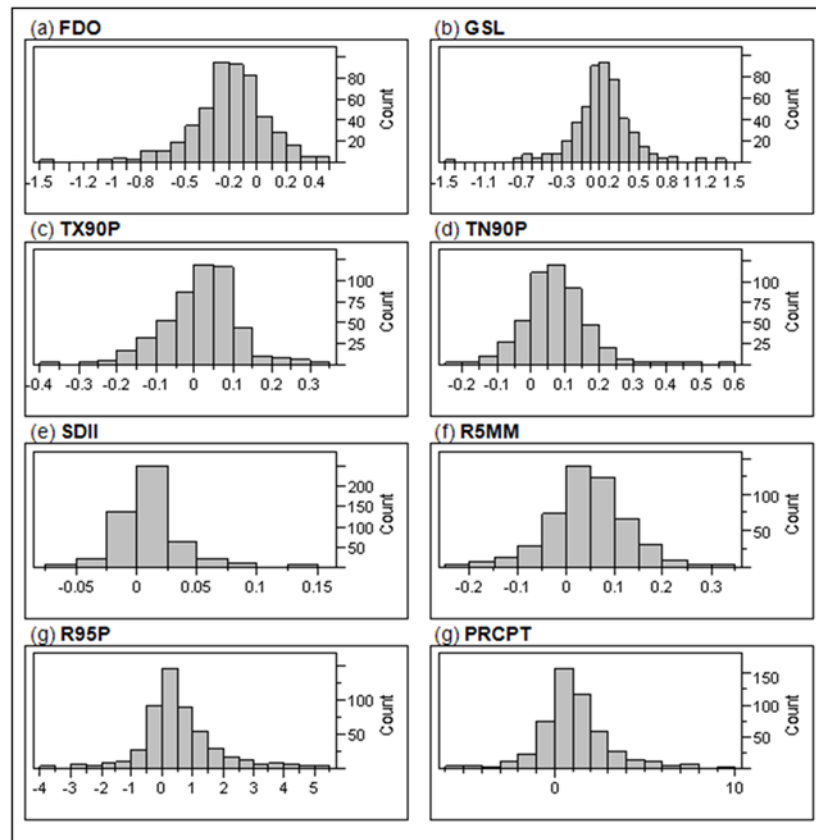


Figure 2.2: Frequency histograms of weather station trend slopes for the period 1950-2005, for each climate indicator over WNA.

The objective was not to examine the exact shape of the relationship, or to compare variation on shorter time scales, but to compare overall trends. If there were no regional trends, the distribution of slopes for an index would be expected to have a mean value not statistically discernible from zero, given the variability among sites. To test against the hypothesis that the expected value of any given mean slope was equal to zero, distributions were examined and then a t-test and a non-parametric Wilcoxon test was applied to each index. A two-tailed test was used because the overall expected value of the slope for an index could be either negative or positive, and no prejudice was imposed over which way it was likely to be. In all cases the conclusions of the parametric and non-parametric tests agreed. Regional time-series were also produced by calculating the annual average index value for all stations in each region. These values were then plotted to provide visualization of regional trends.

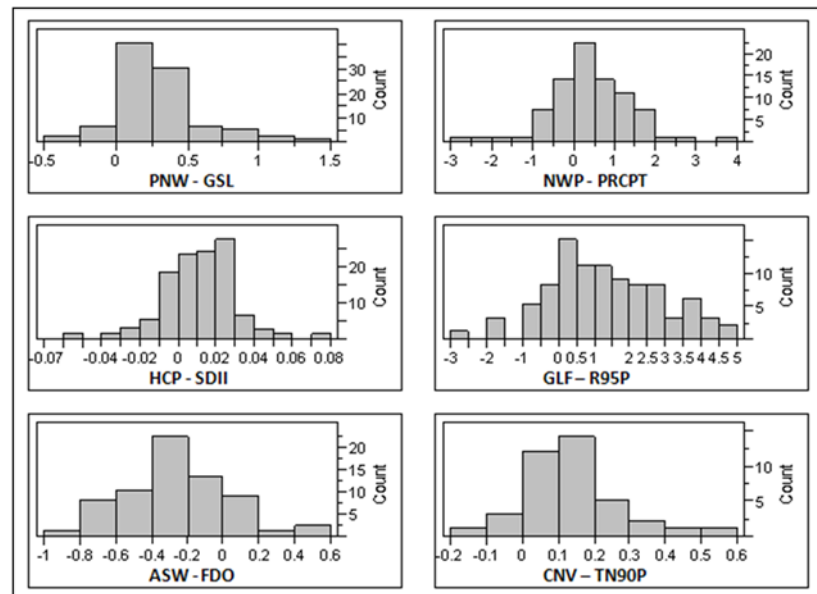


Figure 2.3: Frequency histograms of weather station trend slopes for the period 1950-2005, for selected climate indicator over each region in WNA.

Output data were integrated into a GIS to identify the spatial patterns of trends in the selected climate indices across WNA. The sign of the slope for indices calculated at each station was plotted over the study area. Station results by region are presented in Table 2.2. Additional trend surface analysis was used to interpolate spatial patterns based on station-specific output. The calculated slopes for each station were interpolated over the study area to smooth the results from the individual stations and give a sense of the rate of change over WNA. Results for temperature indices are presented in Figures 2.6 and 2.7, precipitation in Figures 2.8 and 2.9. A combination of Global and Local polynomial interpolation was chosen as the method best suited to analyze trends over an area as large as western North America. Basic Global polynomial interpolation uses a single polynomial to create a surface that varies gradually through the points over the entire study area. However, this method fails to capture the regional variability of trends over such a diverse area. Local Polynomial interpolation uses many polynomials to better represent trends over user-specified local neighborhoods (Johnston *et al.*, 2001). Error in the fitted surface was minimized by varying influence of surrounding points on the surface values produced by the interpolations. Varying the width of the neighborhood used to define the weight of calculated slopes allowed for the production of smooth surfaces over WNA while preserving smaller regional trends.

Although exact interpolations are not possible over such a large area, they are a valuable visualization tool to identify possible spatial trends; particularly given that trends should be more uniform in space if they are in fact driven by large-scale climatic change (Pryor *et al.*, 2009). No interpolation is able to eliminate all error through the

entire predictive surface. The method used here is no different. Error is exaggerated towards the edges of the fitted surface, particularly in areas with limited data availability like Northern Canada. Error in the final maps was reduced by presenting the interpolated surfaces in classes. Exaggerated values were curtailed by displaying the amount of historical change as being either greater than, or less than, a plausible value. Regional averages presented in the maps were calculated based on the station data, and therefore are not influenced by any errors present in interpolated surfaces.

Table 2.2: Summary of station specific trends by region for all indices. The positive/negative signs (+/-) denotes any trend where the slope is > 0 or < 0 respectively.

Station trends were considered to be significant (Sig. +/-) when $p < 0.1$.

A.

PNW - STATION TRENDS				
INDEX	Sig. (+)	(+)	Sig. (-)	(-)
FD0	3	10	55	86
TN90P	65	89	1	7
TX90P	46	77	4	15
GSL	39	86	1	8
PRCPT	11	57	6	39
SDII	19	48	9	42
R5MM	10	50	4	43
R95P	7	56	9	40

B.

NWP - STATION TRENDS				
INDEX	Sig. (+)	(+)	Sig. (-)	(-)
FD0	9	18	42	64
TN90P	56	71	4	12
TX90P	46	73	3	9
GSL	31	76	1	7
PRCPT	18	58	2	25
SDII	14	52	3	27
R5MM	15	54	5	28
R95P	13	55	0	28

C.

HCP - STATION TRENDS				
INDEX	Sig. (+)	(+)	Sig. (-)	(-)
FD0	9	26	47	86
TN90P	68	93	6	18
TX90P	26	69	2	43
GSL	29	86	0	26
PRCPT	28	88	1	24
SDII	31	78	4	28
R5MM	19	77	1	34
R95P	29	89	1	22

D.

GLF - STATION TRENDS				
INDEX	Sig. (+)	(+)	Sig. (-)	(-)
FD0	8	23	45	70
TN90P	35	57	15	35
TX90P	3	14	35	79
GSL	4	38	12	55
PRCPT	42	86	0	7
SDII	35	71	2	22
R5MM	38	84	0	8
R95P	27	76	1	17

E.

ASW - STATION TRENDS				
INDEX	Sig. (+)	(+)	Sig. (-)	(-)
FD0	3	12	44	54
TN90P	43	53	7	13
TX90P	29	41	3	25
GSL	13	40	5	26
PRCPT	32	57	1	9
SDII	14	43	8	22
R5MM	28	59	2	7
R95P	16	49	1	17

F.

CNV - STATION TRENDS				
INDEX	Sig. (+)	(+)	Sig. (-)	(-)
FD0	4	4	27	36
TN90P	28	36	4	4
TX90P	11	21	7	18
GSL	11	31	1	9
PRCPT	8	36	0	4
SDII	4	22	1	17
R5MM	7	36	0	4
R95P	3	30	1	10

Table 2.3: Regional analysis statistics. Mean slopes for each index by region were tested to determine if trends over each region were significantly different from zero. Shaded areas denote regional trends that are significant at the $p < 0.001$ level.

Region	FD0	GSL	TN90P	TX90P	SDII	R5MM	R95P	PRCPT
ASW	-0.272	0.021	0.079	0.048	0.006	0.071	0.389	1.209
GLF	-0.140	-0.088	0.026	0.015	0.025	0.096	1.325	2.807
HCP	-0.113	0.145	0.068	0.020	0.010	0.036	0.696	1.060
NWP	-0.165	0.241	0.073	0.059	0.005	0.024	0.252	0.408
PNW	-0.244	0.312	0.094	0.047	0.001	-0.002	0.047	-0.022
SNV	-0.248	0.068	0.126	0.018	0.003	0.061	0.185	1.012
ALL WNA	-0.185	0.127	0.072	0.015	0.009	0.018	0.045	0.530
								$P < 0.001$

2.6. Results and Discussion

2.6.1. Pacific Northwest

Many of the calculated trends for the Pacific Northwest (PNW) vary as much as the micro-climatology of the cordillera. An overwhelming majority of stations in the region have experienced warming over the period of study (Table 2.2a). All regional mean temperature indices are reporting significant trends for the region (Table 2.3). One indicator that shows very strong trends throughout the entire region is FDO (Figure 2.6a). As stated above, FDO measures the annual count of days when the daily minimum temperature falls below 0°C , roughly indicating the length of winter. Negative trends are clearly evident over the entire Pacific Northwest, with an average reduction in the number of annual frost days of 2.4 per decade, significant at $p < 0.001$ (Figure 2.7a). It is possible that a reduction in the number of frost days may potentially lengthen the growing season. Highly significant trends in the GSL index support this notion. This region has experienced the most amount of change in WNA for this index,

with an average increase in the annual GSL of 0.31 days per year (Figure 2.7b). The general increase in GSL can be seen in the annually averaged time-series in Figure 2.4. The 1906-2005 trend calculated for Agassiz BC also agreed with the regional results (Figure 2.5). Significant positive trends were also found in the TN90P, TX90P, and WSDI indices (Table 2.3). Based on these results, there is little doubt that the Pacific Northwest experienced significant warming from 1950 to 2005.

The precipitation-based indices are much more varied over the Pacific Northwest, with some areas experiencing wetter conditions while others appear to be receiving less precipitation. This type of diversity is expected in a region with such mountainous

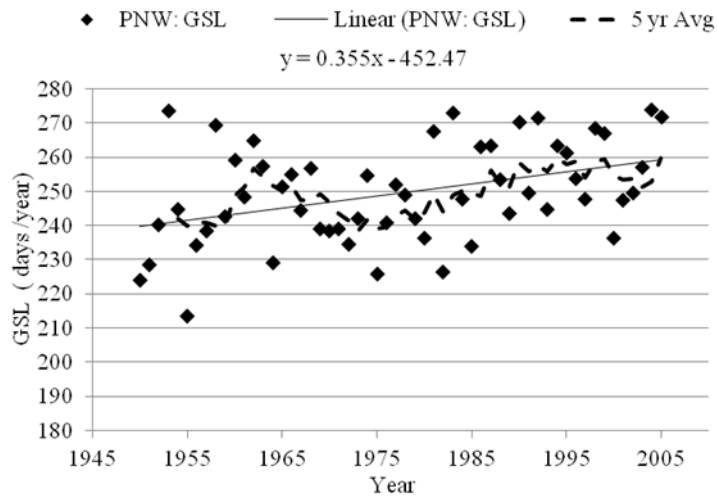


Figure 2.4: PNW regional mean time series for GSL index. Annual mean index counts were calculated and plotted over time. Linear trends are shown with solid line. 5 year moving averages were calculated and are shown with dashed line.

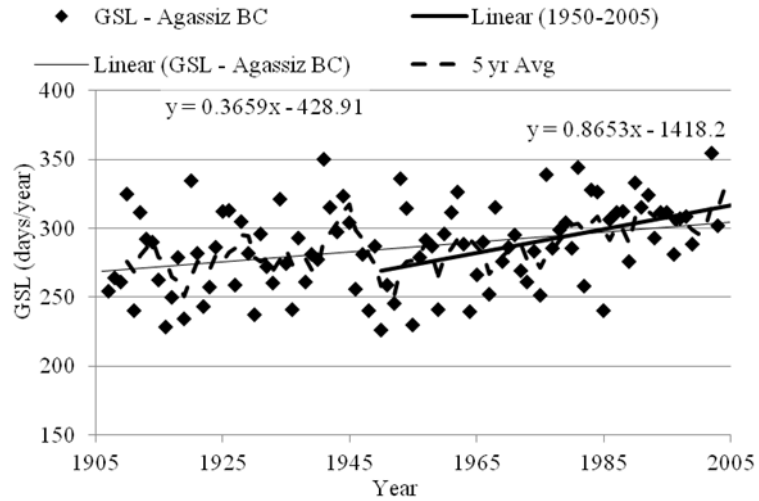


Figure 2.5: 100 year GSL time series for Agassiz, BC. 1906-2005 linear trends are shown with thin solid line. 1950-2005 linear trends are shown with bold solid line. 5 year moving average shown with dashed line.

topography. The spatial variability of trends in the precipitation indices over the PNW resulted in no significant trend in the region-wide means (Table 2.3). Although a number of stations in the interior of British Columbia are reporting significant increases in PRCPT (Figure 2.8d), a drying cell located over Oregon stands out in the interpolation (Figure 2.9d). Strong significant negative trends in PRCPT are found in station records in the south and central areas of the region. This decline in total annual precipitation seems to be driven by negative trends in the number of high-intensity events, as the SDII and R95P indices are also reporting significant negative trends over the area (Figure 2.8a and 2.8c). Even when considering the cell centered on Oregon, precipitation intensity seems to be increasing in some areas, as indicated by moderate positive trends found in SDII over much of British Columbia, Washington, and Idaho (Figure 2.9a).

Results from the Pacific Northwest region have a number of potentially serious ramifications. Strong negative trends detected in the FDO are important because a reduction in the number of frost days in alpine regions indicates a shortening of the winter season, and a potential change in the timing of the spring snowmelt runoff, which has been noted in a number of other studies (Easterling, 2002; Kunkel *et al.*, 2004; Barnett, 2005; MacDonald *et al.*, 2011). Shorter and warmer winters in high alpine areas are partially responsible for the outbreak of the mountain pine beetle that has been devastating forests in many areas throughout the PNW and other regions over the last decade. According to the mean of the future models investigated by the IPCC, inland and higher elevation areas in the PNW are expected to see dramatic increases in temperature over the next century (Christensen *et al.*, 2007). As the temperature rises, some pest species are able to move into new areas in higher elevations and latitudes where they were previously not able to survive (Kurz *et al.*, 2008). Some areas in the region have also clearly received less precipitation than in the past. When combined with a potential earlier onset of spring and an increase in summer temperatures, a reduction in rainfall substantially increases the risk of forest fire. An earlier onset of spring means that forests will lose their snow-cover earlier and have more time to dry out, thus lengthening the fire season throughout northern regions (Running, 2006; Westerling *et al.*, 2006). An intensification of precipitation events in some areas of the PNW may increase the risk of flooding and landslides, especially in mountainous areas that have previously succumbed to pest infestation and/or fire. The significant negative trends detected in the precipitation indices over Oregon potentially signifies a northward expansion of the warmer and drier Köppen-Geiger Mediterranean climate

zone historically found in central and northern California (Peel *et al.*, 2007). Northern portions of Pacific Northwest region are expected to receive 5 to 10% more precipitation by 2099 (Christensen *et al.*, 2007). However, the drying cell over Oregon may continue into the future as many model projections show negative trends in precipitation over the southwest portion of the continent extending into Northern California and Oregon.

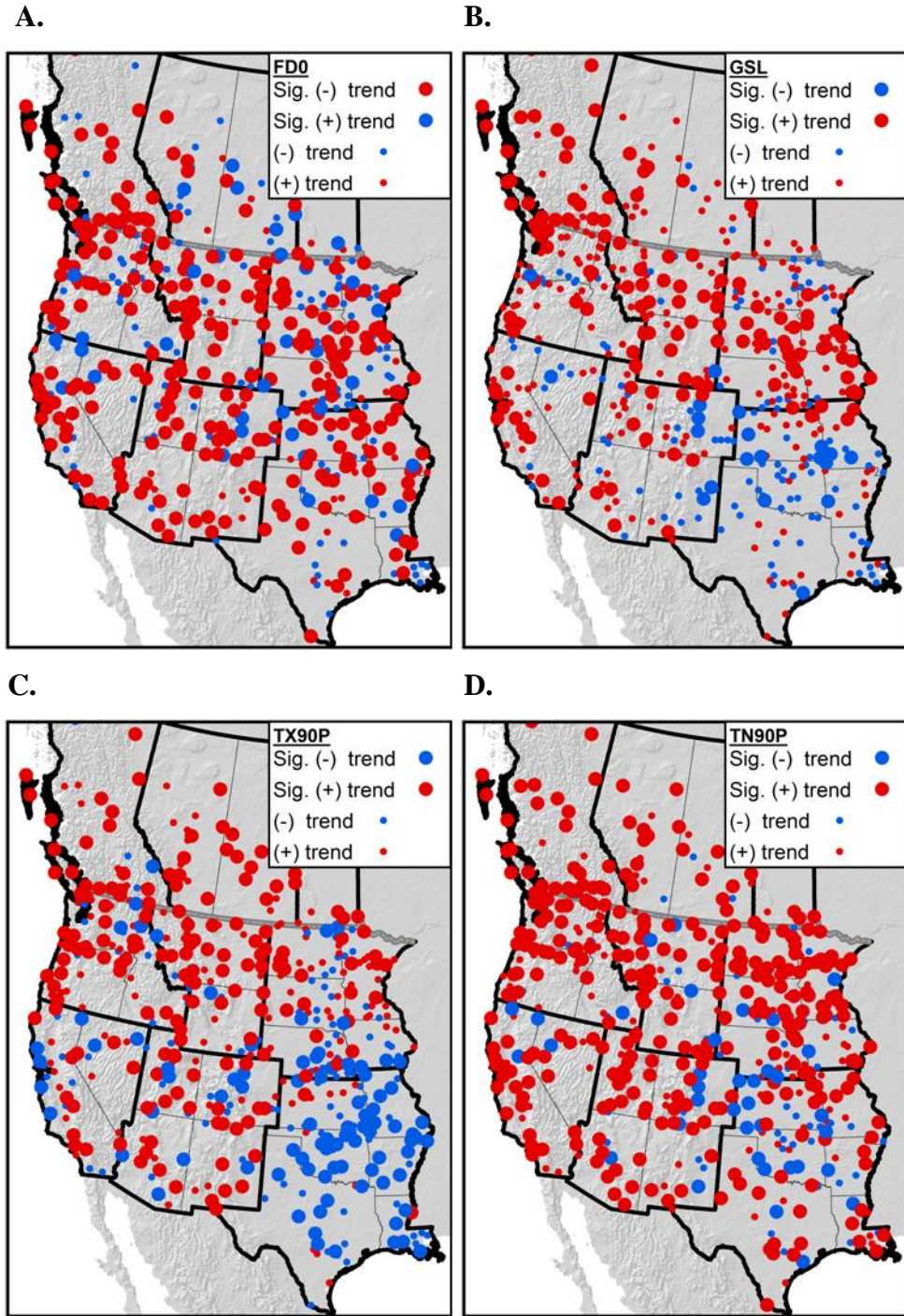


Figure 2.6: Calculated trends in temperature indices across WNA by station. Red points indicate warming trends and blue dots indicate cooling. Larger points are significant at the $p < 0.1$ level.

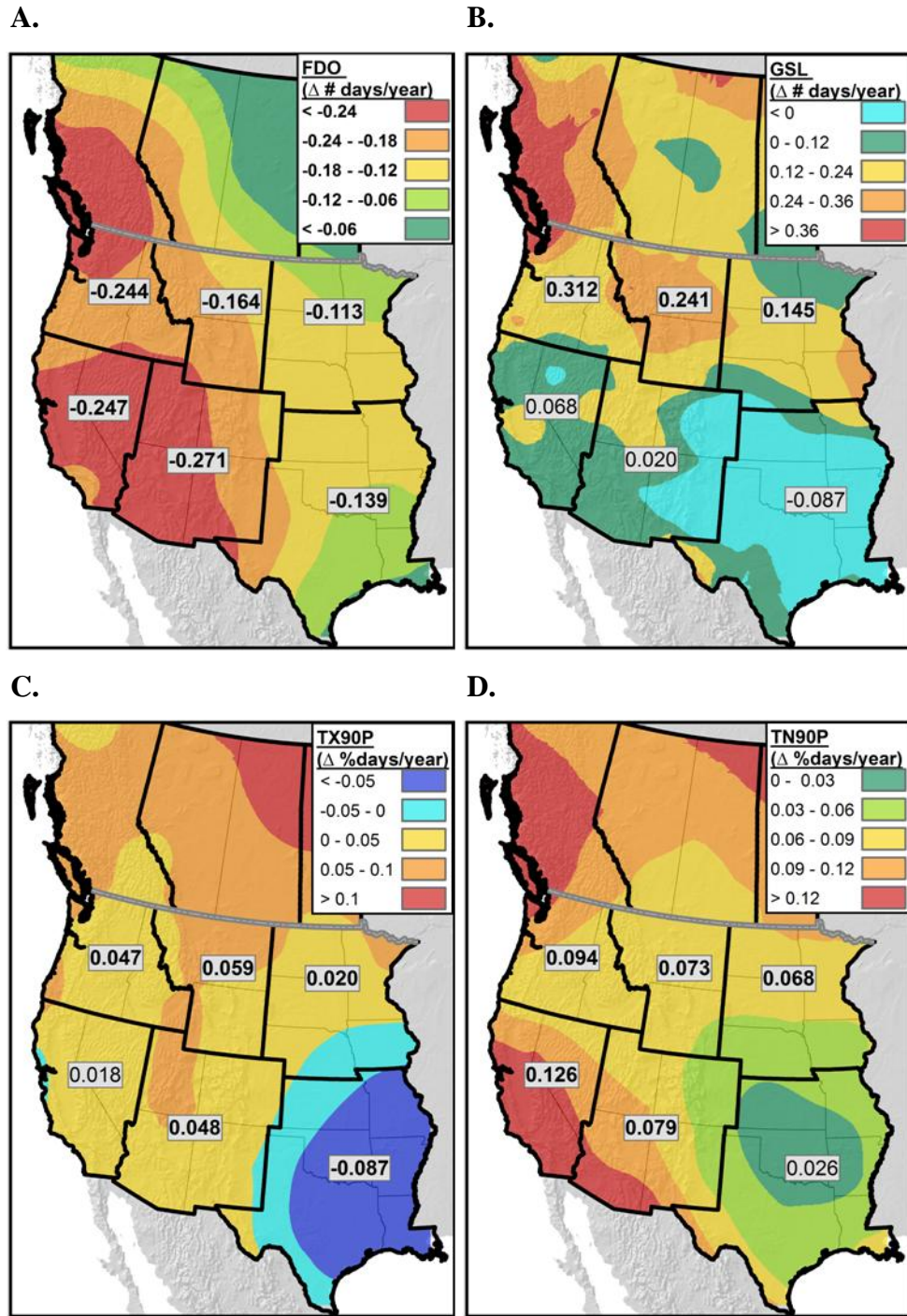


Figure 2.7: Spatial interpolation of calculated trends in temperature indices across WNA. Regional mean trends calculated using station-specific trends and are displayed over their respective regions. Bold numbers were found to be significant at the $p < 0.001$ level.

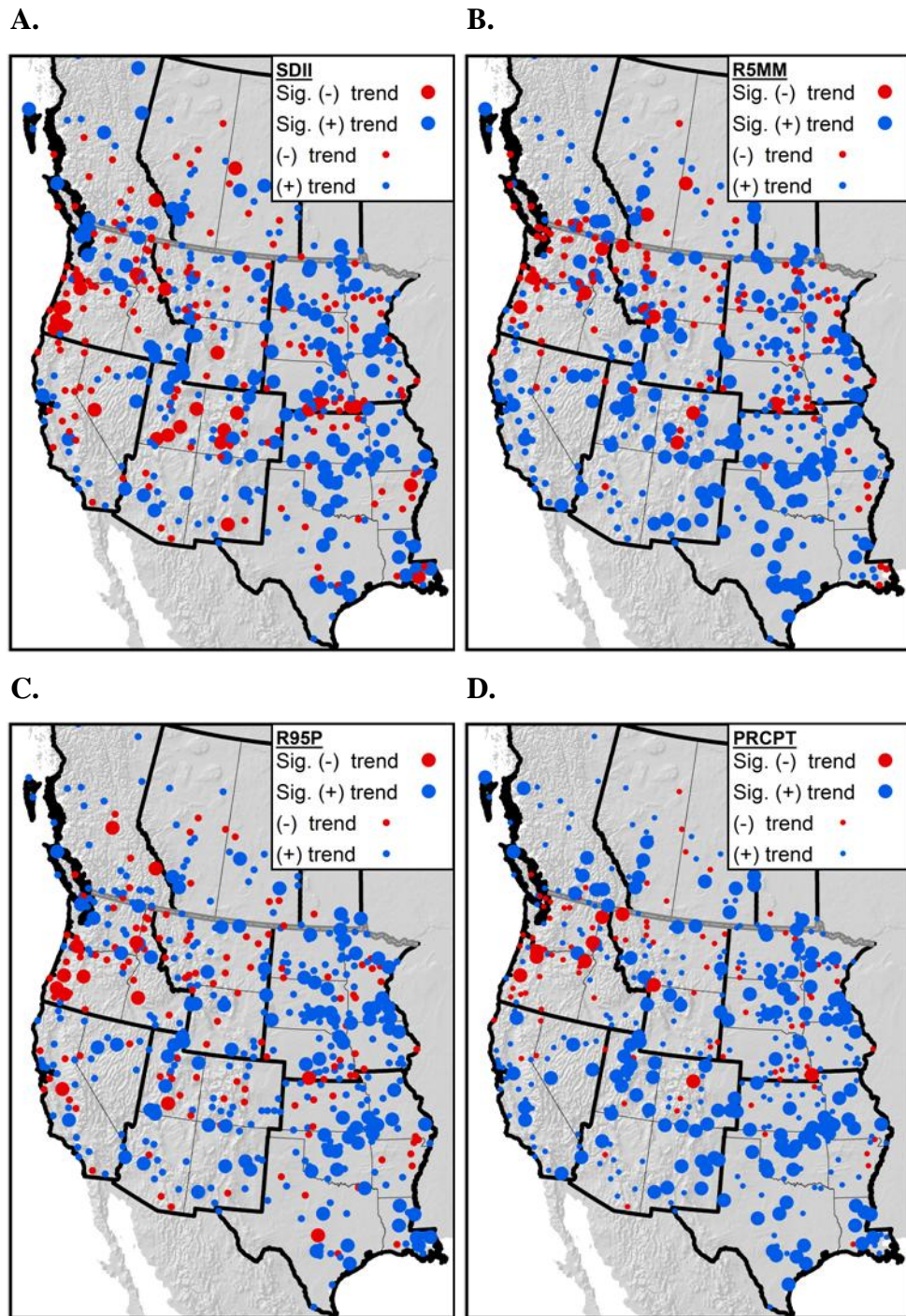


Figure 2.8: Calculated trends in precipitation indices across WNA by station. Blue points indicate increasing precipitation trends and red dots indicate decreasing precipitation. Larger points are significant at the $p < 0.1$ level.

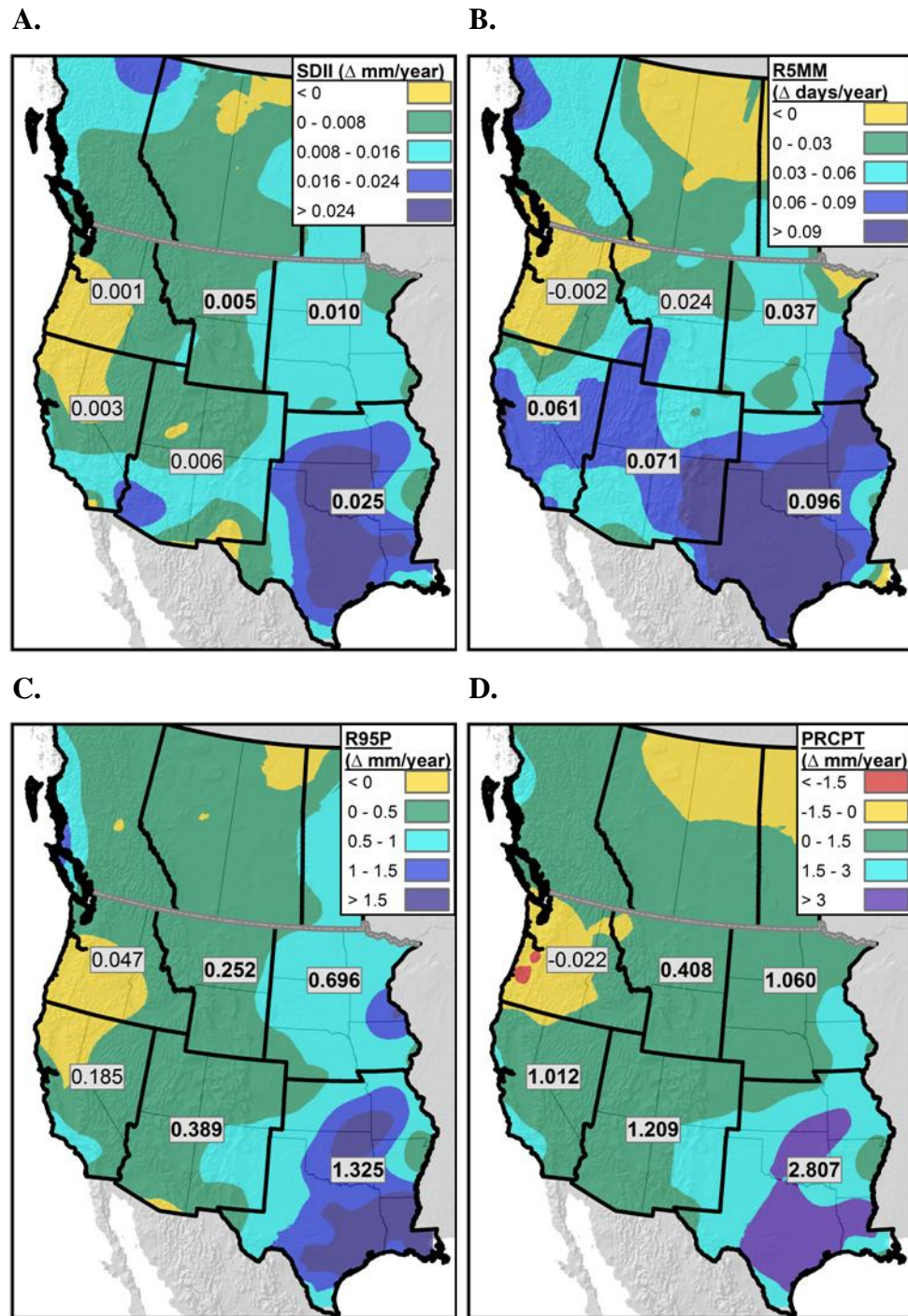


Figure 2.9: Spatial interpolation of calculated trends in precipitation indices across WNA. Regional mean trends calculated using station-specific trends and are displayed over their respective regions. Bold numbers were found to be significant at the $p < 0.001$ level.

2.6.2. Northwest Plains

The Northwest Plains (NWP) region is characterized by the Rocky Mountains and the semi-arid steppe that sits in their rain shadow. Climatic trends are not as strong as in the Pacific Northwest but they appear to be more spatially coherent, likely due to the more uniform landscape. Temperature-based indices overwhelmingly show moderate to strong warming over the region as a whole (Table 2.2b and Figure 2.6). The calculated regional trends for the FD0, GSL, TN90P, and TX90P indices were all significant at the $p < 0.001$ level (Table 2.3). Although a few stations are reporting significant positive trends in the number of frost days per year, the vast majority display significant declines in their annual FD0 count, with an average reduction in the number of annual frost days of 0.16 per year, significant at $p < 0.001$ (Figure 2.7a). Negative trends in FD0 are consistent with the positive trends in the GSL index (Figure 2.7b). GSL trends for the Northwest Plains region are among the strongest in WNA, with some stations reporting a lengthening of the annual growing season of about 4 days per decade with a calculated region-wide average of 0.24 days per year. Significant increasing trends are also found throughout the region in the TN90P and TX90P station-specific temperature indices (Figures 2.7c and 2.7d).

Much fewer significant trends were found in the precipitation-based indices over the Northwestern Plains region (Table 2.2b). The lack of overwhelming station-specific significant trends for the extreme-based R95p indicator makes it difficult to conclude for certain that an intensification of the hydrologic cycle has accompanied the clear warming trend over the Northwestern Plains. Stations that are reporting

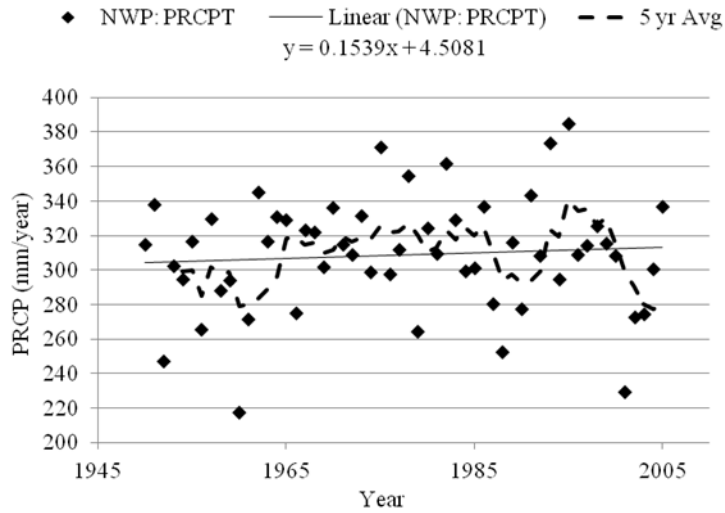


Figure 2.10: NWP regional mean time series for PRCPT index. Annual mean index counts were calculated and plotted over time. Linear trends are shown with solid line. 5 year moving averages were calculated and are shown with dashed line.

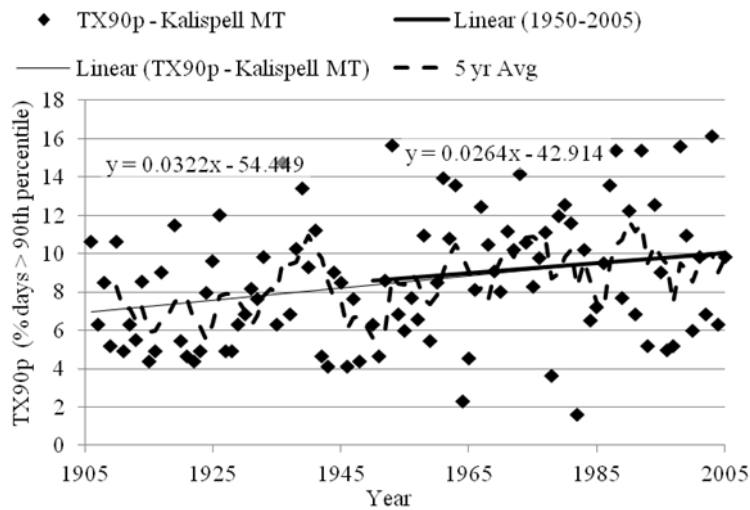


Figure 2.11: 100 year TX90p time series for Kalispell, MT. 1906-2005 linear trends are shown with thin solid line. 1950-2005 linear trends are shown with bold solid line. 5 year moving average shown with dashed line.

significant trends indicate moderately increasing precipitation over the region.

Regional analysis results for the NWP suggest that precipitation has increased over the

area, with the SDII, R5MM, and PRCPT indices all reporting trends that are significantly different from zero (Table 2.3). The regional time series plot (Figure 2.10) suggests that this positive trend is quite weak owing to large inter-annual variability. The 1906-2005 time-series at Kalispell MT also shows moderately increasing PRCPT (Figure 2.11).

Due to the semi-arid climate in the Northwest Plains region, any change in the hydrologic regime could pose serious problems for areas dependent on irrigation-based agriculture. Overall results suggest that most of the region is receiving as much or more precipitation as in the past (Figures 2.8 and 2.9), and IPCC mean modeled projections suggest that the area will likely receive more precipitation in the future. However, the significant warming, especially in the mountainous areas in the west, may negate the effects of any overall increase in precipitation. Higher temperatures indicate higher potential evapotranspiration which can have a negative impact on soil-moisture content and the productivity of grassland and crop-based ecosystems (Hughes and Diaz, 2008; Liu *et al.*, 2009). The shortening of winter as depicted by the FDO and GSL indices has resulted in an earlier onset of spring throughout the highlands of the eastern slopes (Lapp *et al.*, 2005; Barnett *et al.*, 2005; MacDonald *et al.*, 2011). If warming trends continue into the future as forecasted by research presented by the IPCC reports, it is likely that watershed managers throughout the region will have to adapt to an earlier spring runoff and prepare for potentially longer periods of low-flow. The problem is compounded by shrinking alpine glaciers that traditionally supply a substantial proportion of summer flows in dry years, and may have already passed the peak of melt water generation (Moore *et al.*, 2009).

2.6.3. Humid Continental Plains

The Humid Continental Plains region is similar in relief to the eastern portion of the Northwest Plains but is lower in elevation and largely falls within a wetter climate zone. Calculated temperature trends vary from north to south in the region, roughly following the climatic zones according to Köppen-Geiger classification (Peel *et al.*, 2007). While most stations are reporting significant negative trends for FDO, a number of stations are actually reporting significant increases in the number of frost days per year which substantially reduces the average regional trend (Table 2.2c and Figure 2.6a). The resulting mean trend in FDO for the region amounts to a reduction in the number of annual frost days of 0.11 per year, significant at the $p < 0.001$ level, but it is the weakest trend in FDO among all regions in WNA (Table 2.3). Trends calculated for TN90P are overwhelmingly positive, outnumbering negative trends by a ratio of more than 5 to 1, indicating a highly significant increase in the number of days per year when the minimum temperature is above the baseline 90th percentile. A general warming of the region is also indicated by trends in GSL, with a moderate region-wide lengthening of the annual growing season of 1.4 days per decade. Strong significant positive trends are concentrated in the southern half of the region, with more northern stations reporting less significant historical trends (Figure 2.6b). The region is reporting significant increases in TX90p, indicating that from 1950-2005 there was a moderate increase in maximum temperatures, especially in the northern HCP (Figures 2.6c and 2.7c).

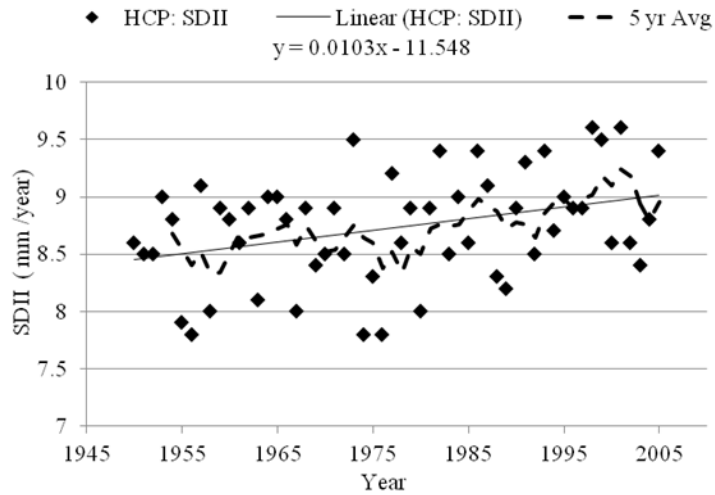


Figure 2.12: HCP regional mean time series for SDII index. Annual mean index counts were calculated and plotted over time. Linear trends are shown with solid line. 5 year moving averages were calculated and are shown with dashed line.

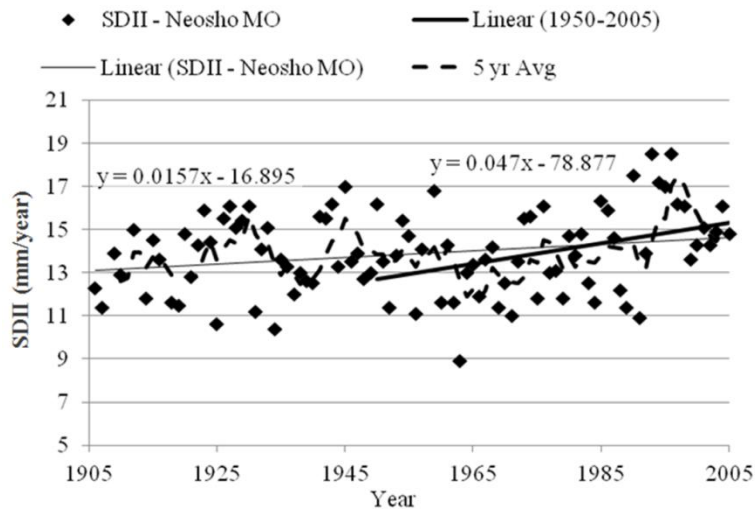


Figure 2.13: 100 year SDII time series for Neosho, MO. 1906-2005 linear trends are shown with thin solid line. 1950-2005 linear trends are shown with bold solid line. 5 year moving average shown with dashed line.

Positive trends heavily outweigh negative trends for the precipitation based indicators (Table 2.2c), which are all reporting significant regional trends during the period (Table 2.3). Significant increases in PRCPT are found throughout the region, with an average increase of 0.11 mm per year (Figure 2.9d). Increases in PRCPT over the region appear to be driven by an intensification of the hydrologic cycle. The SDII and R95P intensity-based indicators are depicting significant increases over the Humid Plains, with greater increases found in the eastern portion of the region (Figures 2.9a and 2.9c). The regional SDII mean time-series (Figure 2.12) supports the hypothesis that precipitation intensified in the region, as does the 1906-2005 analysis performed on station data from Neosho, MO (Figure 2.13). This means that more precipitation was likely delivered from heavy and extreme events, supported in part by the more moderate trends found in the R5MM index (Figure 2.9b). These findings support the work done by Pryor *et al.* (2009) who found that some of the largest positive trends for extreme precipitation events could be found in North America's central Great Plains.

Overall results indicate that the Humid Plains region has generally become wetter and warmer over the period 1950-2005, although maximum temperatures have not increased at the same rate as minimums, based on the TN90P and TX90P results. The increases in GSL may benefit this region whose economy is heavily dependent on the agricultural sector. However, the significant increases found in precipitation-based indices pose serious problems for the populations living in the Northern Humid Plains. A rise in the number and severity of heavy and extreme precipitation events places the region at an increased risk of flooding. According to Kunkel *et al.* (2003), flooding over the region has increased during the latter part of the study period. Many urban

areas and much prime agricultural land are located on the floodplains of major rivers in the region, meaning that they are directly at risk when prolonged heavy precipitation coupled with a faster spring snowmelt causes the rivers to rapidly rise. Modeled future changes in precipitation over the Humid Plains seem to vary depending on the model you look at, with a mean increase of around 5% by 2099, meaning that there is great uncertainty as to what effect global change will have on the climatology of the region (Christensen *et al.*, 2007).

2.6.4. Gulf

Between 1950 and 2005, the Gulf Region in the southeast corner of the study area experienced significant changes in both temperature and precipitation indices (Table 2d). Overall, the minimum-temperature-based FDO index is reporting significant negative trends, despite the fact that some stations in the region have experienced significant increases in the number of frost days (Table 3, Figures 6a and 7a). The TN90P index is showing more stations with significant negative trends than the FDO, although overall the average trend still suggests some moderate warming over the region (Figures 6d and 7d). In contrast, the maximum-temperature-based indices have seen strong significant negative trends throughout the Gulf region. TX90P results showed a clear majority of stations in the Gulf Region have experienced significant historical reductions in the number days exceeding the 1961-1990 90th percentile (Figures 6c and 7c). The GSL signal is by far the weakest of the temperature indices. The regional mean does depict a slight reduction in growing season length over much of the area (Figure 6b).

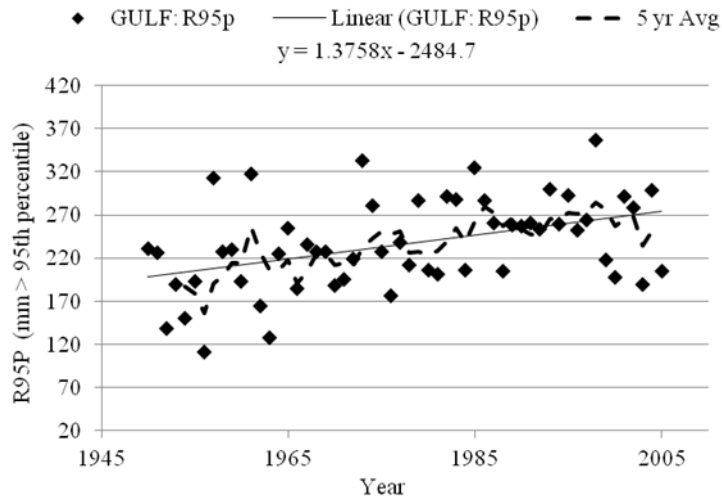


Figure 2.14: GLF regional mean time series for R95p index. Annual mean index counts were calculated and plotted over time. Linear trends are shown with solid line. 5 year moving averages were calculated and are shown with dashed line.

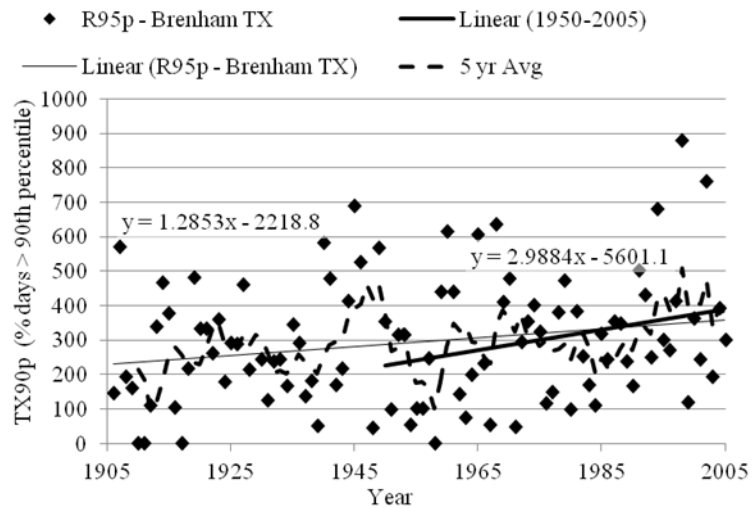


Figure 2.15: 100 year R95p time series for Brenham, TX. 1906-2005 linear trends are shown with thin solid line. 1950-2005 linear trends are shown with bold solid line. 5 year moving average shown with dashed line.

Precipitation-based trends calculated for the Gulf Region are the greatest throughout all of WNA (Table 3). Calculated trends were overwhelmingly positive across the region (Table 2d). PRCPT has increased at an average rate of 2.8 mm per year, placing the region in a class by itself. It appears this increase in annual precipitation may be due to increases in the amount of precipitation delivered by heavy events. The region is reporting the strongest significant increases in the SDII in WNA, indicating an intensification of the hydrologic cycle (Figure 9a). Trends calculated for the R5MM and R95P indices also follow the same pattern of intensification (Figures 9b and 9c). The regional time-series shows a strong trend for the R95P index (Figure 2.14), echoed by the 1906-2005 trend found at Brenham TX (Figure 2.15). Overall trends in temperature are difficult to quantify for the Gulf region.

While minimum temperatures are rising, this increase is offset by apparent declines in daily maximum temperature. Although not reporting significant trends over the region as a whole, the GSL appears to be significantly decreasing in the northern states of the region. This decrease may be connected to an increase in the number of frost days found at a number of stations in the same areas. These trends may pose a challenge for agricultural operations that could be devastated by an early or late frost. The cooling trend found in the maximum temperature index TX90P may be tied to the strong increases found in the precipitation indices. Portman *et al.* (2009) showed that the largest warming trends were found in dry areas, whereas wetter areas have experienced some negative trends in temperature. This decrease in maximum temperatures may be partially explained by increased cloudiness associated with more

precipitation and a partitioning of heat units to evapotranspiration rather than to daytime sensible heating.

The expected future mean temperature response to anthropogenic forcing in this region is about 3.5° C by 2099 (Christensen *et al.*, 2007). The increases in precipitation over the Gulf region could be caused by a number of factors, but perhaps the strongest argument could be made in favor of an increase in extreme weather events like tropical depressions and super-cell convective systems (Groisman *et al.*, 2004). Elsner *et al.* (2008) has found an increasing intensity of tropical systems originating over the Atlantic Ocean and the Gulf of Mexico which often make landfall in the region and deliver massive quantities of precipitation. This region also includes the southern portion of ‘tornado-alley’, and an increase in the frequency of intense convective storms associated with a general warming of the lower atmosphere may also be partly to blame for increases in precipitation over the southern interior of the United States. Many future climate scenarios forecast a significant reduction in precipitation over the region, while others project a continuing increase over the next century, more similar to areas in eastern half of North America (Christensen *et al.*, 2007).

2.6.5. American Southwest

The arid Southwest region is characterized by a mix of hot desert, arid steppe, and highland terrain. Trends in the temperature indices vary spatially over the region, but overall results seem to indicate a general warming (Table 2e). Similar to the other mountainous regions, very strong negative trends in the FD0 were found across the Southwest (Figure 6a). The FD0 regional average was the highest among all regions,

experiencing a reduction in the number of annual frost days of 2.7 per decade, significant at the $p < 0.001$ level (Table 3 and Figure 7a). The ASW annually averaged FDO time series also supports the argument for a significant reduction over the period (Figure 2.16). Analysis run for 1906-2005 for Fort Collins, CO shows a consistent warming trend in the FDO over the period, with an acceleration post 1950 (Figure 2.17). The TN90P and TX90P indices also displayed significant regional trends. The TN90P is strongest in the southern and western areas of the region (Figure 7d). Stations located in and around the Colorado Plateau display a significant positive trend in the TX90P (Figure 7e). Trends in GSL were positive in the western portion of the region but not strong enough overall to result in a significant regional trend, perhaps owing to the normally higher average temperatures of the region (Figures 6b and 7b).

Significant regional trends were found in 3 of 4 precipitation indices for the American Southwest (Table 3). Trends in precipitation are strongest in Utah and New Mexico, with a majority of stations in those states receiving significant increases in PRCPT (Figures 8d and 9d). In some stations, this increase in precipitation seems to be coming from an increase in the number of small events, as trends in R5MM seem to mimic PRCPT while the SDII does not (Figure 8). Groups of stations in the region have experienced significant increases in the SDII although results were too mixed for a significant regional trend to be detected. Overall, precipitation trends were relatively weak over desert areas, likely owing to the small amount of precipitation they receive per year, and the infrequent nature of big events.

Although overall precipitation trends for the Southwest indicate that the climate may have become wetter between 1950 and 2005, rising temperatures will likely negate

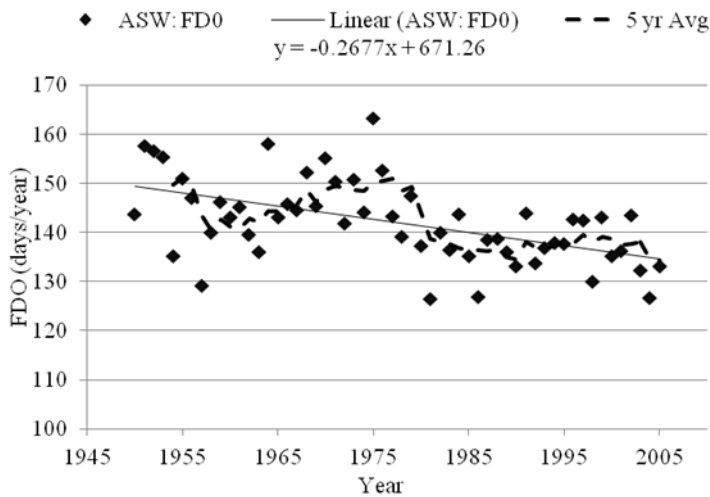


Figure 2.16: ASW regional mean time series for FDO index. Annual mean index counts were calculated and plotted over time. Linear trends are shown with solid line. 5 year moving averages were calculated and are shown with dashed line.

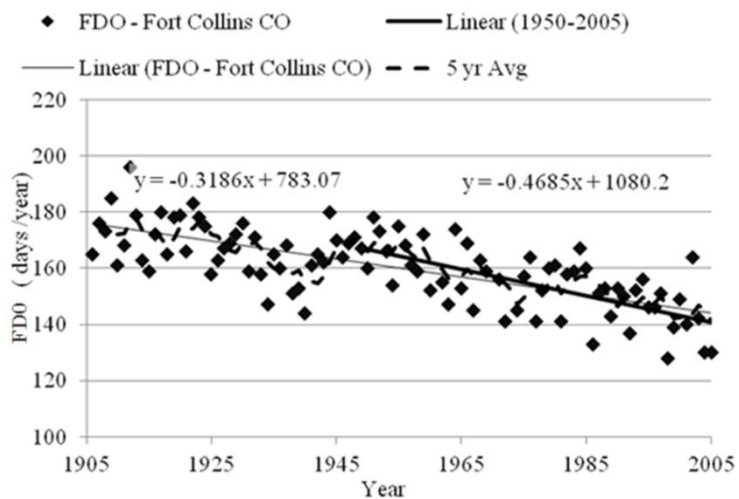


Figure 2.17: 100 year FDO time series for Fort Collins, CO. 1906-2005 linear trends are shown with thin solid line. 1950-2005 linear trends are shown with bold solid line. 5 year moving average shown with dashed line.

any positive influence for this arid region. Shorter winters, as indicated by a decline in FDO, potentially mean a shorter snow accumulation season in the mountains and

highlands that feed the Colorado River and the Rio Grande. Watersheds in the region are currently over-allocated and any further stresses placed upon them could result in a crisis (Barnett and Pierce, 2008). Additionally, the majority of modeled scenarios for precipitation show the region receiving less precipitation in the future than it has in recent history (Seager *et al.* 2007; Christensen *et al.*, 2007; Seager and Vecchi 2010). Hoerling *et al.* (2010) modeled precipitation change over regions around the globe from 1977 to 2006. The study linked SSTs in the Pacific Ocean to precipitation patterns in the American Southwest, finding negative trends that agree with the majority of modeled future projections. The difference in time period studied directly influences the contrast in trend calculated, due to sampling different phases of the PDO. It is important to note that long term natural variability in precipitation may be masking the changes expected due to anthropogenic forcing of the climate, and calculated past trends cannot necessarily be expected to continue into the future (Hoerling *et al.* 2010). Higher temperatures and projected decreases in precipitation will have a negative impact on soil moisture level, further increasing the demand for irrigation, and contributing to the desertification of some areas (Wilcox 2010). Reservoir levels in the Colorado River system are currently hovering at an all time low, running the risk of crippling hydro-electric generation and irrigation agriculture depended upon by millions living in the southwestern United States (Barnett and Pierce, 2008). While best management practices may be able to mitigate the risk of widespread system failure (Rajagopalan *et al.* 2009), current levels of development in arid areas of the region may be unsustainable, especially if warming trends continue to increase the stress on critical water resources.

2.6.6. California-Nevada

Trends indicate increasing daily minimum temperatures throughout the CNV region, which has experienced a substantial reduction of frost days (Figure 2.7a). The region displays the greatest amount of warming in WNA according to the TN90P index, with an annual average increase of 0.12% of days per year registering above the baseline 90th percentile (Table 2.3; Figure 2.7d). The regional time-series for TB90P (Figure 2.18) shows a dramatic increase in minimum temperatures, as does the 1906-2005 trend for Ukiah CA (Figure 2.19). Stations across California show a slight significant increase in GSL, especially in central and northern areas (Figure 2.6b). The maximum temperature TX90P index is more varied spatially, and as such it did not report a significant regional trend. Warming trends are most apparent for this index in Southern and Northern California as well as in California's central valley, while the central coastal area seems to have experienced a slight lowering of maximum temperatures (Figures 2.6c and 2.6d).

Precipitation trends over CNV were weaker than in other regions, with a majority of stations reporting no statistically significant trend. However, an argument can be made in favor of increasing precipitation across the region as a whole if the sign of the individual trends is taken into account (Figure 2.8d and 2.9e). This notion is based on the fact that 36 out of 40 stations in the region reported positive sign trends with respect

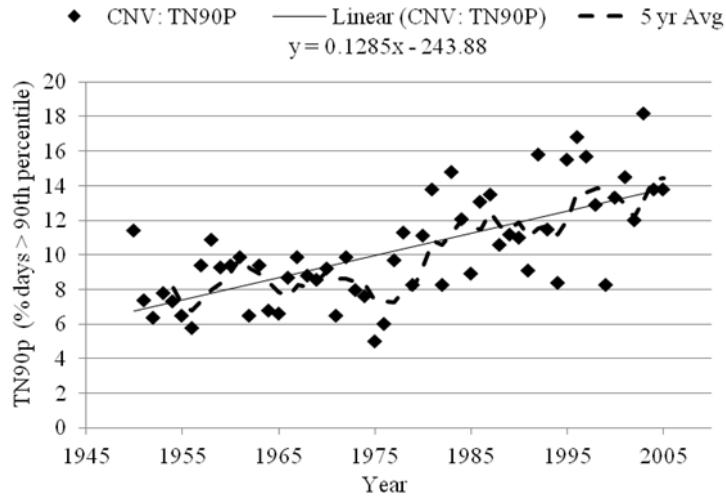


Figure 2.18: CNV regional mean time series for TN90P index. Annual mean index counts were calculated and plotted over time. Linear trends are shown with solid line. 5 year moving averages were calculated and are shown with dashed line.

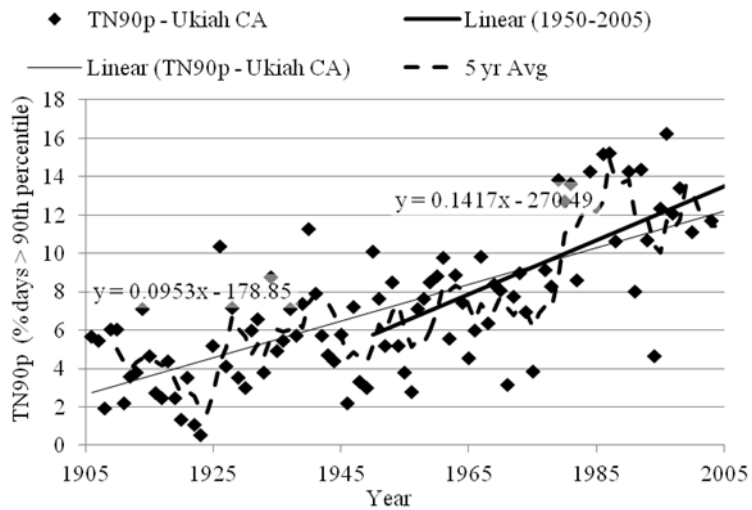


Figure 2.19: 100 year TN90P time series for Ukiah, CA. 1906-2005 linear trends are shown with thin solid line. 1950-2005 linear trends are shown with bold solid line. 5 year moving average shown with dashed line.

to PRCPT (Table 2f), and the regional mean slope of 1.01 mm per year was found to be significantly different from zero at the $p < 0.001$ level (Table 3). Similar spatial trends are found in R5MM whose regional mean is also significantly positive (Figure 9b). Although the majority of stations indicate positive trends in intensification, only a few stations in the region are reporting statistically significant trends for the intensity based indices and the regional means for the SDII and R95p indices were not found to be statistically significant.

The California-Nevada region is heavily populated and represents one of the most productive irrigation-based agricultural areas in North America. The substantial warming and no significant increase in precipitation over the region may pose a serious threat to both agricultural operations and large population. Significant positive trends were found in the extreme temperature index TX90P at stations located in the vicinity of Los Angeles in southern California (Figures 6c). Demand for power will likely continue to increase as more people seek relief from the warming temperatures (Franco and Sanstad, 2008). An increase in the frequency and intensity of wildfires in the region as a whole has been tied to rising temperatures, especially at higher elevations (Fried *et al.*, 2008; Westerling *et al.*, 2008; Miller *et al.*, 2009). Modeled forecasts for the region predict that temperatures will continue to rise and precipitation will likely decrease as part of a larger trend affecting nearly all of southwest North America (Christensen *et al.*, 2007; Seager and Vecchi, 2010). During the study period, stations in northern California have become drier and warmer, representing the southern portion of a spatially coherent trend found over Oregon and southern Washington. Central California has also experienced a significant amount of warming. As in the other

mountainous regions of WNA, the sharp decline in the number of frost days may have altered the hydrologic regime. Crops grown in the region place a very heavy demand on the water resources of the area. A decline in the availability of water supplies may make the current intensive agriculture industry in California's Central Valley unsustainable in the long term (Purkey *et al.*, 2008), and threaten hydropower operations that supply 15% of California's in-state electricity use (Vicuna *et al.*, 2008). It is clear from the results that the CNV region has already experienced substantial climatic change over the period 1950 to 2006.

2.7. Summary and Conclusion

Across the western half of North America, climate change is already well underway. Significant historical trends were found in all indices tested, although it is clear that different regions have changed in different ways over the last half century. Many regions have experienced similar changes for the indices tested, but for no index has the amount of change been uniform across WNA. One area that stands out is the Gulf Region, where the calculated mean trends are significantly different from all other regions in 7 out of 10 indices. Increasing precipitation in the Gulf region during the study period has driven this separation from the other regions. The regions that make up the western cordillera have experienced significant trends for temperature-based indices. If they continue as projected by most future models, warming trends in mountainous regions will continue to substantially alter the climatology and hydrology of the Cordillera, and the Great Plains and populated centers that receive their runoff. The problems identified in this study will likely become exacerbated in the near future,

with temperatures projected to continue increasing throughout the 21st century due to anthropogenic forcing. As the climatic zones of North America shift due to changing temperature and precipitation patterns, society must adapt in order to achieve a more sustainable future.

CHAPTER 3

MODELING THE EFFECTS OF CLIMATE CHANGE ON GLACIATED ALPINE RIVER BASINS

3.1. Introduction

Earth surface air temperatures have significantly increased over the period 1850-2008 (Solomon *et al.*, 2007). Anthropogenic influences on the atmosphere in the form of the burning of fossil fuels are contributing to the warming observed at climate stations across the globe (Karl *et al.*, 2003). It has been noted that the effects of climate change are amplified in high elevation environments (Beniston, 2003; Barnett *et al.*, 2005). Irrigated areas in western Canada are dependent on snowmelt and glacial runoff from the Canadian Rocky Mountains, which means that any climatic shifts in the high alpine region could have a profound impact on the hydrologic regime in water scarce regions downstream (Lapp *et al.*, 2002; Barnett *et al.*, 2005; MacDonald *et al.*, 2009, Kienzle *et al.*, 2011). Increasing temperatures have caused glaciers in North America to lose mass at an increasing rate (DeBeer *et al.*, 2007; Jiskoot *et al.*, 2009). This is of particular concern because of the large contribution that alpine glaciers have on late-summer stream flow, as well as their potential to significantly contribute to sea level rise (Hirabayashi *et al.*, 2010).

This literature review serves as an introduction to glacier modeling concepts and methodologies in order to determine the methods best suited for large scale simulations of glacier fluctuation in response to climatic change. An assessment of current knowledge regarding snow and ice hydrology in changing alpine environments is

presented. A brief exploration of the present state, and recent history, of alpine glaciers worldwide will place the study area in global context. Glacier response to climate change in the Canadian Rocky Mountains is examined in more detail. Progress made in recent years relating to modeling alpine hydrology, coupled with an increase in computing power, has improved forecasting tools for watershed management. Approaches to modeling snow accumulation and melt will be explored, with a focus placed on the Generate Earth Systems Science (GENESYS) hydro-meteorological model, developed at the University of Lethbridge (Sheppard, 1996; Lapp *et al.*, 2005; MacDonald *et al.*, 2009; Larson *et al.*, 2010). The GENESYS model is used in chapter 4 to model the effects of climate change on glaciers in the Upper North Saskatchewan River watershed.

3.2. Climate Change in Alpine Environments

One of the environments most susceptible to rising temperatures is the alpine cryosphere, specifically the glaciers and ice caps that store the largest quantity of fresh water on the planet. The rate of temperature change at higher elevations is generally more pronounced than in lowland areas (Hall and Fagre, 2003; Nogues-Bravo *et al.*, 2007). Further, the effects of a warming climate are stronger in cryospheric environments primarily due to movement in the 0°C isotherm across time and space. Warmer temperatures lead to an earlier onset of melt (Stewart *et al.*, 2004; Barnett *et al.*, 2005), which alters the annual hydrologic cycle bringing spring and summer conditions earlier to alpine ecosystems.

During the last century and a half, glaciers across the globe have experienced a severe decline (Figure 3.1) that is well documented in the literature (Oerlemans, 2005; Lemke *et al.*, 2007; Zemp *et al.*, 2008). A recent study by Hirabayashi *et al.* (2010) found that the global annual average glacier mass loss has accelerated since 1990, with the Sea Level Equivalent melt from glaciers increasing to 0.76 mm/yr, up from an average of 0.34 mm/yr during the period 1948 – 1989. Alpine glaciers in North America’s Rocky Mountains have been subject to the same warming trends that are driving glacier retreat around the world. In Glacier National Park, Montana, it has been estimated that over two-thirds of the glacier area that existed in 1850 had disappeared by 1980, and the ablation rate has not slowed since (Hall and Fagre, 2003). Similarly, by 1995, Peyto Glacier had lost approximately 25% of its 1966 volume, and around 60% of its 1896 volume (Demuth and Pietroniro, 2002).

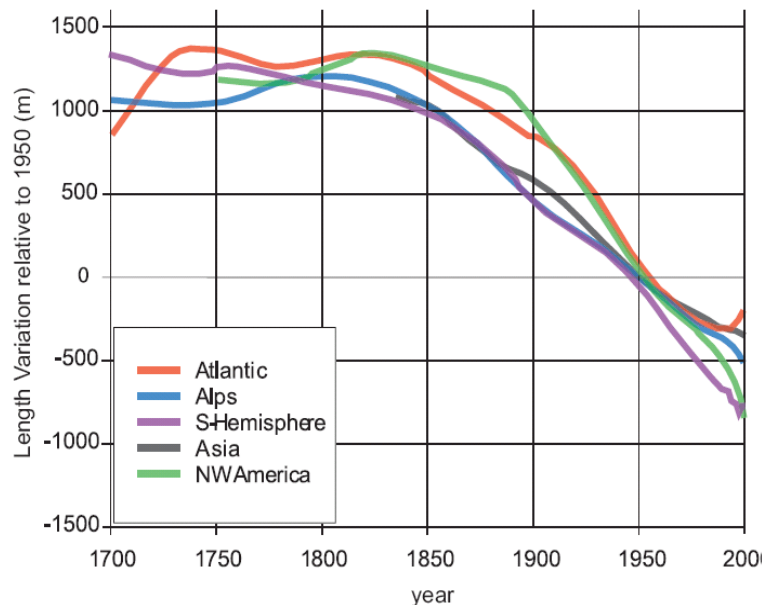


Figure 3.1: Large-scale mean length variations of glaciers across a number of global regions. (Source: Oerlemans, 2005).

Jiskoot *et al.* (2009) found that glaciers in the Clemenceau Icefield and Chaba Group, located nearby in British Columbia, retreated an average of 14 m per year in the period 1850-2001. Glaciers across North America appear to have begun receding around the same time during the middle of the nineteenth century (Luckman, 2000; Berger, 2010). The most recent maximum extent of Peyto Glacier is estimated to have occurred between 1836 and 1841, at the tail end of the Little Ice Age (Østrem, 2006). The acceleration of glacial retreat in the Rocky Mountains in recent decades has been attributed to a mid-1970s shift in the climatic regime towards a drier phase of the Pacific Decadal Oscillation (Demuth and Keller, 2006). Evidence suggests that the current rate of warming is bringing about a change in glacier mass balance in the North Saskatchewan River Basin that is unprecedented during the Holocene (Demuth and Pietroniro, 2002; Luckman, 2006; Comeau *et al.*, 2009).

Climate projections indicate that the rate of warming of global mountain systems during the next century will be greater than that observed during the last century, when glaciers in the Canadian Rockies decreased in volume by around 25% (Luckman, 2000). North America's mountain ranges are expected to experience an average warming of 2.7°C by 2055 under the most conservative emission scenario (Nogues-Bravo *et al.*, 2007). Snow water equivalent (SWE) may be reduced due to an earlier onset of spring which has already been observed in mountains across western North America (Stewart *et al.*, 2004; Barnett *et al.*, 2005; MacDonald *et al.*, 2011). Changing precipitation patterns and temperature regimes threaten to radically change the nature of watersheds in the Canadian Rocky Mountains.

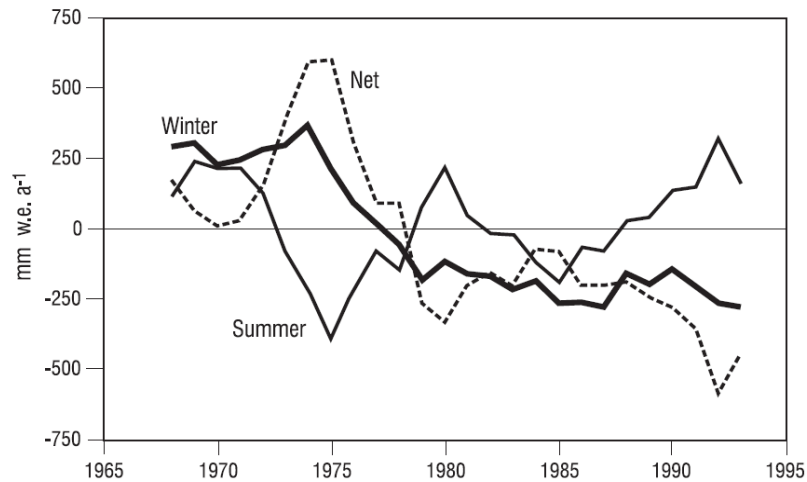


Figure 3.2: Five year moving averages of Peyto Glacier seasonal and net mass balance (Source: Demuth and Keller, 2006).

3.3. Glacier Mass Balance: Response to Climate Change

Alpine glaciers act as barometers of climatic change, responding directly to long-term changes in precipitation and temperature with changes in glacier mass balance, defined as the difference between accumulation and ablation during the hydrologic year (Cogley *et al.*, 2011). Advancing glaciers typically exhibit a long-term positive mass balance, while retreating glaciers are associated with negative values, when total ablation (melt, calving, sublimation, etc) from the glacier exceeds accumulation. Annual fluctuations in glacier mass balance are considered a direct response to climate change while glacier advance and retreat represent a cumulative and delayed response to new climatic conditions (Cogley *et al.*, 2011). In response to a change in the climate, glaciers readjust their size towards an equilibrium state where the annual net mass balance would be zero. Due to the long lag times inherent in glacial response, the state of equilibrium with their surrounding environment is likely never

attained, meaning that glaciers are almost always in a state of adjustment (Lemke *et al.*, 2007).

An important concept that deals with the response of glaciers to changes in climate is the equilibrium line altitude (ELA), which is defined as the boundary between the accumulation and ablation zones of a glacier. The ELA is often closely associated with the permanent snowline over the glacier surface. The ELA fluctuates annually with the climate, therefore controlling the mass balance gradient, which in turn controls the long-term growth or decline of a glacier (Cogley *et al.*, 2011). Determination of the ELA is necessary in many glacier modeling methodologies. When climate data or satellite imagery are not readily available, the area-weighted mean altitude can be used as a proxy for the long-term ELA, known as the ‘Kurowski’ method (Jiskoot *et al.*, 2009). Glacier areal extent can be an important determination of its sensitivity to changes in climate and associated changes in the ELA (Munro, 2006). Smaller glaciers are usually much more sensitive to changes in climate simply because they have a smaller accumulation area, extending over a limited vertical range. A projected rise in the ELA of 200-300 m for mid-latitude regions means that many small glaciers will likely disappear during the next century (Beniston, 2003).

Precipitation is a critical climate control on glacier mass balance. Glaciers are fed by winter snowfall, which transforms from snow to firn to ice over a number of years. In humid climatic regions glaciers can exist at lower elevations with higher annual temperatures, as a result of the large amount of solid winter precipitation they receive. Some glaciers in northern maritime regions may actually experience growth during periods of global warming due to changes in the precipitation regime that bring

large increases in winter mass-balance (Calkin, 1999; Berger, 2010). Norwegian and New Zealand Glaciers experienced this warming-associated growth during the 1990s, although glaciers in both areas are now conforming to the general global pattern of retreat (Hirabashi *et al.*, 2010), as the effect of warming (higher ablation) has overwhelmed the effect of increased solid precipitation (higher accumulation). Glaciated areas receiving less precipitation during the winter can be severely impacted by decreases in winter mass balance. The effect of a declining winter balance can be seen at Peyto Glacier, Canadian Rocky Mountains (Figure 1), where overall mass balance has been driven by a decline in the amount of snowfall over the glacier surface (Figure 3) (Demuth and Pietroniro, 2002; Demuth and Keller, 2006; Pederson *et al.*, 2011).

In addition to a decline in accumulation from decreasing winter precipitation, a declining winter balance can also influence the amount of summer melt, primarily due to the higher albedo values of snow versus ice. Albedo refers to the reflectivity of a surface with respect to incoming solar radiation. Higher albedo values indicate that more radiation is reflected away from the physical surface, leaving less shortwave radiation energy available to contribute to the heat budget associated with snow and ice ablation. When albedo is low, shortwave radiation is the main energy contributor to the melt budget. Decreasing winter snowpack thickness means that the ice surface of a glacier will be exposed earlier in the season, prolonging the ablation period and increasing the total amount of mass lost to summer melt (Cogley *et al.*, 2011). For this same reason, a late spring or mid-summer snowfall can induce a dramatic reduction in ablation due to an immediate increase in the albedo of the glacier surface (Hock, 2005).

As soon as glacier ice loses its snowpack, ablation increases dramatically and ice melt is able to take place (Schuster and Young, 2006). Albedo and associated absorption of incoming solar radiation are one of the most important controls on glacier melt rates (Hock, 2005). Small scale spatial variations in albedo across the glacier can cause large differences in ablation. Differences in the albedo of a glacier surface are usually due to the differential melting of snow, and the presence of sediment and rock debris in the ice (Cogley *et al.*, 2011).

3.4 Simulating Mountain Hydrometeorology

With the rapid advancements made in computing power over recent decades, it is now possible to simulate hydrometeorology over large, diverse watersheds. The ultimate goal of hydrological modelers is to construct and operate a model that simulates as closely as possible all facets of the hydrologic cycle over a large area. Because glacier mass balance is largely controlled by the amount of snow it receives annually, any attempts to model the response of glaciers to a change in climate must first ‘realistically’ simulate the distribution of Snow Water Equivalent (SWE) across the ice surface. Generally, an alpine hydrological model can be considered to have at least two components: a snow and ice accumulation/melt routine, and a routine that uses the melt generated as input to calculate runoff (Hock, 2002, Hock, 2005, Morris, 2006). If entire catchments or regions are modeled as a single unit the hydrological model is classified as a “lumped model”, where accumulation and ablation can take place simultaneously over different spatial domains. Lumped models are generally used on regional to global scale studies, such as the study done by Hirabayashi *et al.* (2010)

which modeled global glacier mass balance using a grid resolution of $0.5^\circ \times 0.5^\circ$. If a catchment is divided into multiple response units based on elevation and/or other variables, the model is classified as being “distributed”. Fully distributed hydrologic models can have many components that represent different elements operating in the hydrologic cycle over a wide range of scales. A good example of a fully distributed hydrologic model is the ACRU model, which has been employed in the North Saskatchewan Basin by Kienzle *et al.* (2011) to model the future effects of climate change on the hydrology of the watershed. The study found a clear shift in the hydrologic regime, with spring runoff coming as much as four weeks earlier.

The physically based GEnerate Earth Systems Science (GENESYS) distributed hydrometeorological model in development at the University of Lethbridge has been used to simulate snow accumulation and ablation using temperature and precipitation observations in a number of watersheds across the eastern slopes of the Rocky Mountains, including the North Saskatchewan River Basin, using limited data inputs (Sheppard, 1996; Lapp *et al.*, 2005; Macdonald *et al.*, 2009; Macdonald *et al.*, 2010; MacDonald *et al.*, *in review*). GENESYS simulates climate conditions for Hydrologic Response Units (HRUs) spread over geographically diverse terrain. The concept of the HRU allows homogenous areas with similar landcover and elevation to be grouped together to facilitate easier calculation of hydrometeorological variables within a distributed model (Kouwen *et al.*, 1993; Gurtz *et al.*, 1999; MacDonald *et al.*, 2009; Kienzle *et al.*, 2010). The assumption is made that the area within each HRU will respond in a similar fashion to climatic events. One obvious drawback of using HRUs in a distributed hydrometeorological model is that detail is lost as large areas of non-

adjacent land units are grouped together as a single entity. However, the computational efficiency of an HRU-based model may make it one of the better choices for simulating hydrological processes on a large scale by blending the computational efficiency of a lumped model with the detailed modeling routines of a distributed model.

3.4.1. Simulating Micrometeorology

In order to simulate temperature and precipitation, meteorological variables are usually extrapolated across a watershed from observed values recorded at nearby stations (Ferguson, 1999). The level of complexity chosen for simulating hydrological variables depends largely on the objectives and scale of the study. Accurately predicting climatic conditions in alpine areas is difficult because observed data are usually quite sparse due to the costs associated with monitoring programs. Climate data used to generate daily weather variables across large mountainous watersheds are typically recorded at much lower elevations than the areas of significance. However, Shea *et al.* (2009) suggests data collected at lower elevations are more likely to capture the characteristics of regional winter air masses than stations located at high elevation sites as the effects of localized orography are reduced. A number of methods have been developed to adjust temperature and precipitation values based on geographical conditions. The most common method is to use simple temperature and precipitation lapse rates defined through regression analysis, that extrapolate measured data based on relative elevation. Air temperatures generally decrease with an increase in elevation, due to adiabatic processes, based on the fact that as air density decreases, so does its ability to retain heat (Beniston, 2000). The average free-air environmental lapse rate is

6.0° C/km, meaning that air temperatures decrease by 6° C for every 1000 m increase in altitude. Lapse rates in mountain environments generally differ throughout the year, with higher rates in the summer than in the winter (Rolland, 2003). Cold-air drainage during the winter months can result in very shallow lapse rates, and in some cases temperature inversions, where temperature actually increases with elevation (Beniston, 2000; Pigeon and Jiskoot, 2008). The biggest limitation to accurately simulating air temperature is a lack of data on which to base lapse rate estimates. In addition, there are a number of climatological controls that cannot be reproduced from a simple elevation-based adjustment. Solar radiation in mountainous regions has been shown to vary considerably due to the effects of slope, aspect, and effective horizon and can have a profound effect on the temperature regime (Hock, 2005).

The GENESYS model attempts to account for the high spatial variation present in complex mountain terrain. Simulations are driven by historical climate observations extrapolated over the study area from a station in close proximity, using the GENGRID component of the model (MacDonald, 2009). Air temperature, precipitation, daily solar radiation, and humidity are simulated for HRUs based on elevation, slope, and aspect values derived in a Geographic Information System (GIS). The MTCLIM microclimate simulator, originally developed by the U.S. Department of Agriculture, Forest Service (Hungerford *et al.*, 1989) was adapted by Sheppard (1996) to simulate snowpack in the upper Oldman River basin, Alberta. MTCLIM is able to simulate microclimate hydrometeorological data for a given site, based on observed data at a base weather station. GENGRID uses MTCLIM to simulate climate data at a watershed scale through integration of the FORTRAN program and a GIS (Section 4.5).

The extrapolation of observed precipitation observations across space requires that a correction factor be applied to account for differences in the microclimatology of the site compared to the base station (Kienzle, 2011). The complex topography of mountain ranges exerts a powerful influence on the distribution of precipitation across a watershed. Perhaps the most important control on precipitation is elevation. As a result of orographic forcing, many high-elevation areas receive much more precipitation than areas in the same watershed that are located at a lower elevation. When moist air is uplifted due to obstruction by a mountain barrier, cooler temperatures at higher elevations can result in the air parcel reaching the critical condensation threshold at which point it can no longer hold water in its vapor form, thereby producing more precipitation as moisture is released from the air (Beniston, 2000). This same orographic process is responsible for the ‘rain-shadow effect’, whereby the moisture holding capacity of an air parcel increases with temperature as it descends down a slope, causing areas on the leeward side of a mountain range to receive far less precipitation than areas on the windward side. This effect is particularly discernible along the W-E gradient crossing the Canadian Rocky Mountains, as moist air is usually associated with westerly winds from the Pacific Ocean source region (Lapp *et al.* 2002). Sheppard (1996) and Lapp (2005) used simple linear regression based on elevation and published isohyet maps for the study region. Simulation of precipitation was relatively weak, owing in large part to the crude precipitation-elevation relationship used to interpolate values over diverse terrain (Sheppard, 1996).

In an effort to better account for the distribution of climate variables across complex mountainous terrain, MacDonald *et al.* (2009), Kienzle *et al.* (2011), and

MacDonald *et al.* (in review) utilized *Parameter-elevation Relationships on Independent Slopes Model* (PRISM) datasets (Daly *et al.*, 2008) in their studies. PRISM surfaces are gridded GIS datasets that report 1971-2000 monthly normals for precipitation, maximum and minimum temperature. The model generates the 2 km gridded datasets by taking elevation, location, aspect, and a number of other variables into account to provide realistic predictions of the monthly climate normals. Use of PRISM output allows each HRU to be assigned a unique ‘normal’ monthly precipitation value, from which relationships between the base station and the specific HRU can be made. Monthly lapse rates for minimum and maximum temperatures can also be derived from the PRISM grids, which have been deemed to be more accurate than simply adopting a static rate for use throughout the year (Kienzle *et al.*, 2011). The performance of the GENESYS model improved significantly when PRISM data was used (MacDonald *et al.* 2009) compared to earlier studies where it was not employed (Sheppard, 1996; Lapp *et al.*, 2005).

3.4.2. Simulating SWE and Mountain Hydrology

A snowmelt algorithm, developed by Pipes and Quick (1977), was adapted within GENGRID to simulate snowpack ablation across the watershed using simple daily maximum, minimum, and mean air temperatures (Sheppard, 1996; MacDonald *et al.*, 2009). GENESYS model development was continued by Lapp *et al.* (2005), where improvements in computing power allowed for an increase in complexity over previous simulations. GENGRID was modified to include a sublimation sub-routine originally modified by Dery *et al.* (1998) from the method developed by Thorpe and Mason

(1966). General Circulation Models (GCMs) were utilized in an attempt to simulate future snowpack conditions under a range of possible scenarios. Results showed a substantial decline of maximum SWE in the upper Oldman River watershed for the selected future climate scenarios (Lapp *et al.* 2005).

Subsequently, MacDonald *et al.* (2009; 2010) and Larson *et al.* (2010) increased the ability of GENESYS to simulate hydrometeorological variables across the physically diverse Upper St Mary watershed, located in Glacier National Park, Montana. Larson *et al.* (2010) refined the capabilities of the model to account for rain on snow events, to model snowmelt and rainfall runoff, and compare these to observed stream discharge at the watershed outlet. MacDonald *et al.* (2009 and 2010) introduced a number of elements to better simulate hydrology over a large, diverse watershed:

- A new method was incorporated to seasonally vary the precipitation-elevation functions used in previous applications (Figure 3.3).
- HRUs were redefined based on land cover and elevation to better represent the spatial variability over the St. Mary River watershed.
- A new method developed by Kienzle (2008) to partition precipitation between rain and snow based on air temperature was included to improve SWE simulations.
- Soil moisture storage capability was built into the GENESYS model and canopy interception was also taken into account to improve runoff comparisons.

When the snowpack in a given terrain category is exhausted, the model switches to simulate soil moisture. Using this improved GENESYS Model, the potential impacts of

climate change on SWE distribution were explored by downscaling an ensemble of GCM scenarios to simulate future climate on a watershed scale (MacDonald *et al.*, 2010). The study found statistically significant reductions of future SWE due to climatic warming and an earlier onset of spring. Overall, GENESYS was able to reasonably simulate snowpack accumulation and melt over the mountainous St. Mary Watershed.

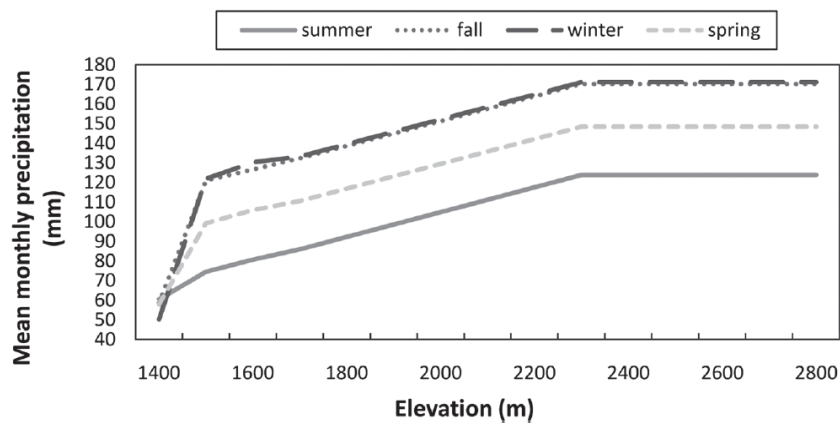


Figure 3.3: Mean monthly changes in precipitation as a function of elevation and season (Source: MacDonald *et al.* 2009).

Recently, the GENESYS model was employed in the upper North Saskatchewan River watershed (MacDonald *et al.* (in review)). This watershed, with an area over 20,000 km², is significantly larger than the basins previously simulated by the model. Due to the large size of the study area, the number of HRUs was increased to 997, compared to the 82 used by MacDonald *et al.* (2009; 2011) in the upper St Mary River watershed. Historical SWE was simulated for all HRUs (Figure 3.4) and GCM scenarios were applied to simulate potential future change in the watershed (expand

discussion on GCM future scenarios). The study found that the greatest changes in the amount and timing of maximum SWE were at higher elevations (MacDonald *et al.*, (in review)). This finding presents a number of concerns over how the glaciers that feed the headwaters of the North Saskatchewan River will react to a rapidly changing climate.

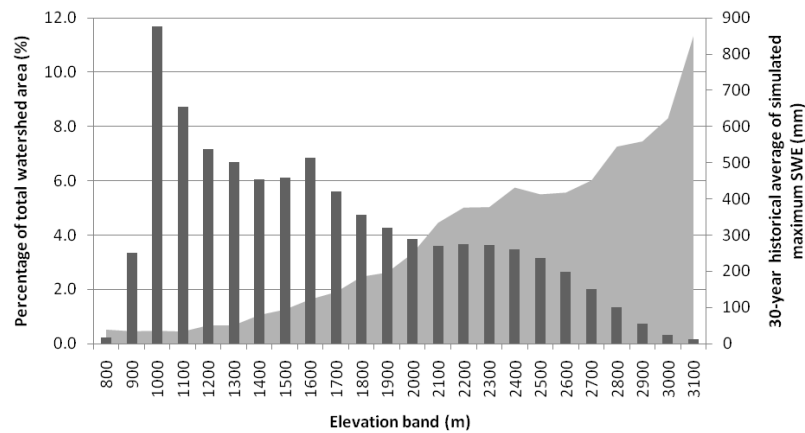


Figure 3.4: Upper North Saskatchewan River watershed elevation-area distribution and associated historical average of simulated maximum SWE (Source: MacDonald *et al.*, (in review)).

3.5. Modeling Glacier Mass Balance

To better capture hydrologic change over time in a glaciated watershed, fluctuations in ice volumes must be quantified by incorporating a glacial mass balance routine into a distributed hydrometeorological model (i.e. GENESYS). There are normally two stages in the modeling of glacier response to climate change. The first stage is the calculation of the short term mass balance over the glacier area, known as the static response, and includes calculations of annual snow accumulation and total snow and ice ablation over the glacier surface. The second stage is the determination of

long term changes in glacier area and volume that result from fluctuations in mass balance, known as the dynamic response (Braithwaite and Zhang, 1999; Raper and Braithwaite, 2009).

3.5.1. Static Response: Temperature Index Models

A distinction between glacier models can be made based on how snow- and ice-melt is calculated. Simple Temperature Index (TI) models, also known as degree-day models, are based on empirical relations between melt and air temperature, generalizing a very complex process by using a melt factor representing the amount of melt normally generated by a given air temperature (Hock, 2005). TI models have proven to be very effective for catchment sized studies, due in large part to their modest data requirements (Shea *et al.*, 2009). The assumption is made that there is an empirical relationship between air temperature and the amount of melt, based on the high correlations found between air temperature and the variables used in the energy balance equation. The melt factor used in TI models is usually expressed in terms of the amount of daily water equivalent (mm) melted per 1° K increase of temperature above freezing (Hock, 2005). Melt factors used for the estimation of ice ablation are often higher than the ones used to model snow melt, largely due to the lower albedo values of sediment-laden glacier ice which absorbs and retains more solar energy than the ice matrix. Shea *et al.* (2009) found melt factors for snow in Western Canada to range from 2.32 to 3.62 mm °C⁻¹ d⁻¹, and 3.61 to 5.57 mm °C⁻¹ d⁻¹ for ice (Table 3.1). Melt factors calculated for snow and ice at Peyto Glacier were 2.32 and 5.57 respectively. Melt factors were found to be

relatively consistent across a number of glaciers across western Canada, generally agreeing with values found in previous studies (Hock, 2005; Stahl *et al.*, 2008)

TI models are by far the most widely used method of simulating ablation. However, use of the TI method can vary depending on the spatial and temporal scale of the simulation. The past decade has seen many studies involving TI modeling of glacier mass balance. Braithwaite and Zhang (1999) applied a simple degree-day model to 37 glaciers around the globe, focusing mainly on Storglaciären, Sweden. The study showed that degree-day models can perform reasonably well for regional or global studies, which is ideal due to the lack of data in mountain environments. More recently, Hirabayashi *et al.* (2010) calculated glacier mass balance on a global scale using a simple degree day approach for the period 1948 - 2006. Monthly mass balance was calculated for $0.5^{\circ} \times 0.5^{\circ}$ grid cells treating all glaciers within the cell as one. The coarse resolution used in this study prevented detailed examination of local or regional impacts of climate change on glaciers. However, the model performed well on a global scale, providing good estimates of glacier loss for the period 1948 to 2006 when compared to observed values (Hirabayashi *et al.*, 2010).

Table 3.1: Melt factors for snow (k_s) and ice (k_i) determined for a number of glaciers in western Canada (Source: Shea *et al.*, 2009).

Glacier	k_s mm °C ⁻¹ d ⁻¹	k_i mm °C ⁻¹ d ⁻¹	R^2	n	S_T m w.e. a ⁻¹ K ⁻¹
Bench	2.81	4.17	0.80	52	-0.43
Bridge	3.21	4.22	0.86	94	-0.55
Helm	3.62	5.27	0.65	35	-0.56
Peyto	2.32	5.57	0.90	239	-0.49
Place	2.71	4.69	0.81	165	-0.55
Sykora	3.27	4.22	0.84	37	-0.54
Tiedemann	2.97	4.79	0.83	67	-0.54
Woolsey	3.21	4.58	0.75	67	-0.45
Zavisha	3.23	3.61	0.37	28	-0.52
Mean	3.04	4.59			-0.51

3.5.2. Static Response: Energy Balance Method

Energy Balance (EB) models usually involve much more complex melt routines because they incorporate the full range of factors to calculate the energy balance at the Earth's surface. Many additional climate variables are needed to simulate ablation based on the energy balance of the snowpack (Hock 2003; Morris 2006). EB methods take into account all possible heat fluxes to and from the surface that can influence melt in snow or ice. The full energy balance (*EB*) for melt calculations can be expressed as (Hock, 2005):

$$EB = Q_n + Q_h + Q_l + Q_g + Q_r - Q_m \quad [\text{Eq. 3.1}]$$

where Q_n is net radiation, Q_h the sensible heat flux, Q_l the latent heat flux, Q_g the ground heat flux, Q_r the sensible heat flux supplied by rain, and Q_m the energy consumed by melt. EB models have been shown to perform very well for simulating mass balance and runoff at daily and even hourly intervals (Hock, 2005). However, as

stated above, EB models have very intense data requirements which are only available for a small number of glaciers around the world, making the method unsuitable for large scale simulations.

One of the most important controls on the heat fluxes associated with the glacier surface energy balance melt is the amount of shortwave and longwave radiation at the ice/snow surface (Hock, 2005). Ice and snow melting can occur even when the air temperature is below freezing. Föhn (1973) reported results from Peyto Glacier indicating as much as 20% of daily melt took place as a direct result of incoming short-wave solar radiation. The amount of radiation received by a glacier surface varies over time and space. The albedo values on a glacier can range from between 0.1 for very dirty ice near the glacier terminus, to 0.9 for areas with freshly fallen snow (Hock, 2005). The modeled reflectivity parameters for snow and ice albedo in glacier models are often treated as constants across the glacier surface. Snow albedo values are replaced by the lower albedo value for ice as soon as the overlying snowpack has been removed (Hock, 2005). Oerlemans and Fortuin (1992) suggests the incorporation of an albedo parameterization based on the assumption that albedo on a glacier will increase with altitude, owing to concentration of debris in the ablation zone and cleaner ice and permanent snow at higher elevations. The low albedo values and high thermal capacity of bare rock surfaces usually result in the end-of season snowline on terrain surrounding glaciers being at much higher elevations than the snowline on the glacier surface. This is due to a combination of low albedo, high longwave radiation, high sensible heat, that result higher air temperatures and faster melt (Schuster and Young, 2006). Wei *et al.*

(2010) found that debris cover on a glacier surface can cause an increase in ablation of up to 59%, compared to areas assumed to be debris-free.

3.5.3 Dynamic Response of Glaciers

Long term fluctuations in the areal extent and mass balance of glaciers represent a cumulative and dynamic response to changes in climate. The response time to a change in climate largely depends on a glacier's size and its geographic position, and ranges from decades for small alpine glaciers to centuries for large icefields and millennia for ice sheets (Lemke *et al.*, 2007). Glacier hypsometry, defined as the distribution of terrain area over elevation, is the topographical, hence local, component, and may also play a large role in determining a glacier's annual response to a change in climate (Jiskoot *et al.*, 2009). Factors such as the slope, the longitudinal profile, and the hypsometry of a glacier all determine the rate at which climate perturbations propagate through the system (Oerlemans, 1989). Ice moves downslope through the force of gravity, largely at a rate determined by the thickness of the ice mass and the slope of the ice surface. In this way, accumulation areas at higher elevations supply ice volume to ablation areas at lower elevations, allowing a glacier to maintain a steady long-term mass balance through its dynamic component (ice flow). Any attempts to model the dynamic response of glaciers to climate change must take this redistribution of ice volume into consideration, even if ice flow models are not directly incorporated.

3.5.4. Estimating Glacier Volume

Modeling the dynamic response of a glacier to climate change requires initial ice area and volume distributions from which to calculate mass balance as it gives a starting value from which to add or subtract annual calculations. Due to a lack of observational measurements of ice thickness on the majority of glaciers world-wide, volume often has to be estimated based on the areal extent of the glacier surface (Bahr *et al.*, 1997). Similarly, it is possible to estimate changes in glacier area based on simulated mass balance changes in volume. The use of remotely sensed data is becoming increasingly important for the estimation of snow and ice cover in regions where data availability is sparse. Based on the work of Chen and Ohmura (1990), Bahr *et al.* (1997) observed relationships between area and volume for 144 glaciers world-wide (Figure 3.5). DeBeer and Sharp (2007) used an empirically derived exponential method adopted from Bahr *et al.* (1997) to approximate the volume of glacial ice in the southern Canadian Cordillera. Glacier extent was determined from Landsat 7 satellite imagery for September 2002, and from historical air photos acquired in the 1950s and 1960s. Volumes were then calculated to estimate the amount of change experienced by the glaciers during the study period. Area-volume scaling was also used by Stahl *et al.* (2008) to model glacier mass balance and associated streamflow in a small alpine watershed in British Columbia. Their initial glacier volumes were estimated based on 2005 glacier areas, and their mass balance was simulated based on these initial estimations, and area was recalculated using the same equation based on future modeled Ice Water Equivalent (IWE). Their results suggest the glacier-volume scaling process performed well in estimating initial glacier volumes for use in hydrological models

investigating the impacts of glacier change. The ability to reasonably estimate the volume of IWE present in glaciers is crucial to regions that depend on their runoff.

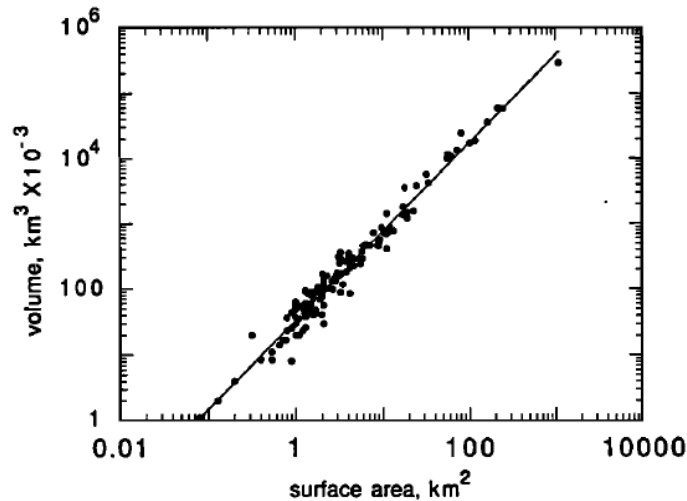


Figure 3.5: Surface area vs. glacier volume for 144 glaciers world-wide, plotted on a log-log scale. (Bahr *et al.* 1997).

A different method to estimate the IWE volume in alpine glaciers was developed by Marshall *et al.* (2011), who modeled the future mass balance through 2100 of glaciers on the Eastern Slopes of the Canadian Rocky Mountains. Results obtained using the area-volume scaling method were compared to results using a novel method that estimates depth based on the slope of the glacier surface. The estimation of glacier depth using the slope of the surface is based on the maximum shear stress that glacier ice can withstand before it is forced to flow downslope under the force of gravity. The principle is that the depth of ice decreases as the angle of slope increases across a glacier surface. Marshall *et al.* (2011) derived estimates of volume using a glacier-averaged slope-thickness and found that they compared well with estimates made using

the traditional area-volume scaling approach. The benefit in using a slope-based estimation is that the area-volume scaling method tends not to be as accurate when applied to individual glaciers, but is better suited to estimating IWE volume on a regional basis.

3.5.5. Glacier Runoff

Glacier runoff models add another component to the accumulation and melt routines developed to model ice- and snowmelt. One critical reason to model runoff from glaciers in a changing climate is to determine when they will reach their peak annual melt water discharge, or if in fact the peak has already passed. By comparing historical glacier melt to measured runoff it is possible to gauge how changes in mass balance will affect streamflow levels in glacierized basins. Ye *et al.* (2003) modeled the response of glaciers to climate change in western China. The study showed that emergence and magnitude of peaks in glacial runoff depend on both the size and hypsometry of the glacier and on the rate of warming. Runoff peaks were found to be higher and occurred earlier with a rapid simulated rise in temperature.

DeBeer and Sharp (2007) report that the ability of glaciers to moderate low flow periods in the North Saskatchewan River is already in decline. Similar studies have reported that the majority of glaciated basins in British Columbia may too already be past the peak discharge from glaciers (Stahl *et al.*, 2008; Moore *et al.*, 2009). Glaciated basins have a distinct annual hydrograph compared to watersheds with no glacier cover. Glacier fed streams generally have a lower winter and spring discharge with enhanced flow during the summer and early fall due to the melting of ice and the delays

associated with a glacial system (Comeau *et al.*, 2009). The incorporation of a glacier routine in a hydrologic model substantially increases the complexity, due to the lag times associated with runoff on, through, and under the glacier. In many ways, the hydrology of a snowpack operates much like an extra layer of soil, except that its thickness and extent may vary throughout the year (Morris, 2006). When the snowpack melts over a glacier, runoff enters the glacial system where it can remain for a substantial period of time. Time lags present in glacial runoff systems include melt storage within snowpack and firn, standing water stored in surficial holes on the ice surface, and poorly formed englacial drainage structures (Schuster and Young, 2006; Harper *et al.*, 2010). A model with a glacier drainage component may attempt to describe this process and better represent delays in the system, either as a physically based distributed model that traces the flow of water through the ice, or a lumped model that treats the entire glacier as a single reservoir (Morris, 2006). Delays in meltwater runoff are usually more pronounced early in the season, before runoff channels in the system are fully developed. A reduction in firn over the glacier associated with warming temperatures and declining SWE inputs may amplify the amount of runoff from a glacier, as the storage capacity of the system is reduced (Demuth and Pietroniro, 2002).

3.6. Summary and Conclusions

Anthropogenic warming of the earth is projected to continue well into the twenty-first century (Solomon, 2007). The declines seen in glaciers around the world during the twentieth century serve as a stark indicator of the rapid change experienced

by the global climate system. Many watersheds have already passed the peak phase of glacial discharge and may now be entering a phase of continued steady decline in glacier streamflow contribution (Moore *et al.* 2009). However, it has been suggested that some areas, such as the upper North Saskatchewan River Basin may actually see a resumed phase of enhanced glacial runoff if large alpine ice fields with top heavy hysometries (Clemenceau, Columbia, etc.) become subject to melt due to a further rise in ELA (Demuth and Pietroniro, 2002). The incorporation of a glacier mass-balance routine within an existing hydrologic model will allow for previously developed methods of SWE accumulation to be used to model the effects of potential future climate change on glaciers. Due to limitations in available data, the most widely applicable method for modeling snow and ice ablation remains the temperature index method. Variants of this method have been shown to approximate mass balance almost as well as the more complex energy balance methods. Distributed hydrologic modeling of these crucial alpine watersheds represents a powerful tool that must be employed by human populations that depend on the seasonal runoff from snow and ice melt.

CHAPTER 4

DEVELOPMENT AND APPLICATION OF A GLACIER MASS BALANCE MODEL IN THE UPPER NORTH SASKATCHEWAN RIVER BASIN

4.1. Introduction

Since the end of the Little Ice Age in the mid to late 19th century, the climate of the earth has been warming at a rate likely unprecedented during the Holocene (Solomon *et al.*, 2007). Sustained increases in temperatures have had a dramatic effect on the Earth's cryosphere, causing a reduction in ice sheets, ice caps, and glaciers around the world (Lemke *et al.*, 2007). Irrigated areas in western Canada are dependent on snowmelt and glacial runoff from the Canadian Rocky Mountains. Historically, glacier melt contributes ~3% annually to the Saskatchewan River system, and up to 27% during hot dry summers when rivers are at low flow (Comeau *et al.*, 2009). Glacier contributions to streams and rivers in upper headwater regions are typically much higher. Continued alpine warming and an associated reduction in glacier ice volumes on the eastern slopes of the Canadian Rocky Mountains will likely have a profound impact on the hydrologic regime in water scarce regions downstream, and aquatic ecosystems in headwater regions like the Upper North Saskatchewan River Basin (UNSRB – Figure 4.1).

The objective of this study was to develop a mass balance glacier model for incorporation within the GENErate Earth SYstems Science (GENESYS) physically-based hydrological model developed at the University of Lethbridge (Sheppard, 1996; Lapp *et al.*, 2005; MacDonald *et al.*, 2009; Larson *et al.* 2011) with the goal of

modeling the effects of climate change on the glaciers in the UNSRB. The FORTRAN-based GENESYS model was previously used in watersheds on the eastern slopes of the Rocky Mountains to simulate daily hydro-meteorological processes at a high resolution (~100 m) over complex terrain, focusing on modeling snow water equivalent and soil moisture conditions. Glacier model development was focused on creating a new, simple yet dynamic, model routine that could be applied to individual glaciers across the UNSRB. Historical glacier mass balance was modeled and compared to observed records at Peyto Glacier to determine the operational capability of the model. Future mass balance in the UNSRB was simulated using downscaled GCM ensembles, applied to the model to predict changes in UNSRB glacier volume under a range of climate scenarios. Results include time series of changes in glacier mass balance and hydrologic response to changing ice volumes up to 2100.

4.2. Study Area

The primary area of focus for this assessment is the watershed of the Upper North Saskatchewan River, which forms part of Canada's hydrologic apex on the continental divide. The study basin (3858 km²) feeds the North Saskatchewan River, which flows northeast from its headwaters on the eastern slopes of the Canadian Rocky Mountains, through Edmonton, Alberta (Figure 4.1), representing a crucial portion of the headwaters of the Nelson watershed that spans the interior of the continent and empties into Hudson's Bay over 1500 km away. The upper watershed study area is dominated by mountainous terrain, ranging in elevation from about 1200 to 3500 meters above sea level (m a.s.l.). The Bighorn Hydroelectric Dam, built in 1972, created

Abraham Lake and serves as the outlet for the study watershed. Although this area makes up only around 14% of the total watershed area above Edmonton, it is responsible for about 40% of average annual streamflow due to the large volume of water derived from snow and glacier melt (Kienzle *et al.* 2011). The climatic regime can be characterized as continental, experiencing cold dry winters with wetter summers. The hydrology of the area is snowmelt-dominated with peak flows usually occurring in late spring to early summer.

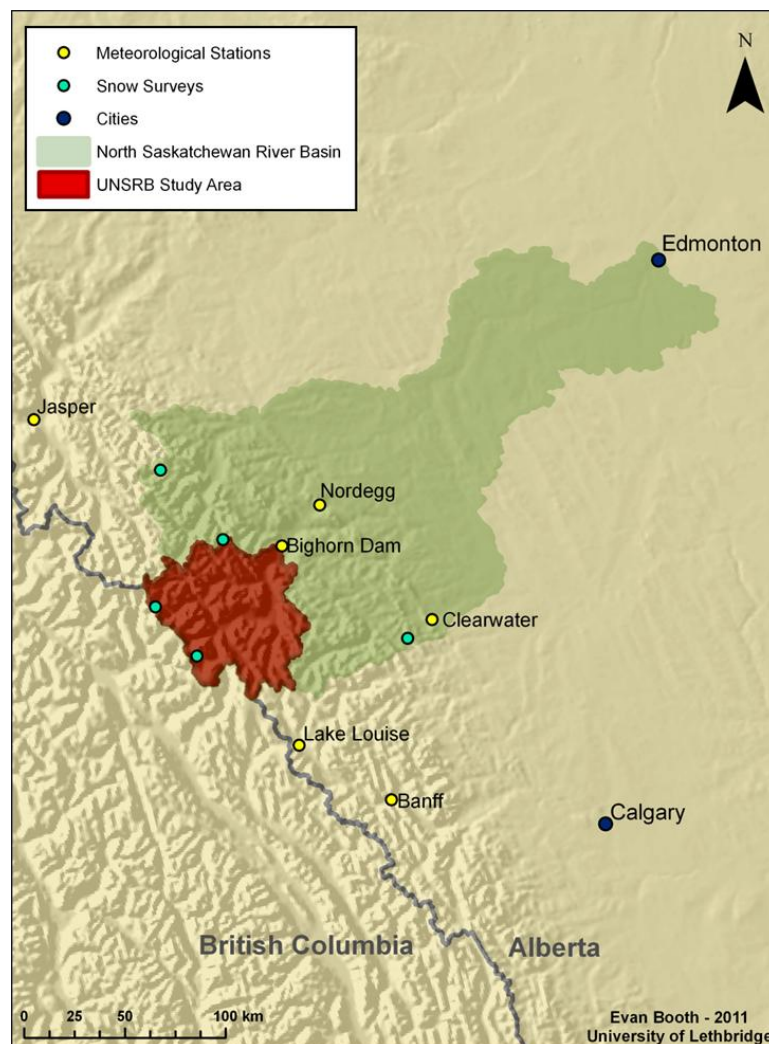


Figure 4.1: Study Area Map for the North Saskatchewan River Basin above Edmonton, Alberta.

The UNSRB is approximately 7% glaciated and includes 73 continuous ice masses (ice divides have not been separated) (Figure 4.2). The glaciers include outlet, valley and mountain glaciers. Outlet glaciers from the Columbia Icefield (e.g. Saskatchewan Glacier) and Peyto Glacier have been extensively studied since the 1950s (Østrem, 2006). Peyto Glacier is located in the southernmost portion of the UNSRB, sharing an ice divide with Bow Glacier in Banff National Park. The glacier serves as a “benchmark” for glaciers on the eastern slopes of the Canadian Rocky Mountains, chosen because of its relative ease of access, average size, and hypsometry representative of other glaciers in the area (Østrem, 2006). Detailed mass balance measurements were made at Peyto Glacier from 1966-1995 (Demuth and Keller, 2006), and yearly measurements continue to the present. These records have been used by numerous studies to gain understanding of how glaciers in this portion of the Rocky Mountains respond to changes in climate (DeBeer and Sharp, 2007; Shea *et al.*, 2009; Marshall *et al.* 2011). Because they represent the only long-term data available in the UNSRB, the published mass balance observations from Peyto Glacier have been relied on in this study for the calibration and verification of the model. The long-term Equilibrium Line Altitude (ELA) is at approximately 2700 m a.s.l., which is in the upper portion of the area-elevation distribution of the UNSRB (Figure 4.3). The fact that the majority (~63%) of the glaciated area in the UNSRB is situated below the Peyto Glacier ELA likely indicates that overall the glaciers in the basin are currently receding due to a long-term negative glacier mass balance.

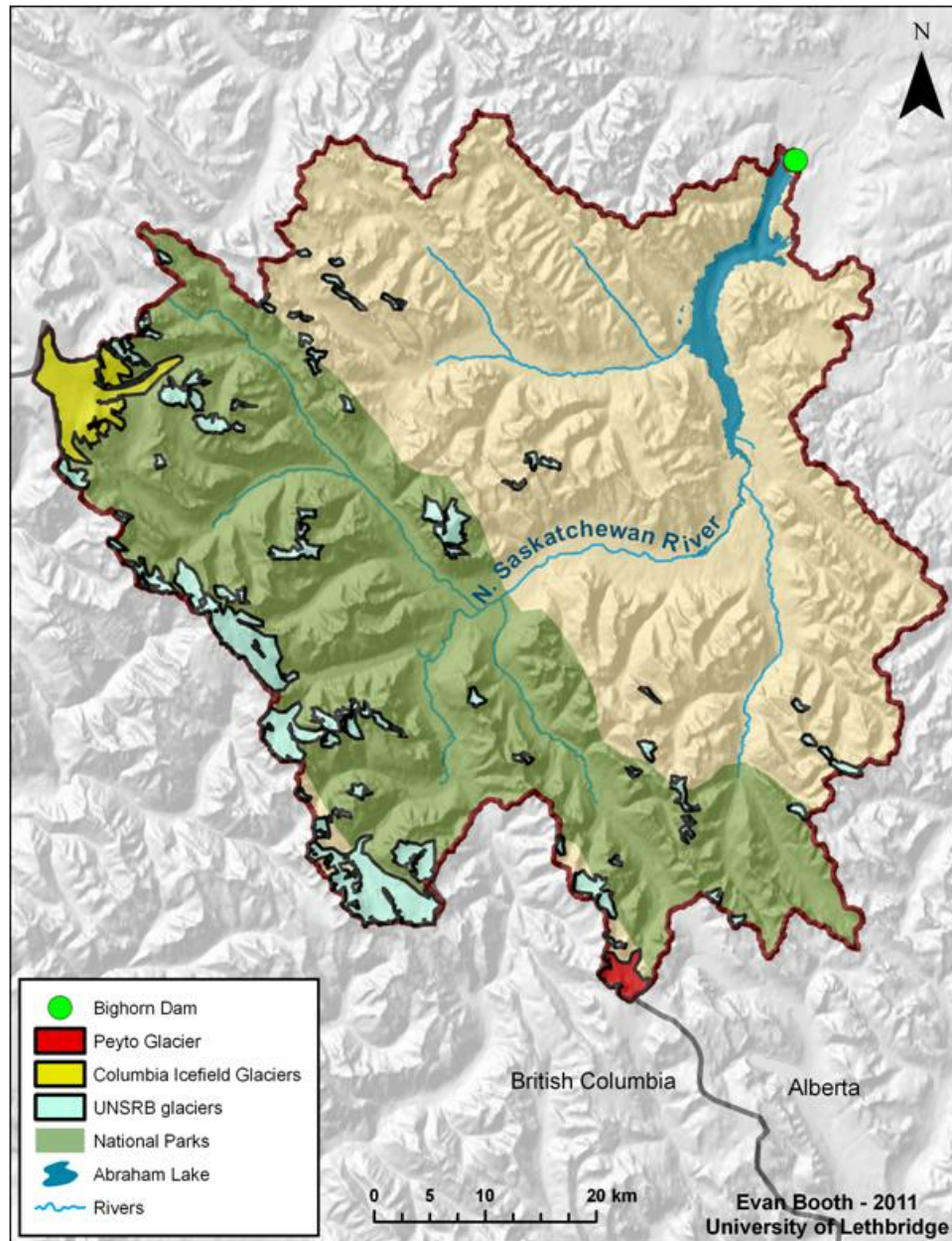


Figure 4.2: Study Area Map for the UNSRB

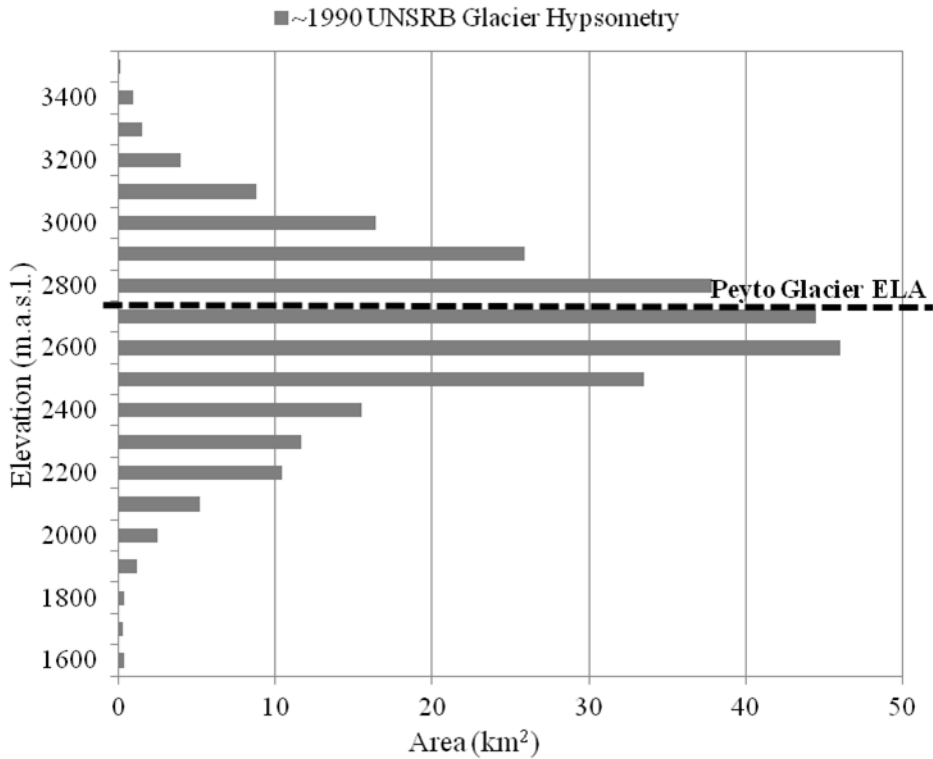


Figure 4.3: Area-elevation distribution of glaciers in the UNSRB.

4.3. Methods: Meteorological Data

Operation of the GENESYS modeling routine requires a meteorological driver station located within, or in close proximity to, the study area to extrapolate daily air temperature and precipitation across the watershed. Meteorological data dating from 1960-2010 were downloaded for stations in close proximity to the UNSRB (Figure 4.1) from Environment Canada’s website (www.ec.gc.ca). Recent hydrologic modeling efforts in the UNSRB by Kienzle *et al.* (2011) and MacDonald *et al.* (in review) employed a driver station located at Bighorn Dam (Figure 4.2), with data gaps in-filled from nearby stations using linear regression. Despite the reasonable performance of the Bighorn Dam station in the previous studies, a change in focus towards glaciers found

at high elevations in the basin necessitated a sensitivity analysis, comparing a number of nearby climate stations with long-term records to the observed mass balance measurements made at Peyto Glacier between 1966-1995 (Demuth and Keller, 2006).

The GENESYS model was originally designed to operate using a combination of precipitation driver stations as it was shown to be more representative of spatial precipitation trends over a basin (Sheppard, 1996). Lapp *et al.* (2005) used only one precipitation station to drive the model and efforts since then have operated in a similar fashion (MacDonald *et al.*, 2009; MacDonald *et al.*, 2011). For this study, the possibility of utilizing two stations to drive the model was revisited in an attempt to better represent precipitation at high elevations across the watershed by incorporating the regional climatology. A hybrid precipitation driver was created by combining the daily precipitation between two stations. It should be noted that the use of two climate records to drive precipitation across the watershed results in a loss of daily resolution due to an enhanced frequency of daily precipitation, as precipitation events at either station are represented in the model input. However, this was deemed acceptable if the monthly and annual performance improved, especially since the objective was to model changes over long time periods. To create the hybrid precipitation driver station, daily precipitation records from Lake Louise and the infilled Bighorn station (Kienzle *et al.* 2011) were averaged. The 30 year monthly normals for precipitation at Bighorn Dam and Lake Louise are presented in Figure 4.4. Bighorn-Lake Louise Hybrid (BLH) station data were evaluated in a sensitivity analysis along with other potential driver stations. Winter precipitation (October through April) was tested against the observed winter balance (~May 1 accumulation) at Peyto Glacier. Results of the study are shown

in Table 4.1. Bighorn Dam, Banff, and Lake Louise performed the best with Pearson correlation coefficients of 0.493, 0.582, and 0.672 respectively, all significant at the $p < 0.01$ level. Results show that the total annual winter precipitation derived from the BLH driver station had the highest Pearson's correlation with the observed data at 0.748, significant at the $p < 0.01$ level.

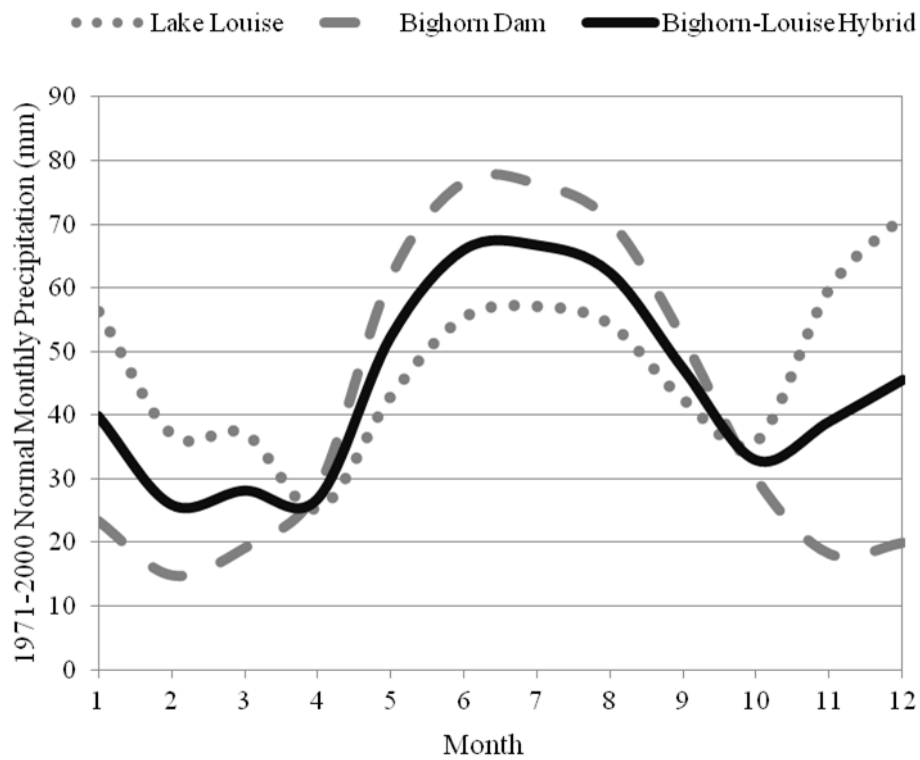


Figure 4.4: Driver station average monthly precipitation (1971-2000).

Table 4.1: Correlation analysis results comparing observed winter mass balance at Peyto Glacier with total winter precipitation (Oct –Apr) at stations in proximity to the UNSRB.

Meteorological Stations	Pearson Correlation	Sig. (2-tailed)
Nordegg	0.461*	0.014
Clearwater	0.131	0.505
Jasper	0.317	0.100
Bighorn	0.493**	0.008
Banff	0.582**	0.001
Louise	0.672**	0.000
Bighorn-Louise	0.748**	0.000
* p < 0.05 (2-tailed).		
** p < 0.01 (2-tailed).		

Kienzle *et al.* (2011) and MacDonald *et al.* (in review) used a number of high elevation snow surveys for model calibration and verification, obtained from Alberta Environment (Figure 4.1). To further determine the suitability of the BLH station driving the model, annual winter precipitation was tested against observed snow water equivalent (SWE) from snow surveys using bivariate correlation. As above, annual winter precipitation totals from other stations in the regions were also tested to provide a comparison of performance in relation to BLH. Results of the sensitivity analysis are shown in Table 4.2. BLH showed significant ($p < 0.01$) correlations at all 5 snow surveys tested, and had the highest correlation at 0.627 when tested against an annual average computed for all the surveys. Based on these results, the BLH station was chosen to drive simulations in the UNSRB as it was deemed the most representative of winter precipitation on a basin-wide scale.

Table 4.2: Correlation analysis results comparing observed ~May 1 SWE totals at snow surveys with stations in proximity to the UNSRB.

Pearson Correlations						
Stn. / Survey	Avg SWE	Golden Eagle	Job Creek	Limestone Ridge	Southesk	Watchman
Bighorn	0.527**	0.446*	0.562**	0.646**	0.545**	0.334
Nordegg	0.519**	0.411*	0.529**	0.600**	0.537**	0.347
Clearwater	0.224	0.288	0.156	0.088	0.342	0.215
Louise	0.451*	0.442*	0.361	0.155	0.445*	0.595**
Jasper	0.611**	0.653**	0.655**	0.396	0.659**	0.522**
Banff	0.522*	0.561**	0.622**	0.377	0.558**	0.520**
Bighorn-Louise	0.627**	0.577**	0.575**	0.451*	0.638**	0.637**
* p < 0.05 (2-tailed).						
** p < 0.01 (2-tailed).						

4.4. Methods: Spatial Data

The GENESYS modeling routine is able to provide realistic estimates of climate across complex mountain terrain through its integration with a Geographic Information System (GIS). Many of the variables required for operation of the model are derived or extracted using a GIS, and generated output is linked back into the software for further analysis and presentation.

One of the most important spatial datasets used in the modeling routine is a Digital Elevation Model (DEM), which is a gridded raster file where each individual pixel is assigned a unique elevation based on interpolated measurements. The DEM used for this study was compiled by Nemeth *et al.* (2011) from digitized 1:50,000 National Topographic System (NTS) map sheets, downloaded from Natural Resources Canada's (NRCan) Geogratis website (www.geogratis.ca). The original NTS map sheets date from the early 1990s, and have a contour interval of 40 m with a vertical

accuracy of 20 m. Topographic map sheets were combined with a stream network file, and the ArcGIS 9.3 ‘Topo to Raster’ tool was used to convert the data to a DEM with a resolution of 100 m (Nemeth, 2010). Watersheds delineated and used in the UNSRB study have been used successfully for previous hydrological modeling applications (Kienzle *et al.* 2011; Nemeth *et al.* 2011; MacDonald *et al.* (in review)). The final DEM for the UNSRB is presented in Figure 4.5, clipped using the delineated watershed above the Bighorn Dam.

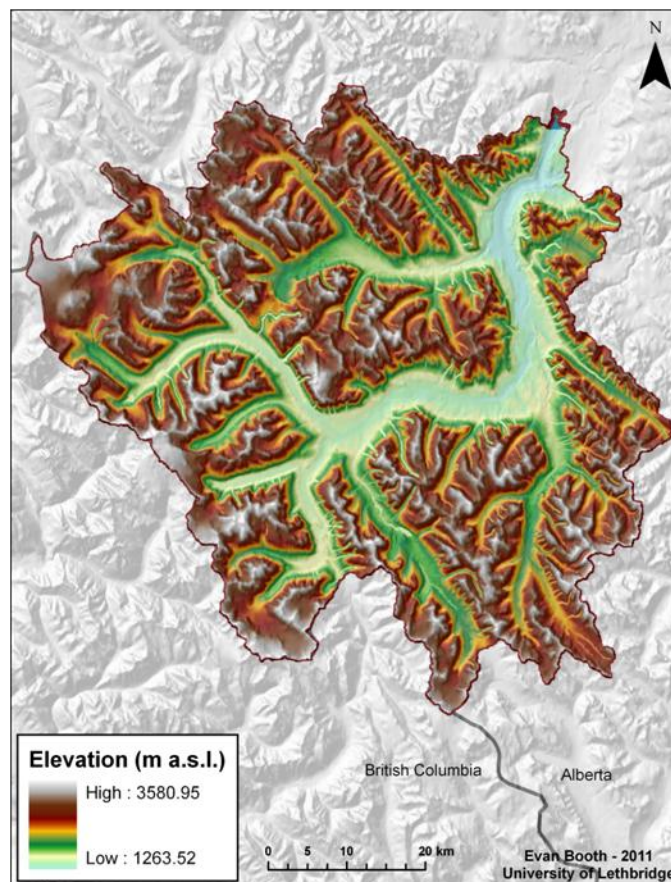


Figure 4.5: Digital elevation model for the UNSRB.

To aid in the interpolation of climate data, *Parameter-elevation Relationships on Independent Slopes Model* (PRISM) datasets (Daly *et al.*, 2008) were acquired for the UNSRB by Kienzle *et al.* (2011). The gridded 2 km PRISM raster datasets report normal monthly values from 1971-2000 for precipitation, maximum temperature, and minimum temperature. These gridded surfaces were interpolated from observed data over complex terrain factoring in a number of variables including elevation, aspect, coastal proximity, and orographic effects (Daly *et al.* 2008). Monthly PRISM grids were downscaled by converting the grids into point data, and interpolating those points using the ArcGIS 9.3 ‘Spline with Tension’ tool to match the 100 m DEM grid for use in the GENGRID setup (Figure 4.6).

Land cover data, including glacier extents, were downloaded from the NRCan website (www.geogratis.ca). The glacier extents included in the database date from surveys completed in 1985-1987. It is assumed that some minor errors exist in the glacier extents used (e.g. perennial snow may be interpreted as glacier ice). However, the glacier cover datasets were assumed to be of sufficient quality for the development of a dynamic mass balance model and for model runs that were initiated between 1980 and 1990. For model runs beginning before the 1990s, the ice thickness was extrapolated into the past based on the dynamic glacier ice distribution module explained in section 4.6.1.

4.5. Methods: Modeling

Simulating the mass balance of glaciers in the UNSRB requires the operation of a number of different GENESYS components, illustrated in the flowchart in Figure 4.6.

Interpolation of climate variables from the base station to sites throughout the watershed is done through the GENGRID program. The main GENESYS program uses the output generated by GENGRID to model the accumulation and ablation of snow and the potential ice melt at glaciers throughout the basin. The newly developed ICEGEN module is the final component of the modeling routine, simulating the dynamic long-term response of glaciers using output generated by the main GENESYS routine. An in-depth description of each model component follows below.

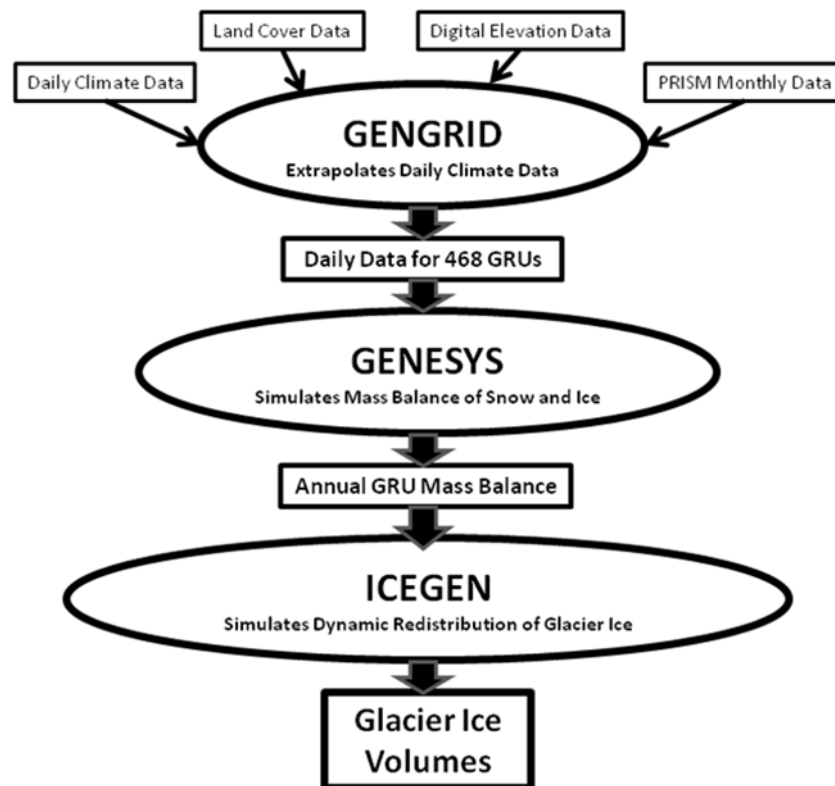


Figure 4.6: GENESYS glacier modeling routine flowchart.

4.5.1. GENGRID

The GENGRID model was originally developed by Sheppard (1996) as part of graduate thesis work completed at the University of Lethbridge. The model is based in large part on the MTCLIM Microclimate Simulator developed by Hungerford *et al.* (1989). Sheppard (1996) integrated the model with a GIS and automated the process to allow for efficient and realistic simulation of climate conditions across a physically-diverse watershed. A brief discussion of the processes involved in setting up and running the GENGRID routine for the purposes of driving the ICEGEN model follows below. Refer to Sheppard (1996), Lapp *et al.* (2005), MacDonald *et al.* (2009), and Larson *et al.* (2011) for a more in-depth discussion on the numerous operations of this component of the modeling routine.

The GENGRID model requires input data in the form of complete long-term records of observed maximum and minimum air temperature and precipitation. The hybrid “BLH station” created for this study was found to perform better than other potential driver stations at representing the accumulation of winter precipitation at sites throughout the area (Tables 4.1 and 4.2). Air temperature values were taken solely from the Bighorn Dam meteorological station record. Extrapolating the daily data from the driver station throughout the watershed requires a significant amount of pre-processing using a GIS.

The first step in setting up the GENESYS model is the creation of Hydrologic Response Units (HRUs). The purpose of HRUs is to ease the computer requirement necessary for modeling the physical climate conditions across a large, geographically diverse, watershed. HRUs allow for areas with similar characteristics (landcover,

aspect, elevation, etc) to be grouped together, operating under the assumption that they will respond in a similar manner under a range of hydrologic conditions (Kouwen *et al.*, 1993; Gurtz *et al.*, 1999; MacDonald *et al.*, 2009; Kienzle *et al.*, 2010). MacDonald *et al.* (in review) used a total of 368 HRUs for the portion of their study watershed corresponding to the area studied here that drains into Lake Abraham with an outlet at the Bighorn Dam. HRUs were classified according to land-cover type and 100 m elevation bands. All glaciers were treated the same, divided only by elevation, regardless of the geographic location, aspect, etc. This classification was deemed inappropriate for a study focusing primarily on the response of glaciers to changes in climate.

For the purpose of this study, Glacier Response Units (GRUs) were developed in an attempt to improve the representation of geographic and climatic conditions at each individual glacier. Each of the 73 continuous ice masses in the glacier extent shapefile obtained for the UNSRB was given a unique identifier based on its geographic location with respect to the DEM grid. Elevation bands of 100 m intervals were derived from the DEM and given a code relating to median elevation. These two codes were combined, resulting in 468 unique GRUs for the UNSRB. GRUs form the basic unit of analysis within the GENESYS modeling routine and their areal extents were used to generate zonal statistics for use within the model.

Air temperatures were interpolated across the UNSRB primarily through the application of vertical lapse rates that define the rate of air temperature change with an increase in elevation ($^{\circ}\text{C}/\text{km}$). MacDonald *et al.* (in review) derived minimum and maximum air temperature lapse rates for the UNSRB using monthly rates calculated

from the Bighorn Dam base-station and elevation-averaged values derived from PRISM datasets (Daly *et al.* 2008). Lapse rates were then calibrated and verified using additional Environment Canada and Alberta Environment weather stations, with varying time periods and levels of completeness (Nemeth *et al.*, 2011; MacDonald *et al.*, in review). It is acknowledged that these lapse rates may not be representative of actual conditions over many of the glaciers in the basin (Shea and Moore, 2010). However, due to a lack of available air temperatures observations over glaciers in the UNSRB for which to derive new lapse rates, it was determined to utilize the lapse rates developed for the previous study, which vary between 3.1 and 6.2 °C/km. A comparison of average monthly air temperature lapse rates derived using the PRISM data with those used in other studies (Shea *et al.*, 2004; Marshall and Losic, 2011) can be found in Figure 4.7. The low PRISM lapse rates in winter months likely result from inclusion of days with temperature inversions which can occur up to 25% of the time in the Southern Canadian Rockies (Shea *et al.*, 2004; Pigeon and Jiskoot, 2008).

Air temperatures were further adjusted within GENGRID using solar radiation values derived using a GIS, altering the interpolated maximum air temperature of a GRU based on the amount of solar radiation it normally receives due to its geographic location. Monthly solar radiation values were derived using the ArcGIS 9.3 Area Solar Radiation tool which calculates flat and slope/aspect-based radiation inputs based on the DEM. Monthly solar radiation values were averaged and extracted for each GRU for use in GENGRID interpolations. Within the GENGRID model, maximum temperatures were adjusted based on the ratio of slope to flat surface radiation (RADRAT). Maximum temperatures in GRUs with north facing slopes (where RADRAT < 1.0) are

reduced, while those on south facing slopes (where RADRAT > 1.0) are increased, based on the amount of direct solar radiation they receive during daylight hours (Sheppard, 1996; MacDonald *et al.*, 2009; Larson *et al.*, 2011).

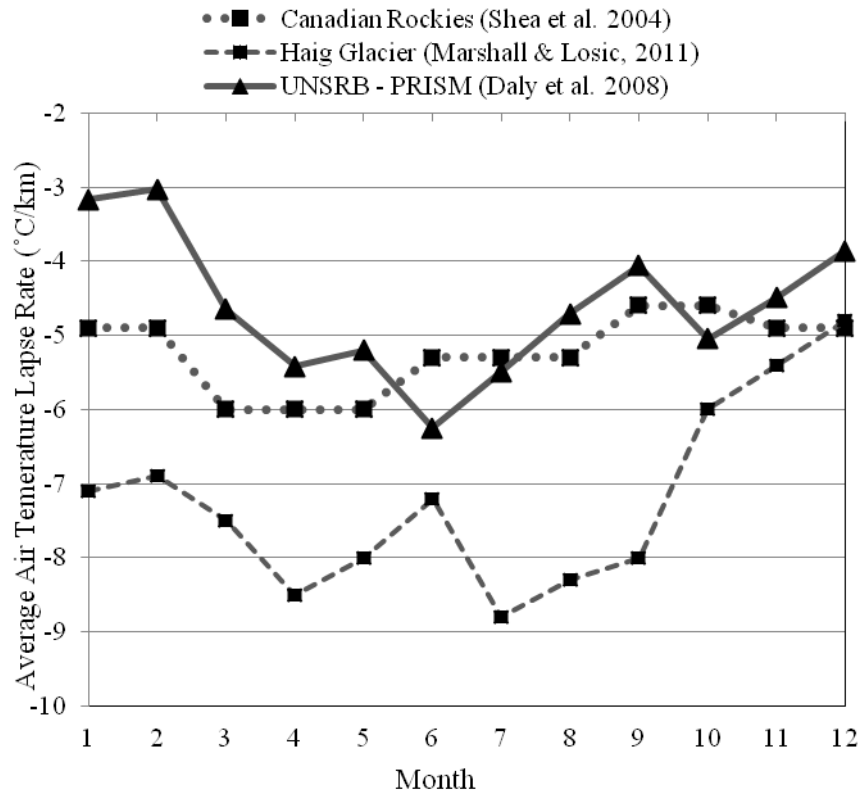


Figure 4.7: Air temperature lapse rate comparison.

Similar to air temperature, precipitation interpolation in GENGRID is primarily governed by downscaled PRISM surfaces (Daly *et al.*, 2008). However, unlike the temperature simulations that operate using basin-wide lapse rates, precipitation is handled on a GRU-specific basis. Monthly 1971-2000 PRISM normals (average total precipitation) were extracted in the GIS for all 468 GRUs, and, together with calculated monthly values for the BLH station, used as input data for the GENGRID model.

GENGRID uses these monthly normals to calculate a ratio between the GRUs and the monthly normal at the driver station, and applies it to the daily input data to extrapolate precipitation across the basin (MacDonald *et al.* (in review)). In order to simulate the mass balance of Peyto Glacier, an analysis comparing PRISM derived winter precipitation totals (Oct-Apr) with the average observed 1966-1995 winter balance (Demuth and Keller, 2006) was completed. The results of this comparison show that the PRISM precipitation surfaces fail to capture the large snow accumulation at high elevations on Peyto Glacier (Figure 4.8), and therefore likely also under-represent SWE at other large glaciers situated near the continental divide.

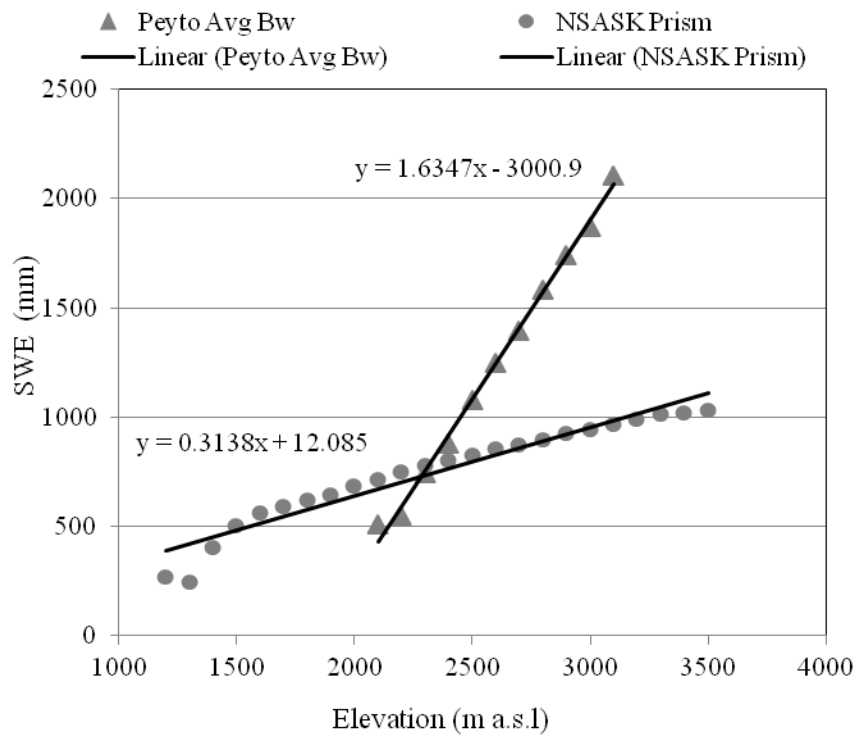


Figure 4.8: Winter precipitation totals by elevation for Peyto Glacier and PRISM datasets.

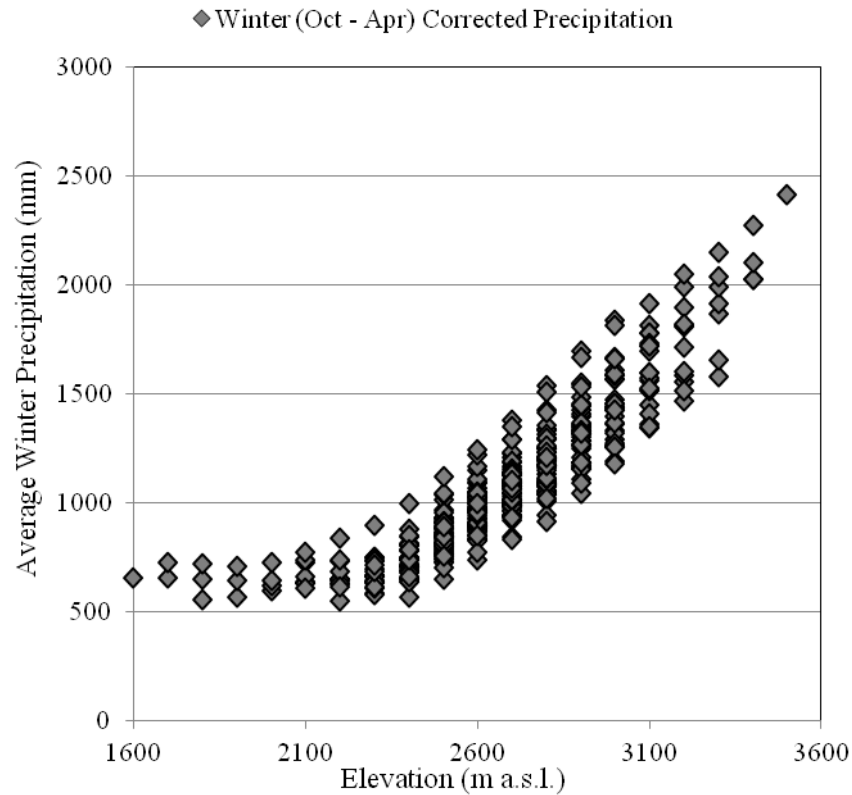


Figure 4.9: Winter precipitation vs. elevation for all GRUs corrected for PRISM underestimation compared to Peyto Glacier winter mass balance.

To accommodate for this under-simulation, a correction factor, based on the difference between the two equations in Figure 4.8, was applied to the GRU normal precipitation amounts for the months of Oct-Apr for areas above 2500 m a.s.l. (Figure 4.9). The high-elevation correction accounts for a combination of elevated snow accumulation processes in the high elevation GRUs, including solid precipitation, wind deposition, avalanching, etc. that contribute to the large amounts of SWE deposited in the accumulation zone of some glaciers (Dadic *et al.*, 2010). After preliminary runs of all components of the model (GENGRID, GENESYS, and ICEGEN) it became apparent that this precipitation correction was not appropriate for a number of smaller

isolated glaciers in the basin, especially (but not limited to) those situated further east of the continental divide (Figure 4.10). Since precipitation rates on the West side of the continental divide are higher than on the East (lee) side, wind distribution was deemed highest for UNSRB close to the continental divide. Monthly precipitation amounts for GRUs in glaciers where the correction caused unrealistic rates of growth following preliminary model runs were instead assigned the original values derived from the PRISM grids.

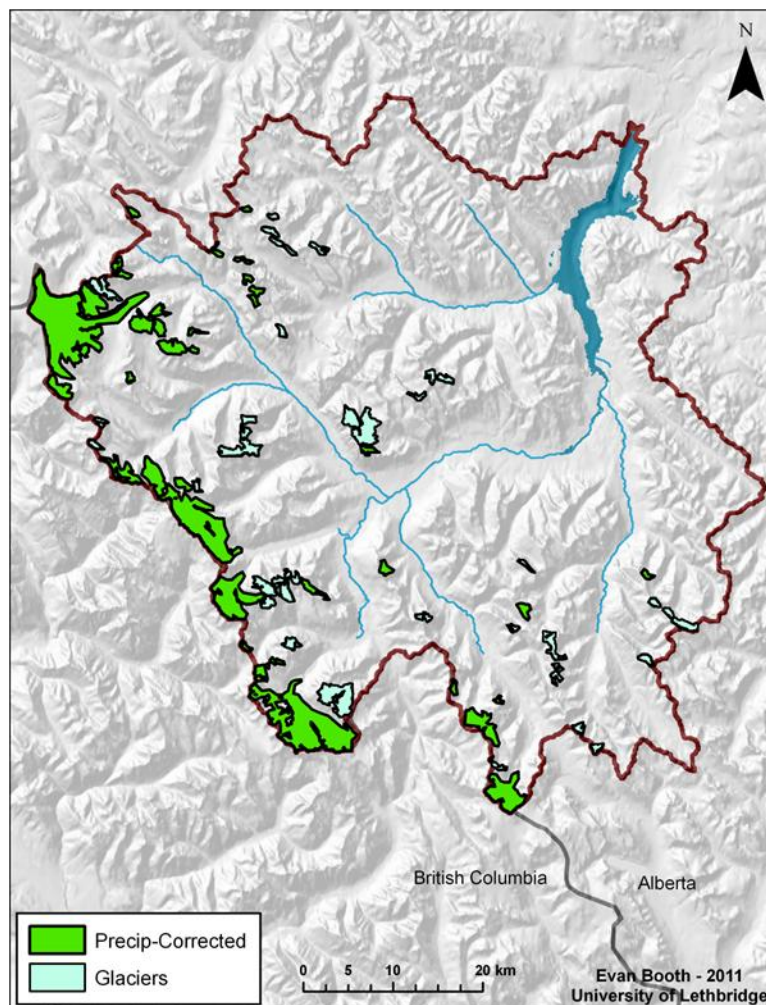


Figure 4.10: Glaciers for which winter precipitation correction was applied (green).

4.5.2. GENESYS

Daily GENGRID output for all GRUs in the UNSRB is used to drive the main GENESYS program for the calculation of snow accumulation and melt, glacier ice melt, glacier mass balance and total runoff (Figure 4.6). The version of GENESYS employed by MacDonald *et al.* (2009) in the St. Mary River watershed, Montana, and MacDonald *et al.* (in review) in the UNSRB, simulates snowpack accumulation and ablation during the winter months. After the seasonal snowpack has melted, soil moisture levels are calculated and daily runoff values for the entire hydrologic year are reported. However, no published attempts were made to model the melting of glacier ice once the overlying snowpack had melted off. To accommodate the simulation of the mass balance of glacier ice, an ice melt subroutine was added to the main GENESYS program.

Daily precipitation generated by GENGRID is partitioned into snow or rain in GENESYS, based on the method developed by Kienzle (2008). Rather than adopting a static or linear temperature partition between rain and snowfall, the method uses an “S-shaped” curve that defines the proportion of “mixed” precipitation that falls as rain. This method was incorporated into the GENESYS model by MacDonald *et al.* (2009) and has remained unchanged for this study.

Snowpack is modeled within GENESYS using a method based on the UBC snowmelt algorithm developed by Quick and Pipes (1977). The model simulates the ‘ripening’ of a snowpack before snowmelt is allowed to take place, through the incorporation of a ‘cold storage’ component. The cold-storage ($TREQ$) of the snowpack is calculated (MacDonald *et al.* 2009) as:

$$TREQ_i = (MLTF * TREQ_{i-1}) + T_{mean_i} \quad [\text{Eq. 4.1}]$$

where $MLTF$ is a decay constant (originally set to 0.85) and T_{mean} is the mean daily temperature. The decay constant $MLTF$ controls how long it takes for the snowpack to ripen. Once the cold-storage factor reaches zero, it is assumed that the snowpack has become ripe and melt/runoff begins to occur.

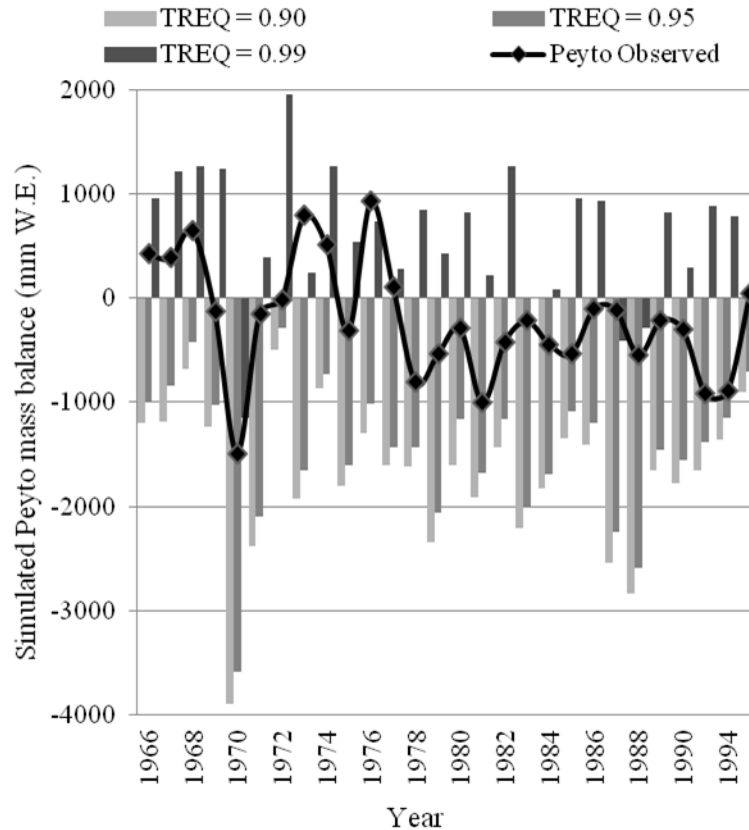


Figure 4.11: Sensitivity analysis on TREQ cold-storage and mass balance.

In order to account for the increased cold-storage of a snowpack over the surface of a glacier (Marshall and Losic, 2011) it was determined that the $MLTF$ value should be substantially increased. A preliminary analysis was carried out to test the effect of changing this constant, keeping all other snowmelt variables consistent with those used by MacDonald *et al.* (in review). Based on the results of the analysis (Figure 4.11), as

well as preliminary model runs, *MLTF* was set to a value of 0.99. Substantially increasing TREQ had the desired effect of reducing the amount of snowmelt, and therefore icemelt, over the glaciers in the UNSRB. Increasing the *MLTF* constant allowed for the other major model parameters (snowmelt and icemelt factors) to be calibrated so that modeled values would be more representative of those observed at Peyto Glacier.

Once the cold-storage of the snowpack has been exhausted it is assumed isothermal, and snow melt (M_s) is calculated using a modified temperature-index model (Quick and Pipes, 1977; MacDonald *et al.*, 2009):

$$M_s = K_s \times (T_{max} + TCEADJ \times T_{min}), \quad [\text{Eq. 4.2}]$$

where, K_s is the snow melt factor ($\text{mm day}^{-1} \text{ } ^\circ\text{C}^{-1}$), T_{max} is the daily maximum temperature, *TCEADJ* is an energy partition multiplier, and T_{min} is the daily minimum temperature. MacDonald *et al.* (in review) used a static K_s value of 2.2 to model snowmelt in the UNSRB. During calibration of the GENESYS routine using observed Peyto Glacier data, it became apparent that a static melt-factor was unable to accurately model SWE amounts at different elevations. A review of the literature reveals that no single melt factor can be expected to perform ideally in all situations and locales (Hock, 2005). Ultimately, melt factors for both snow and ice are entirely dependent on the operation of the model used, the temperature lapse rate used to extrapolate data across a basin, and the local geographic and climatic conditions of the glaciers modeled. For this study, a melt factor that varied linearly with elevation was used, based on calibration with observed summer balances at Peyto Glacier. A melt factor that changes with elevation is adopted based on the assumption that albedo typically increases with

elevation (Oerlemans and Fortuin, 1992; Braun *et al.*, 1994; Hock, 2005). Model runs were completed for the years 1966-1995 using a wide range of melt factors within the published range (Hock, 2005) with the goal of replicating the average observed Peyto Glacier ELA and SWE values in the accumulation area (Demuth and Keller, 2006) as closely as possible. These two values were then used to calculate a linear relationship to interpolate and extrapolate to all elevation bands (Figure 4.12).

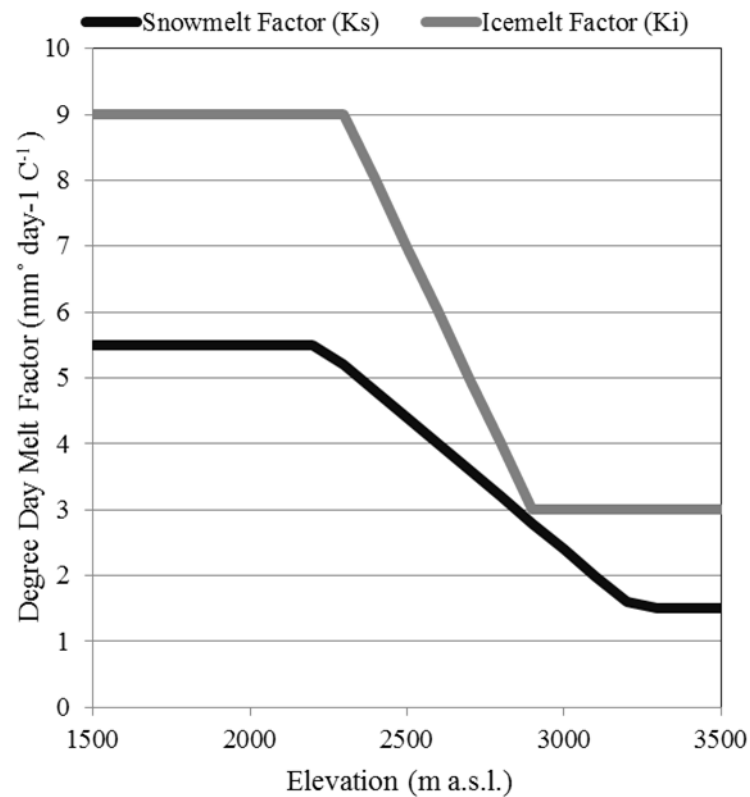


Figure 4.12: Elevation based temperature index melt factors.

Melt factors for snow were capped at $5.5 \text{ mm day}^{-1} \text{ }^{\circ}\text{C}^{-1}$ (due to a lack of data on which to support increasing melt rates with decreasing elevation). For glaciers where no mass balance data are available, the median elevation can be used as a proxy for the ELA

(known as the Kurowski method: ELA_K) (Jiskoot *et al.*, 2009). Since linear melt factors were calibrated to the observed Peyto Glacier ELA, preliminary model runs resulted in a dramatic over-simulation of SWE at glaciers with a higher ELA_K, and an under-simulation of SWE at glaciers with a lower ELA_K. To account for the range in ELA_K at glaciers across the UNSRB, linear melt rates were shifted by applying the median (Peyto) melt rate to the median elevation of the other glaciers and extrapolating from there using linear equations derived from the Peyto Glacier simulations (Figure 4.12).

Once the overlying snow cover is removed from a glacier surface, ice melt can begin to take place. To simulate the melting of ice, a glacier melt subroutine was added to the main GENESYS program. Based on the lack of observed input variables needed to calculate melt using a full energy balance method, a simple temperature index method was adopted (Hock, 2005). Daily ice melt (M_i) is calculated as:

$$M_i = K_i * T_{mean}, \quad [\text{Eq. 4.3}]$$

where K_i is the ice melt factor ($\text{mm day}^{-1} \text{ } ^\circ\text{C}^{-1}$). Similar to K_S , K_i is also adjusted in a linear fashion based on elevation (Figure 4.12), where lower elevations are assigned a higher melt rate than higher elevations, with values adjusted between glaciers based on a different starting ELA_K compared to Peyto Glacier. Ice melt factors were chosen within the range of published values (Hock, 2005), varying between 3 and 9 $\text{mm day}^{-1} \text{ } ^\circ\text{C}^{-1}$. The amount of ice melt generated within the glacier subroutine in the main GENESYS program is considered to be ‘potential melt’, since the main program does not have the capability to determine the long-term dynamic response of the glaciers, and therefore the amount of Ice Water Equivalent (IWE) that is available to melt at each GRU. The winter balance of glaciers is output by GENESYS on May 1, and the

summer balance is reported on October 1, corresponding to the general accumulation and ablation seasons of a hydrologic year. The summer balance SWE and IWE depths in each GRU are used as input for the ICEGEN model that simulates the dynamic response of glaciers to climate change on an annual basis.

4.5.3. ICEGEN

The ICEGEN component of the GENESYS model was developed for this study with the objective of simulating the dynamic mass balance of individual glaciers through the annual redistribution of Ice Water Equivalent (IWE) between GRUs. Model development involved a substantial amount of trial and error, resulting in the formulation of a number of different methodologies for redistributing IWE according to the annual accumulation and ablation calculated by the glacier subroutine in GENESYS. Two versions of ICEGEN are presented here: a volume-based method (Section 4.5.3.1) and a flow-based method (Section 4.5.3.2). For both versions of ICEGEN it is assumed that all accumulated SWE will become glacier ice in the following year, thus removing potential firn accumulation from the calculations. At the end of the hydrologic year, any accumulated SWE is automatically added to the IWE contained in the underlying glacier unit (Figure 4.13).

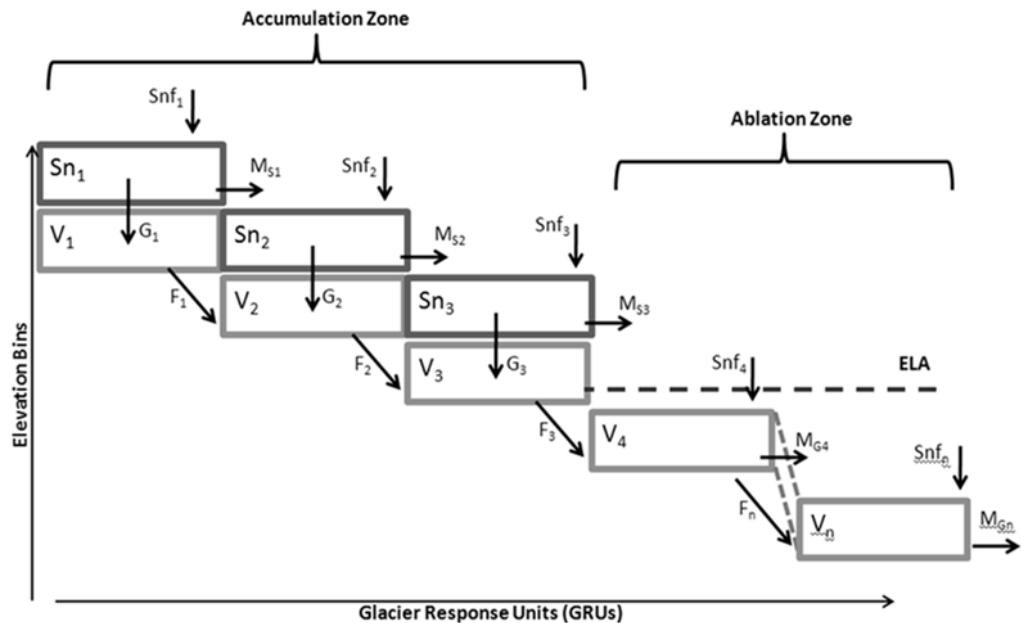


Figure 4.13: Conceptual flow chart of ICEGEN module. Numbered components (1, 2, 3, 4,...n) represent glacier elevation bands. Sn = snowpack, V_i = ice volume, Snf = snowfall, MS = snowmelt, G = ice volume gained from previous year's snowpack, F = redistributed ice volume, MG = ice melt. ELA = the equilibrium line altitude where $G = MG$.

Modeling the long-term dynamic response of glaciers to changes in climate requires an initial estimation of the volume of IWE contained in the glaciers of the UNSRB. Two methods were tested here to provide starting volumes for the operation of the model: area-volume scaling, and slope-based depth estimation. Both methods are based on mid 1980s to mid 1990s measured areas and slope from the NRCan and NTS DEM data used for this region. Area-volume scaling has been used by a number of recent studies (DeBeer and Sharp, 2007; Hirabayashi *et al.*, 2010; Marshall *et al.*, 2011) to provide reasonable estimations of glaciers in western Canada. Originally developed by Chen and Ohmura (1990), and refined by Bahr *et al.* (1997), the method is based on

relationships established by comparing the area and volume of 144 glaciers worldwide (Figure 3.5). By plotting the relationship between area and volume, Chen and Ohmura (1990) developed an equation that can be used to estimate volume (V) in km^3 based on an input area in km^2 :

$$V = cA^y, \quad [\text{Eq. 4.4}]$$

where A is the area of a glacier in km^2 , and C and y are constants, set to 0.0285 and 1.357 respectively for glaciers world-wide (Bahr *et al.*, 1997). Application of the empirical relationship between area and volume based on the glacier extents acquired for the UNSRB provided an overall ice volume estimation of $\sim 19 \text{ km}^3$. Approximations of average glacier depth were then made by dividing the total calculated volumes by the glacier GRU area. Marshall *et al.* (2011) and Meier *et al.* (2007) found that the area-volume scaling method often results in errors at the individual glacier level due to inherent differences in bedrock topography, but that it works well for estimating volume on a basin-wide scale. A major disadvantage of using volumes derived from the area-volume scaling method is that depth estimates can only be made for entire glaciers (or regions), meaning all GRUs are assigned the same averaged value.

A novel method to calculate glacier ice depth for different zones within individual glaciers has been developed by Marshall *et al.* (2011). The method operates under the assumption that the depth of glacier ice is controlled by the topography of the bedrock underneath, with steeper slopes generally having thinner ice than flat areas, in a way in which the basal shear stress remains constant at a value normal for valley glaciers. It is assumed that the surface slope of a glacier is representative of its underlying bedrock (i.e. the two planes are parallel). Surface slopes derived from our

DEM were used as input in the equation used to estimate the depth (H) of a glacier (Marshall *et al.* 2011):

$$H = \frac{\tau_d}{\rho g \nabla s} \quad [\text{Eq. 4.5}]$$

where τ_d is the basal shear stress (assumed to be a constant of 10^5 Pa), ρ is ice density (910 kg/m^3), g is gravitational acceleration (9.801 m/s^2), and ∇s is the sine of the surface slope calculated in radians (Marshall *et al.* 2011). This method can be used locally on a grid-cell basis, or on a larger scale using the slopes averaged over a glacier surface. Depending on the scale of input slopes used to estimate depth, overall measurements differ considerably. Table 4.3 shows total calculated glacier IWE volumes for the UNSRB using area-volume scaling, as well as GRU-based and glacier-wide slope estimated depths. The value we calculated using the area-volume scaling method proved to be much larger (~25%) than those calculated using slopes. Reasons for this over-estimation may include the fact that the area-slope estimation is based on extents from the mid-1980s, while the slope-based estimations use a DEM produced from data acquired in the early 1990s. Another likely error involves the fact that the glacier extents used here have not been separated along ice divides, resulting in much larger individual glacier areas than have been used in previous studies (Marshall and White, 2010; Marshall *et al.* 2011). The slope-based depth estimation is appealing for use in ICEGEN because it is capable of providing unique depth values for each GRU. The GRU-based slope estimates are used here to model the glacier mass balance through to 2100. Irrespective of starting volume used, the results obtained here for relative thinning and retreat trends are not affected. The estimated ~1990 depths for Peyto Glacier are presented in Figure 4.13.

Table 4.3: Glacier volume (IWE) estimates for the UNSRB.

Estimation Method	Volume (km ³)
Area-Volume Scaling	19.03
GRU Slope-Thickness	12.48
Glacier Slope-Thickness	11.75

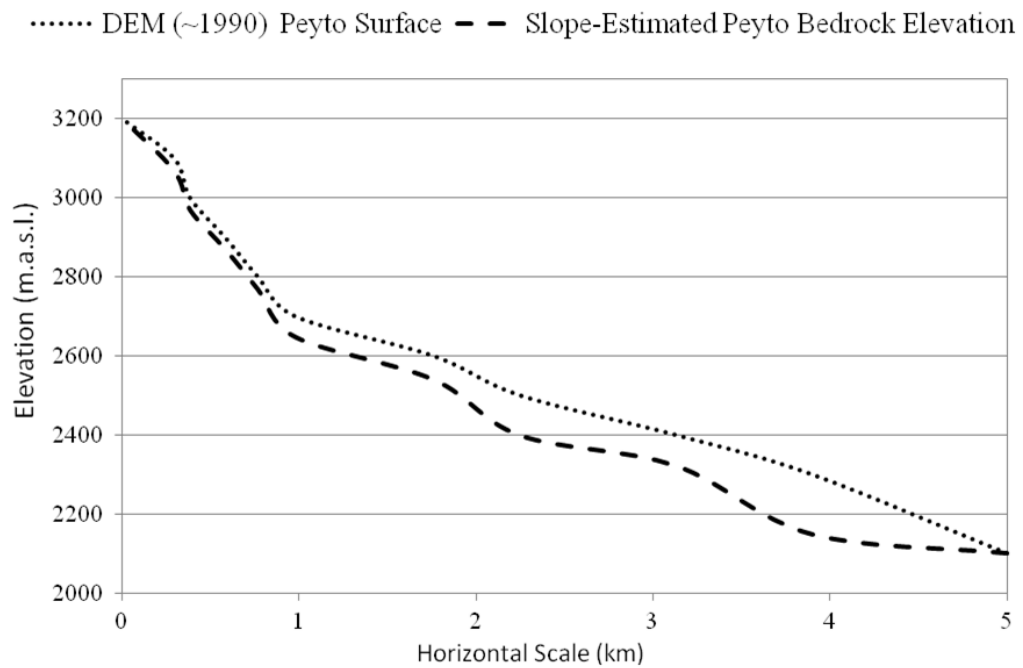


Figure 4.14: Estimated average glacier depth profile per elevation bin for Peyto Glacier

4.5.3.1. ICEGEN v1: Volume-based redistribution

In order to model the contribution of ice flow, from accumulation to ablation zone, to the overall glacier mass balance, ICEGEN v1 simulates the annual dynamic response of glaciers by redistributing all IWE accumulated above the snowline at the end of each hydrological year (30 September) to the GRUs below the snowline, based on their relative volume loss. Annual mass balance estimates from the GENESYS glacier subroutine are used to calculate the net mass balance for each GRU. The total IWE volume loss is determined for each GRU and percentage of loss from each GRU relative to the total IWE volume loss for the glacier is calculated. Accumulated SWE is distributed to GRUs based on the percentage of IWE melted relative to other GRUs. In some cases, the annual mass balance of a glacier would be positive to the point that only one GRU would experience a net loss (i.e. very low snowline). Although this scenario occurs rarely, the lowest elevation GRU would then receive all accumulated IWE, and therefore experience an unrealistic rate of thickening. To correct for this model flaw, a control was written into the code so that if a threshold Accumulation Area Ratio (AAR = 75%) is surpassed, accumulated SWE is distributed evenly to all GRUs. Further, in order to simulate glacier retreat over time, a GRU can cease to exist once all IWE in the GRU is exhausted. In this case, all input variables are set to zero, thus removing them from future calculation and redistribution. Only snow accumulation and melt are possible, but neither the ice melt routine in GENESYS nor ICEGEN is implemented. In the present model only volume growth (thickening) within the starting spatial extent, or glacier retreat, are possible. Advance is not possible as no comprehensive data exist for former glaciers extent (apart from the maximum extent during the Little Ice Age), hence

no possible additional GRUs were defined. Considering that all future climate scenarios result in negative net mass balances, the lack of an advance routine in the model is not important for the timescale at which the model is used (up to 2100).

4.5.3.2 ICEGEN v2: Flow Approximation Redistribution

ICEGEN 2 simulates the dynamic response of glaciers to changes in climate by redistributing IWE annually using a simplified flow function. The initial IWE depths assigned to GRUs are assumed to represent the maximum depth that they can sustain, given the warming experienced in recent history and that expected over the next century. ICEGEN v2 transfers IWE from higher elevation GRUs to those at lower elevations in a cascading fashion (Figure 4.13). Annual mass balance calculations from GENESYS for the highest elevation GRU are used to calculate surplus IWE above the initial depth. Any surplus IWE volume is then directed downslope to the next lower GRU, where it is added to the mass balance calculation along with the annual inputs from GENESYS. If calculated IWE volumes are greater than initial IWE volumes, then flow (F) is equal to:

$$F = (F_{.1} + IWEA + IWEW) - IWES \quad [\text{Eq. 4.6}]$$

where $F_{.1}$ is the flow input from the above GRU, $IWEA$ is the annual input as calculated by GENESYS, $IWEW$ is the working IWE volume from the previous year, and $IWES$ is the initial IWE as calculated from the average GRU slope. Flow is not calculated for the lowest GRU so any additional volume remains there, regardless of whether it is greater than the initial value. Similar to GENICE v1, this can result in an unrealistic buildup of IWE at the lowest elevation in years with positive mass balance. This

situation in nature would likely result in an advance of the glacier (increase in length), which is not currently supported in the design of the model. To overcome this flaw, the AAR based redistribution developed for v1 was applied to v2. GENICE v2 seemed to work reasonably well for many glaciers in the UNSRB although it produced different results compared to v1. The fact that downslope flow is dependent on a GRU surpassing its initial volume means that under the current warming scenario, GRUs at lower elevations may melt off faster because overflow from the accumulation area is “used up” by GRUs at higher elevations and never reaches the lower extents. However, this also had the result of preserving higher elevation GRUs longer than in v1 because they were fully replenished before losing IWE thickness to those at lower elevation.

4.5.4. GCM Future Climate Scenarios

Projections of future conditions are highly speculative given the uncertainty associated with the long-term controls of earth’s climate, perhaps the most important of which is solar forcing. Analysis of geological and glacial history suggests that the earth is currently in an interglacial phase that will inevitably come to an end with the onset of another ice age (Calkin, 1995). However, the anthropogenic warming of the planet introduces a new element to the dynamic earth system for which the long-term results are unknown. Estimating the potential future effects of climate change on the glaciers in the UNSRB was done through the application of General Circulation Model (GCM) future emissions scenarios into the GENESYS modeling routine, identical to the process used by MacDonald (2011) and MacDonald et al. (in review). GCM scenarios were acquired from the Pacific Climate Impacts Consortium (PCIC) website

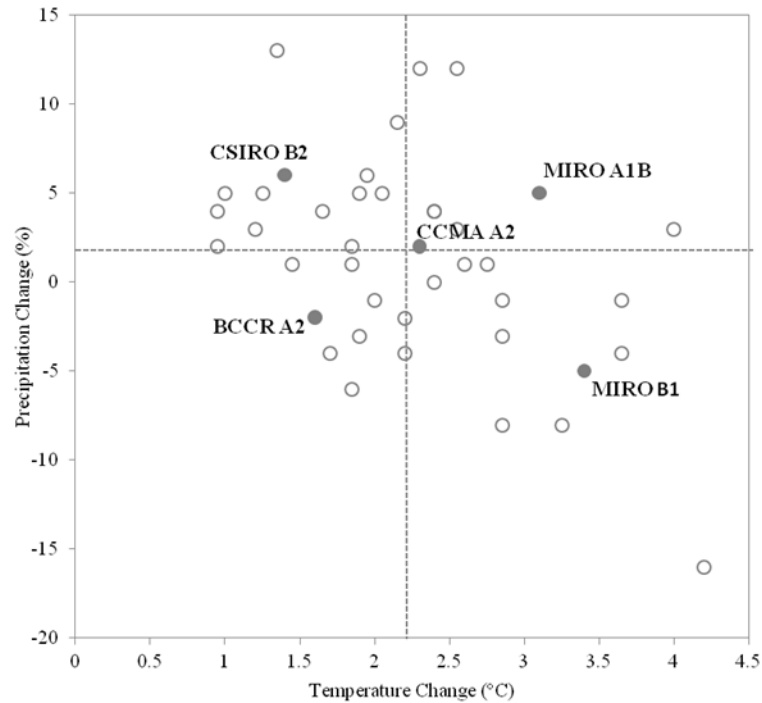


Figure 4.15: Amount of change expected in 2050 for future GCM scenarios selected for use in GENESYS ice modeling routine (source: Dalla Vicenza, *in progress*).

(<http://pacificclimate.org>). Five different future climate scenarios were selected that represent varying amounts of change over 30-year periods centered on the 2020s, 2050s, and 2080s, relative to a historical ‘normal’ base period of 1961-1990. Scenarios were chosen based on the amount of change in air temperature and precipitation for the 2050s, with the goal of selecting scenarios that represent the full range of those available (Figure 4.15). Each scenario is based upon a different set of assumptions about global socio-economic conditions over the next century and associated levels of greenhouse gas (GHG) emissions. For an in-depth discussion on the formulation and design of future scenarios refer to the IPCC Special Report on Emissions Scenarios (Nakicenovic *et al.*, 2000). The ‘delta’ method (Barrow and Yu, 2005) was used to downscale and apply the GCM scenarios to GENESYS. Forecast monthly changes

were applied to the input BLH data and then run through GENGRID and GENESYS for each 30 year future period. For each future scenario, the 30 year output datasets from GENESYS were merged with historical output from 1990-2010 to create input files for the ICEGEN routines for the period 1990-2100.

4.6. Results and Discussion

4.6.1. Peyto Glacier

Initial model development and application were focused on Peyto Glacier as its mass balance measurements represent the only available data within the UNSRB. Calibration of melt factors for snow (K_s) and ice (K_i) were done using the annual observed mass balance measurements from Demuth *et al.* (2006), averaged over the 30 year time series for each elevation. Calibration of the individual melt rates involved a large degree of uncertainty since dates of snowline retreat were not available; only the mass balance at the end of each hydrologic year was available. Despite the inherent difficulties associated with calibration using very limited data, reasonable results were obtained. A regression of simulated GENESYS model output compared to observed mass balance measurements at similar elevations resulted in an R^2 of 0.83, with a slope of 0.9387, significant at the $p < 0.001$ level (Figure 4.16).

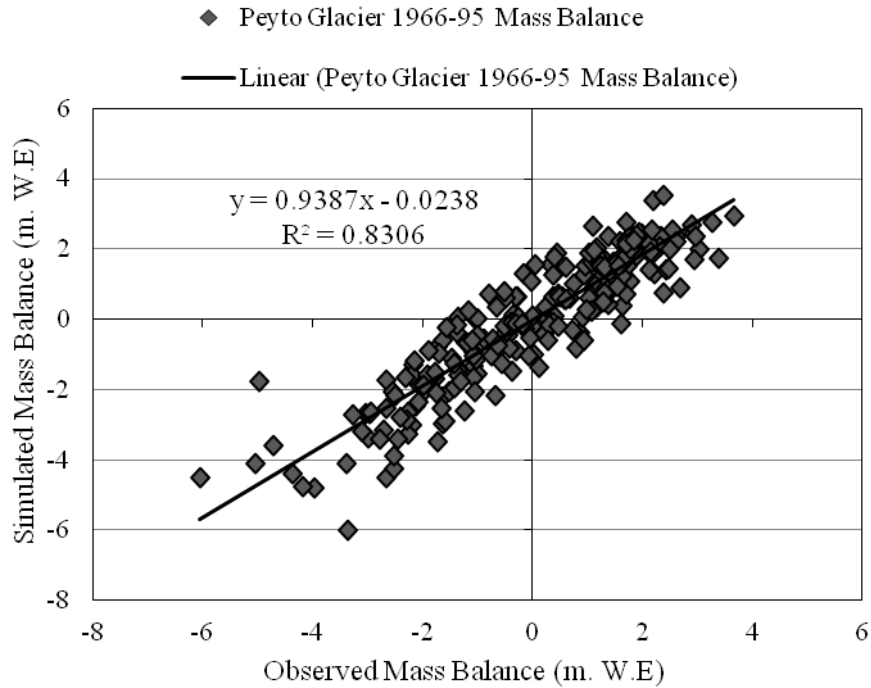


Figure 4.16: 1966-95 Peyto GRUs observed vs. simulated calibration mass balance.

The volume of the glacier was estimated using the slope-based method developed by Marshall *et al.* (2011) and presented above in Figure 4.14. Glacier depths were estimated based on slopes derived from elevation data dating to approximately 1993, and applied to GRUs delineated using glacier extents defined in 1985-87. Due to this discrepancy, it was decided to begin the main modeling routines in the 1989-90 hydrologic year which roughly represents the median year between the data sources. Preliminary historical model runs for Peyto Glacier were done using a uniform depth of 100 m at all GRUs to aid in the development of model mechanics. To provide a more realistic simulation of the historical effects that climate change had on the glacier, 1990 GRU volumes were scaled back to 1966 based on the preliminary modeling efforts. Scaling back the 1990 estimates of IWE volume resulted in a total 1966 IWE volume

for Peyto Glacier of 0.797 km^3 , which compares well with the estimate of 0.745 km^3 made by Holdsworth *et al.* (2006). ICEGEN v1 was then set up to run for the historical period 1966-2010. Figure 4.17 shows results for Peyto Glacier from 1966-2010, plotted with observed mass balance measurements. According to modeling results, the glacier experienced a significant decline over the period, losing over 0.3 km^3 of IWE, representing a loss of about 40% based on our estimates of its 1966 volume. ICEGEN modeled declines are generally in line with changes found by Demuth and Keller (2006), who found that Peyto Glacier lost ~25% of its 1966 volume by 1995. Compared to this, the results derived from ICEGEN were conservative, reporting a loss of 23.2% over the same time period. ICEGEN v1 estimates were also in line with Bolch *et al.* (2010) who estimate a loss in total glacier area of ~25% for the central and southern Rocky Mountains of Alberta between 1985 and 2005.

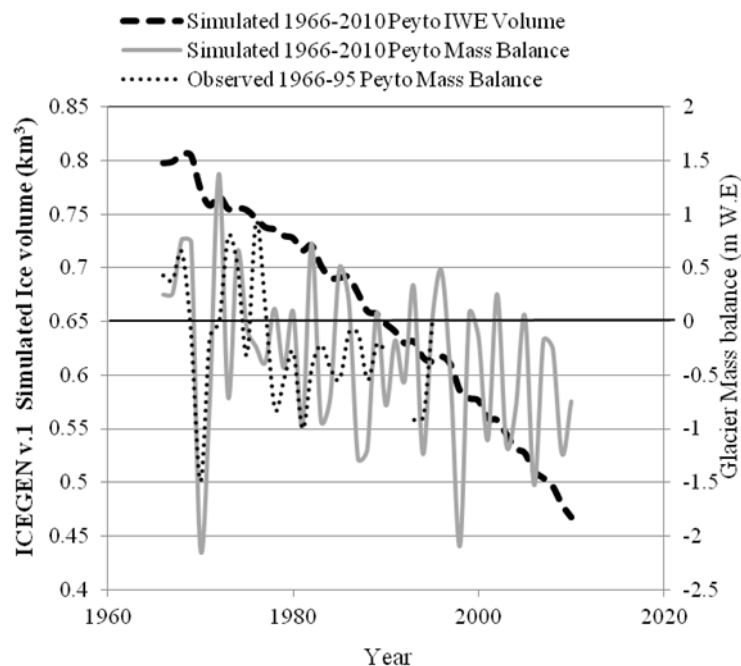


Figure 4.17: Simulated 1966-2010 mass balance and total IWE volume for Peyto Glacier for ICEGEN v1

4.6.2 UNSRB Glacier Modeling

The historical results obtained from Peyto Glacier show a dramatic negative trend in glacier volume in recent decades. If current warming trends continue, the glaciers in the UNSRB will be at risk of disappearing. To determine potential change in glacier mass balance, both GENICE versions were applied to the entire UNSRB for the historical period 1990-2010, and through to the end of this century using the selected range of GCM climate scenarios (Figure 4.15). Although results were somewhat mixed, all forecasts show a severe glacial decline in the UNSRB over the next century. Figure 4.17 shows projected total glacier volumes in the basin through 2100. Results from ICEGEN v1 (Figure 4.18a) depict a much steeper decline in volumes than those from ICEGEN v2 (Figure 4.18b). The difference in the rate of decline between the two models is the result of the method of redistribution. Since ICEGEN v1 distributes IWE according to the percentage lost per GRU compared to net amount lost over the rest of the glacier, more accumulated SWE is transferred to lower elevations where it is subject to high melt rates and lower temperatures in the next hydrological year. ICEGEN v2 retains more of its IWE at higher elevation GRUs, thereby having a smaller, more linear rate of decline, resulting in a slower recession and depletion of the glaciers. Despite the different rates of glacier deterioration over the next century, the end result in 2100 is very similar, with both models predicting dramatic losses. ICEGEN v1 shows a decline of ~86% from 1990 volumes based on the average on the GCM scenario, compared to a loss of ~79% using ICEGEN v2. The shape and trends of the modeled future loss of IWE volume across the basin (Figure 4.18) match well with those reported by Marshall

et al. (2011) who report a projected loss of 79-89% for the eastern slopes of the Canadian Rocky Mountains.

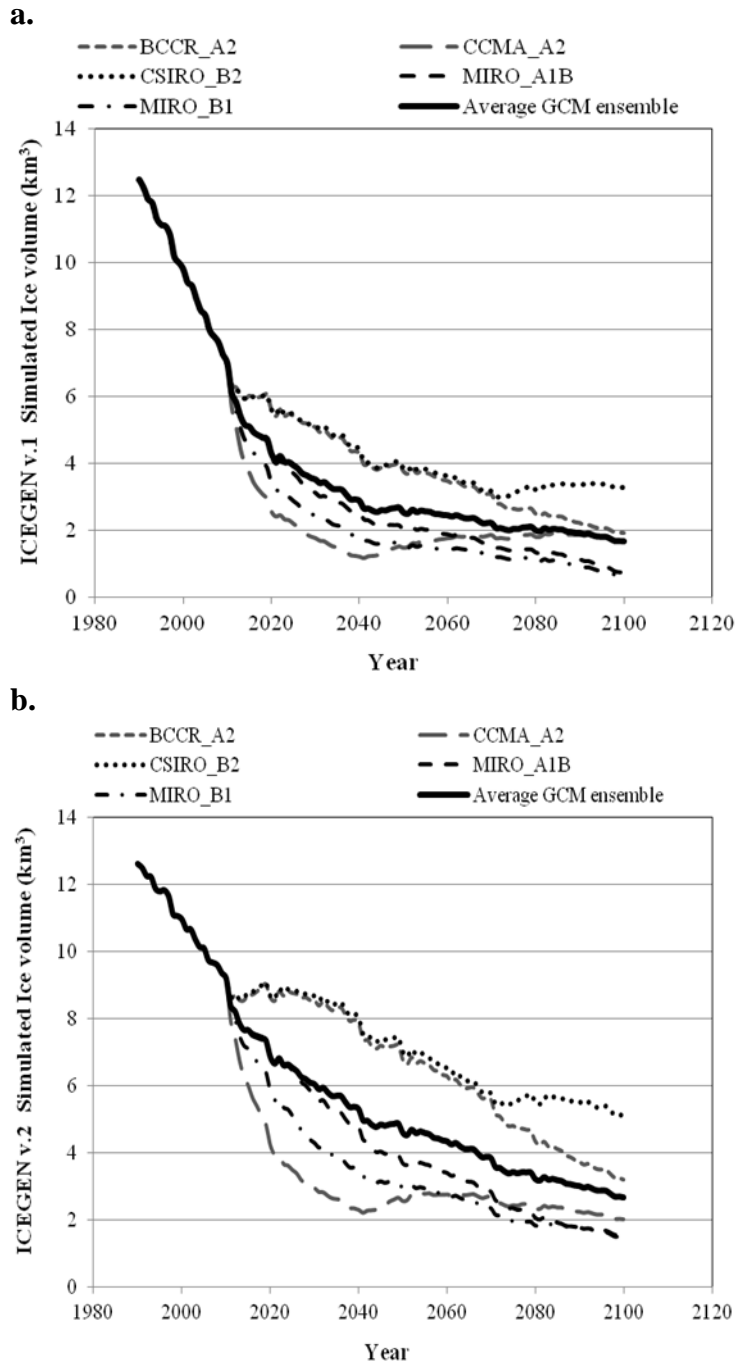


Figure 4.18: Simulated 1990-2100 UNSRB IWE volume using ICEGEN v1 (a) and ICEGEN v2 (b)

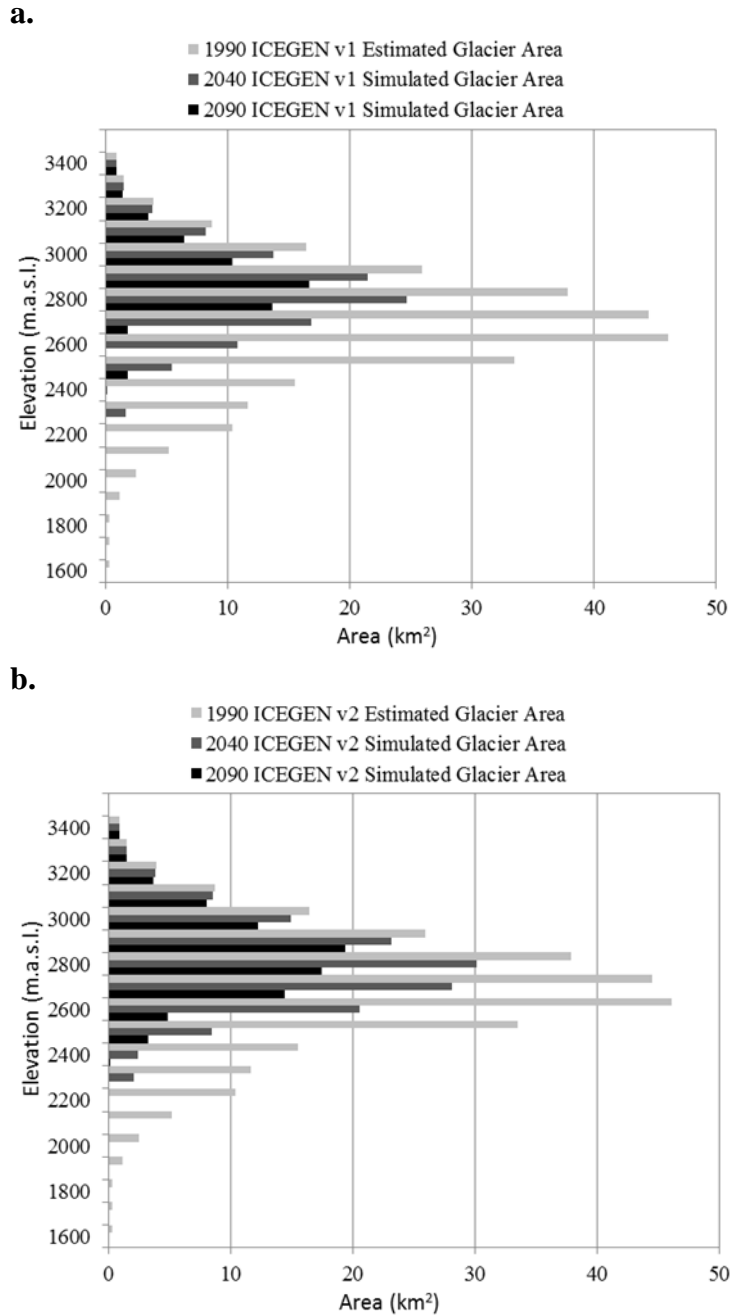


Figure 4.19: Simulated 1990-2100 UNSRB glacier area-elevation relationships using ICEGEN v1 (a) and ICEGEN v2 (b)

The results for both versions of the model presented in Figure 4.18, but especially for ICEGEN v1 (Figure 4.18a) show a leveling out effect in the rate of

glacier decline over the next century. Projected GCM temperature increases cause the ELA to rise in elevation, to which glaciers respond by losing mass as they move towards an equilibrium state. It appears as if the glaciers in the UNSRB reach this equilibrium state around the middle of the century according to the results from ICEGEN v1 (Figure 4.18a), and around 2075 using ICEGEN v2 (Figure 4.18b). Once glaciers in the basin reach equilibrium with the warmer climate regime, their mass balance stabilizes and they maintain their extent at high elevations. Under the future climate scenarios where precipitation is forecast to increase along with a moderate increase in temperature (CCMA A2 and CSIRO B2 – see Figure 4.15), glacier volume actually begins to gain mass after reaching equilibrium in the mid 21st century (Figure 18). Although some of the GCM future scenarios predict moderate gains in glacier volume after equilibrium is achieved, the growth is nowhere near enough to bring the volume back to historical levels.

Figure 4.19 shows the area-elevation relationships for glaciers in the UNSRB for 1990, 2040, and 2090. By 2080, the vast majority of glacier ice in the basin is located above the 1966-1995 Peyto Glacier ELA at 2700 m a.s.l., and has reached a new basin ELA at approximately 3000 m a.s.l., appearing to reach a steady equilibrium. Figure 4.20 shows ICEGEN v1 projected future extents for the glaciers connected to the Columbia Icefield, located in the northwest portion of the watershed (Figure 4.1). Results for 2020 (Figure 4.20) show a dramatic reduction in the glacier

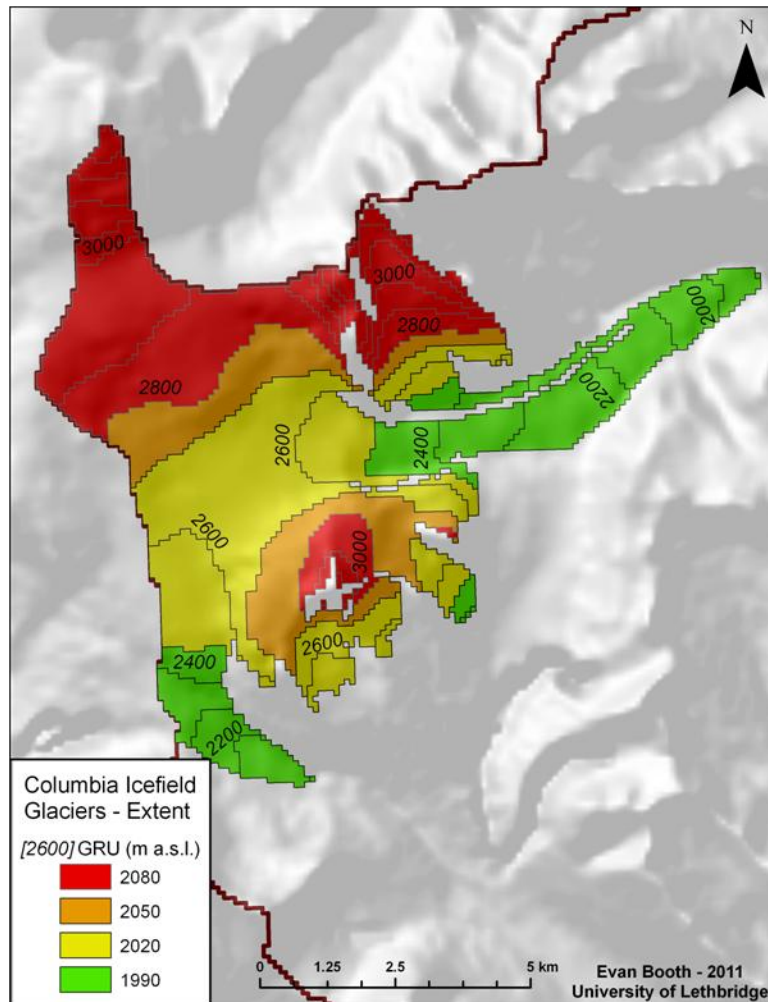


Figure 4.20: Simulated future Columbia Icefield GRU extent for 1900, 2020, 2050, and 2080.

tongue that appears unrealistic compared to the recent historic retreat rates ($\sim 21 \text{ m a}^{-1}$) measured for this region by Jiskoot *et al.*, (2009). While the length of retreat for the glacier tongue shown here may not be realistic, the loss in area experienced by the Columbia glacier group certainly is. The total glacier area for the 2020 period is projected at $\sim 45 \text{ km}^2$, down from $\sim 57 \text{ km}^2$ in 1990, representing a total reduction in area of just over 21%. Jiskoot *et al.* (2009) reported a loss in total glaciated area for the

nearby Chaba Group glaciers of 29% between 1986/87 and 2001, similar to the estimates of ~25% (between 1985 and 2005) loss made by Bolch *et al.* (2010). Based on the results from ICEGEN v1, the Columbia group will lose ~47% by 2050, and towards the end of the century (2080) the glacier group is confined to a much higher elevation, representing a mere fraction (~30%) of its 1990 area.

While these results indicate that the glaciers in the UNSRB may not completely disappear by the end of the century, their impact on the hydrology of the region will likely diminish to the point of insignificance. Figure 4.21 shows the annual glacier melt contributions to the UNSRB to 2100. Results here also strongly agree with those found by Marshall *et al.* (2011). Both ICEGEN v1 and v2 show melt contributions to the UNSRB declining from an average of ~0.3 km³ between 1990 and 2000, to below ~0.05 km³ by 2100. According to the average of all GCM scenarios in the ICEGEN v1 model runs (Figure 4.21a), glacier contribution to streamflow will see reductions from 1990s volumes of ~70% by 2025, ~80% by 2045, and ~90% by 2060. Modeling efforts by Comeau *et al.* (2009) reported that glacier melt and wastage in 1975 and 1998 accounted for approximately 80% of the stream-flow between July and September at a number of gauging stations in the UNSRB. If the projected reductions in melt volumes reported in Figure 4.21 for this study are taken into account, total streamflow in the basin could be reduced from historical volumes during the summer by an average of 55% by the 2020s, 65% by the 2040s, and 75% by the 2060s.

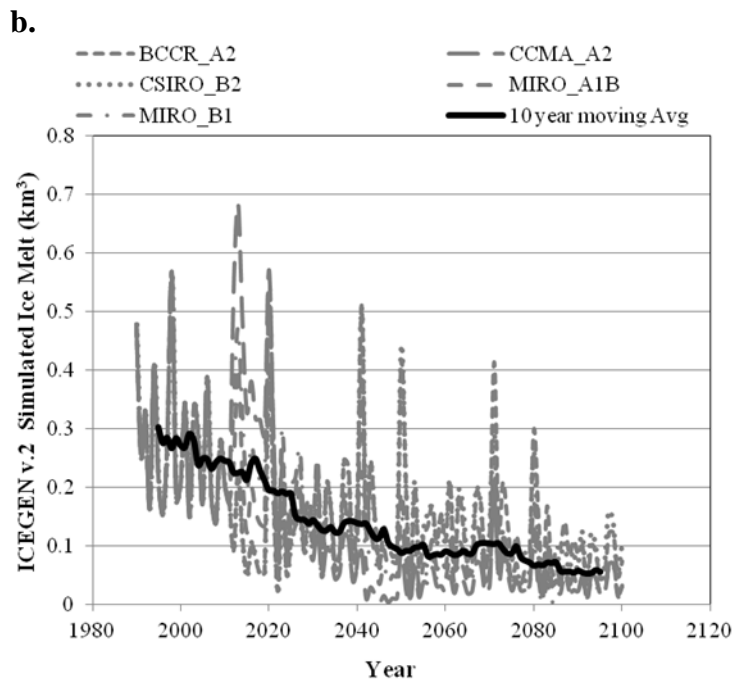
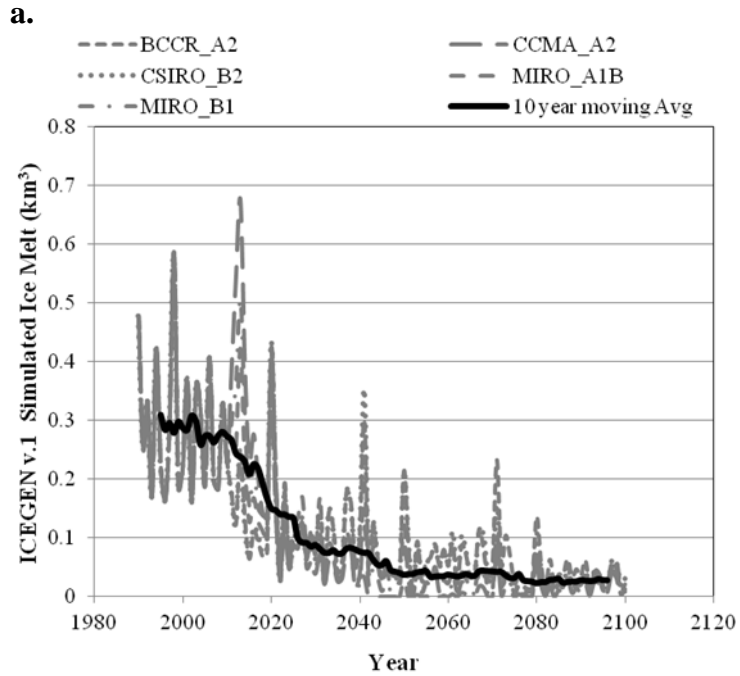


Figure 4.21: Simulated 1990-2100 UNSRB glacier IWE melt runoff modeled by ICEGEN v1 (A) and ICEGEN v2 (B)

4.7. Summary and Conclusions

The development and incorporation of the ICEGEN glacier model components to the GENESYS hydrometeorological physically based modeling routine has provided valuable insights into the historical and potential future mass balance of glaciers in the UNSRB. The new GENESYS glacier subroutine proved capable of simulating the static balance of Peyto Glacier and was applied to the basin as a whole. Two versions of ICEGEN were developed, tested, and used to simulate the dynamic response of glaciers to changes in climate. The objectives of this study were accomplished in that ICEGEN is able to provide reasonable estimations of ice volumes, glacier area, and total glacier melt runoff for the glaciated areas in the UNSRB. Results compared well with other studies done in the area (Demuth and Keller, 2006; Bolch *et al.*, 2010; Marshall *et al.*, 2011, etc.). The modeled reductions in ice volume and glacier area shown here continue the general trend of retreat experienced by glaciers around the world since the end of the Little Ice Age (Lemke *et al.*, 2007). ICEGEN forecasted declines in area of ~60% by 2040, and >80% by the end of century. The rate of future decline is tied to the future GCM emissions scenario used in the simulation. Much uncertainty surrounds the future climate of the region although all current projections indicate significant warming which results in a continued loss of glacial mass (Christensen *et al.*, 2007). Projected reductions to late-summer streamflow in the Upper Saskatchewan River system will pose great challenges to watershed managers in a province that is heavily reliant on alpine runoff for irrigation and industrial processes.

CHAPTER 5

SUMMARY, CONCLUSIONS, AND RECOMMENDATIONS

5.1. Thesis Summary and Conclusions

Chapter 2, “Climatic Changes in Western North America” surveyed the amount of change that has already take place due to modern climate forgings. The rate of change over western North America (WNA) was quantified for 485 climate stations for the period 1950-2005. The indicators used were developed by the World Meteorological Organization (WMO) and the World Climate Research Program’s Expert Team on Climate Change Detection, Monitoring and Indices (ETCCDMI). Four temperature-based and four precipitation-based indicators were selected from the 27 core indices for in-depth analysis. The 8 million km² study area included the twenty-two contiguous U.S. states and four Canadian provinces west of the Mississippi River and Great Lakes. Results were divided into six general regions for interpretation and presentation. GIS interpolation of station-specific statistical output was completed to further aid in the identification of spatially coherent trends across WNA. Mean slopes were calculated over the whole study area and by region for each index, and then tested to determine if they were significantly different from zero.

Results of the study showed statistically significant historical climate trends across the study area. As expected in a region as geographically diverse as WNA, results differed between, and within, regions. Overall, temperature-based indicators showed a general warming trend over the entire study area, with the greatest amount of warming in the higher elevation areas of the North American Cordillera. The trends in

precipitation-based indicators were more varied. General trends indicate moderately increasing precipitation volume and intensity over much of WNA. The strongest precipitation trends were found in areas with climate largely controlled by air masses originating over the Gulf of Mexico. The analysis showed that climate change in WNA is already well underway.

The second objective of this research, the focus of chapters 3 and 4, was to develop a glacier mass balance model that could be incorporated into the GENESYS hydrometeorological model developed at the University of Lethbridge, and applied to the Upper North Saskatchewan River Basin (UNSRB) to quantify the impact that a changing climate would have on the basin. Changing the focus of the GENESYS modeling routine towards simulating daily, annual, and long-term glacier mass balance required a significant amount of model set-up and data preprocessing. Meteorological station records were compiled and analyzed for potential use as a driver from which to extrapolate daily data throughout the UNSRB. Spatial data were analyzed and processed in a Geographic Information System (GIS) for use as input data for the GENESYS modeling routine.

The development of a glacier modeling routine included the creation of a subroutine within the main GENESYS program that would simulate the daily and annual mass balance of glaciers, as well as the formulation of two new routines to simulate the dynamic long term response of glaciers to climate change. The ICEGEN components of the model performed well in historical simulations (1966-2010) of mass balance at Peyto Glacier and were applied to the entire UNSRB basin for the period

1990-2100 using GCM future emissions scenarios to determine the range of potential future change to the glaciers in the basin.

The results of the glacier modeling routine show a dramatic decline in glacier ice volumes in the UNSRB. According to modeling results, Peyto Glacier experienced a significant decline over the period 1966-2010, losing over 0.3 km³ of IWE, representing a loss of about 40% based on our estimates of its 1966 volume. These results were in line with other studies done on the glacier and region. When the model was applied to the UNSRB, results showed a loss in glacier volume of over 80% through the end of 2100. Future summer streamflow estimates for the UNSRB will likely see similar reductions due to the fact that glacier melt historically provides up to 80% of flow during the late summer after the seasonal snowpack has been exhausted.

Based on the results of this research, it appears that the mass balance of glaciers in the UNSRB has already passed the tipping point, meaning that dramatic reductions in glacier area and contribution to streamflow are likely inevitable. While society should still focus on reduction of the GHGs that are driving climate change, local focus should be directed towards adaptation and mitigation of the potential effects.

5.2 Recommendations for Future Research

- An obvious recommendation for future research pertaining to the modeling of glacier mass balance is the acquisition of more high quality data. This study, and many others, relied heavily on the observations made at Peyto Glacier, and daily weather data from low elevation stations many kilometers from the sites being simulated. Up to date remote sensing data should be acquired and glacier extents delineated to more accurately gauge the effectiveness of the model. The acquisition of high-elevation meteorological data would be a valuable addition to the modeling effort as it would allow for better verification of the GENRGID air temperature and precipitation extrapolations.
- A number of improvements could be made to the glacier modeling methods used here. Increasing the overall efficiency of the GENESYS model routine to take advantage of recent exponential growth in computing power would allow for faster calculations and make calibration efforts easier. Increasing the resolution of the raster grid used for GRU creation could potentially improve the accuracy of the simulations. Delineating glacier boundaries based on ice divides could possibly provide more realistic simulations. Finally, incorporating a flow function based on the hypsometry of the glacier may result in a more realistic redistribution of glacier ice.

6. References

- Ahrens CD. 2008. *Essentials of Meteorology: an invitation to the atmosphere, 5th (Instructor's) Edition*. Thompson Learning Inc: Belmont, CA.
- Akinremi OO, McGinn SM, Cutforth HW. 1999. Precipitation trends on the Canadian Prairies. *Journal of Climate* 12: 2996-3003.
- Alexander LV, Zhang X, Peterson TC, Caesar J, Gleason B, Klein Tank AMG, Haylock M, Collins D, Trewin B, Rahimzadeh F, Tagipour A, Kumar R, Revadekar J, Griffiths G, Vincent L, Stephenson DB, Burn J, Aguilar E, Brunet M, Taylor M, New M, Zhai P, Rusticucci M, Vazquez-Aguirre JL. 2006. Global observed changes in daily climate extremes of temperature and precipitation. *Journal of Geophysical Research*, 111: D05109. DOI: 10.1029/2005JD006290.
- Arendt A, Walsh J, Harrison W. 2009. Changes of glaciers and climate in northwestern North America during the late twentieth century. *Journal of Climate*, 22: 4117-4134. DOI: 10.1175/2009JCLI2784.1.
- Bahr DB, Meier MF, Peckham SD. 1997. The physical basis of glacier volume-area scaling. *Journal of Geophysical Research*, 102(B9): 355-362.
- Barnett TP, Adam JC, Lettenmaier DP. 2005. Potential impacts of a warming climate on water availability in snow-dominated regions. *Nature*, 438(17): 303-309. DOI :10.1038/nature04141.
- Barnett TP, Pierce DW. 2008. When will Lake Mead go dry? *Water Resources Research*, 44: W03201. DOI: 10.1029/2007WR006704.
- Barrow E, Yu G. 2005. Climate change scenarios for Alberta. *Prairie Adaptation Research Collaborative (Parc) in co-operation with Alberta Environment*: Regina, Saskatchewan. 73pp.
- Beniston M. 2003. Climatic change in mountain regions: a review of possible impacts. *Climatic Change*, 59: 5-31.
- Beniston M. 2000. *Environmental Change in Mountains and Uplands*. Arnold: London, United Kingdom.
- Berger WH. 2010. On glacier retreat and drought cycles in the Rocky Mountains of Montana and Canada. *Quaternary International* 215: 27-33.
- Braithwaite RJ, Zhang Y. 1999. Modeling changes in glacier mass balance that may occur as a result of climate changes. *Geografiska Annaler*, 81A(4): 489-496.

- Braun LN, Aellen M, Funk M, Hock R, Rohrer MB, Steinegger U, Kappenberger G, Müller-Lemans H. 1994. Measurement and simulation of high alpine water balance components in the Linth-Limmern head watershed (northeastern Switzerland). *Zeitschrift für Gletscherkunde und Glazialgeologie* 30: 161-185.
- Bolch T, Menounos B, Wheate R. 2010. Landsat-based inventory of glaciers in western Canada, 1985-2005. *Remote Sensing of Environment*, 114: 127-137.
- Calkin PE. 1995. Global glacial chronologies and causes of glaciations. In: *Modern glacial environments: processes, dynamics, and sediments*. Menzies, J. (ed.). Butterworth Heinemann Ltd.: Oxford: 9-75.
- Cayan DR, Redmond KT, Riddle LG. 1999. ENSO and Hydrologic Extremes in the Western United States. *Journal of Climate*, 12: 2881-2893. DOI: 10.1175/1520-0442(1999)012<2881:EAHEIT>2.0.CO;2.
- Chen J, Ohmura P. 1990. Estimation of alpine glacier water resources and their change since the 1870s, Hydrology in mountainous regions – I. Hydrologic measurements, the water cycle, Proceedings of the two Lausanne Symposia, *IAHS Publ. No. 193*: 127-135.
- Christensen, J.H., B. Hewitson, A. Busuioc, A. Chen, X. Gao, I. Held, R. Jones, R.K. Kolli, W.-T. Kwon, R. Laprise, V. Magaña Rueda, L. Mearns, C.G. Menéndez, J. Räisänen, A. Rinke, A. Sarr and P. Whetton, 2007: Regional Climate Projections. In: *Climate Change 2007: The Physical Science Basis. Contribution of Working Group I to the Fourth Assessment Report of the Intergovernmental Panel on Climate Change* [Solomon, S., D. Qin, M. Manning, Z. Chen, M. Marquis, K.B. Averyt, M. Tignor and H.L. Miller (eds.)]. Cambridge University Press, Cambridge, United Kingdom and New York, NY, USA.
- Cogley JG, Hock R, Rasmussen LA, Arendt AA, Bauder AA, Braithwaite RJ, Jansson P, Kaser G, Möller M, Nicholson L, Zemp M. 2011. Glossary of glacier mass balance and related terms. *IHP-VII Technical Documents in Hydrology No. 86, IACS Contribution No. 2*, UNESCO-IHP: Paris.
<http://unesdoc.unesco.org/images/0019/001925/192525e.pdf>
- Comeau LEL, Pietroniro A, Demuth MN. 2009. Glacier contribution to the North and South Saskatchewan Rivers. *Hydrological Processes*, 23: 2640-2653.
- Dadic R, Mott R, Lehning M. 2010. Parameterization for wind-induced preferential deposition of snow. *Hydrological Processes*, 24 (14): 1994-2006. DOI: 10.1002/hyp.7776.

- Daly C, Halbleib M, Smith JI, Gibson WP, Doggett MK, Taylor GH, Curtis J, Pasteris PP. 2008. Physiographically sensitive mapping of climatological temperature and precipitation across the conterminous United States. *International Journal of Climatology*, 28: 2031-2064. DOI: 10.1002/joc.1688.
- DeBeer CM, Sharp MJ. 2007. Recent changes in glacier area and volume within the southern Canadian Cordillera. *Annals of Glaciology*, 46: 215-221.
- Demuth MN, Pietroniro A. 2002. The impact of climate change on the glaciers of the Canadian Rocky Mountain eastern slopes and implications for water resource related adaptation in the Canadian prairies: "Phase I" – headwaters of the North Saskatchewan River Basin. *PARC Project P55*.
- Demuth MN, Keller R. 2006. An assessment of the mass balance of Peyto Glacier (1966-1995) and its relation to recent and past-century climatic variability. In: *Peyto Glacier: One Century of Science*. Demuth, M.N., Munro, D.S., and Young G.J. (eds.). *National Hydrology Research Institute Science Report*, 8: 83-132.
- Dore MHI. 2005. Climate change and changes in global precipitation patterns: what do we know? *Environment International*, 31: 1167-1181. DOI :10.1016/j.envint.2005.03.004.
- Easterling, DR. 2002. Recent changes in frost days and the frost-free season in the United States. *Bulletin of the American Meteorological Society*. 83(9): 1327-1332.
- Elsner, JB, Kossin, JP, Jagger, TH 2008. The increasing intensity of the strongest tropical cyclones. *Nature*, 455: 92-95. DOI: 10.1038/nature07234.
- Ferguson RI. 1999. Snowmelt runoff models. *Progress in Physical Geography*, 23(2): 205-227.
- Föhn PMB. 1973. Short-term snow melt and ablation derived from heat- and mass balance measurements. *Journal of Glaciology* 12: 275-289.
- Frich P, Alexander LV, Della-Marta P, Gleason B, Haylock M, Klein Tank A, Peterson T. Observed coherent changes in climatic extremes during second half of the twentieth century. *Climate Research* 19: 193-212.
- Fried, JS. 2008. Predicting the effect of climate change on wildfire behavior and initial attack success. *Climatic Change* 87(Suppl 1): 251-264. DOI: 10.1007/s10584-007-9360-2.
- Franco G, Sanstad, AH. 2008. Climate change and electricity demand in California. *Climatic Change* 87(Suppl 1): 139-151. DOI: 10.1007/s10584-007-9364-y.

- Gleick PH, et al. 2010. Climate change and the integrity of science. *Science* 328(5979): 689-690. DOI: 10.1126/science.328.5979.689.
- Groisman PY, Knight RW, Easterling DR, Karl TR, Hegerl GC, Razuvaev VN. 1999. Changes in the probability of heavy precipitation: important indicators of climate change. *Climatic Change* 42: 243-283.
- Groisman PY, Knight RW, Karl TR, Easterling DR, Sun B, Lawrimore JH. 2004. Contemporary changes of the hydrologic cycle over the contiguous United States: trends derived from in situ observations. *Journal of Hydrometeorology*, 5: 64-84.
- Groisman, PY, Knight RW, Easterling DR, Karl TR, Hegerl GC, Razuvaev VN. 2005. Trends in intense precipitation in the climate record. *Journal of Climate*, 18: 1326–1350.
- Gurtz J, Baltensweiler A, Lang H. 1999. Spatially distributed hydrotope-based modeling of evapotranspiration and runoff in mountainous basins. *Hydrological Processes*, 13: 2751-2768.
- Hall HPH, Fagre DB. 2003. Modeled climate-induced glacier change in Glacier National Park, 1850-2100. *Bioscience*, 52(2): 131-140.
- Harper JT, Bradford JH, Humphrey NF, Meierbachtol TW. 2010. Vertical extension of the subglacial drainage system into basal crevasses. *Nature* 467(7315): 579-582.
- Harrison WD, Raymond CF, Echelmeyer KA, Krimmel RM. 2003. A macroscopic approach to glacier dynamics. *Journal of Glaciology*, 49(164): 13-21.
- Hirabayashi Y, Döll P, Kanae S. 2010. Global-scale modeling of glacier mass balances for water resources assessments: glacier mass changes between 1948 and 2006. *Journal of Hydrology*, 390: 245-256.
- Hock R. 2002. Temperature index modeling in mountain areas. *Journal of Hydrology*, 282: 104-115. DOI: 10.1016/S0022-1694(03)00257-9.
- Hock R. 2005. Glacier melt: a review of processes and their modeling. *Progress in Physical Geography*, 29(3): 362-391. DOI: 10.1191/0309133305pp453ra.
- Hoerling M, Eischeid J, Perlwitz, J. 2010. Regional precipitation trends: distinguishing natural variability from anthropogenic forcing. *Journal of Climate*, **23**: 2131-2145. DOI: 10.1175/2009JCLI3420.1.

- Holdsworth G, Demuth MN, Beck TMH. 2006. Radar measurements of ice thickness on Peyto Glacier – geophysical and climatic implications. In: *Peyto Glacier: One Century of Science*. Demuth, M.N., Munro, D.S., and Young G.J. (eds.). *National Hydrology Research Institute Science Report*, 8: 57-82.
- Hughes MK, Diaz HF. 2008. Climate variability and change in the drylands of Western North America. *Global Planetary Change* 64: 111-118. DOI: 10.1016/j.gloplacha.2008.07.005.
- Hungerford RD, Nemani RR, Running SW, Coughlan JC. 1989. MTCLIM: mountain microclimate simulation model. *Research Paper INT-414*. Ogden UT: U.S. Department of Agriculture, Forest Service, Intermountain Research Station.
- Jiskoot H, Curran CJ, Tessler DL, and Shenton LR. 2009. Changes in Clemenceau Icefield and Chaba Group glaciers, Canada, related to hypsometry, tributary detachment, length-slope and area-aspect relations. *Annals of Glaciology* 50(53): 133-143.
- Johnston K, Ver Hoef JM, Krivoruchko K, Luca N. 2001. Using ArcGIS Geostatistical Analyst. ESRI: Redlands, CA, USA. 300 pp.
- Karl TR, Koss WJ. 1984. Regional and national monthly, seasonal, and annual temperature weighted by area 1895-1983. *National Climatic Data Center Tech. Rep. Historical Climatology Series 4-3*: 33 pp.
- Karl, TR, Trenberth, KE. 2003. Modern global climate change. *Science*, 302: 1719-1723. DOI: 10.1126/science.1090228.
- Kienzle SW. 2008. A new temperature based method to simulate rain and snow. *Hydrological Processes*, 22: 5067-5085. DOI: 10.1002/hyp.7131.
- Kienzle SW, Nemeth MW, Byrne JM, MacDonald RJ. 2011. Simulating the hydrological impacts of climate change in the upper North Saskatchewan River basin, Alberta, Canada. *Journal of Hydrology (In Press)*. DOI: 10.1016/j.hydrol.2011.01.058.
- Kouwen, N., Soulis, E.D., Pietroniro, A., Donald, J., Harrington, R.A. 1993. Grouped response units for distributed hydrologic modeling. *Journal of Water Resources Planning and Management*, 119(3): 289-305.
- Klein Tank, AMG, Können, GP. 2003. Trends in indices of daily temperature and precipitation extremes in Europe, 1946-99. *Journal of Climate*, 16: 3665-3680. DOI: 10.1175/1520-0442(2003)016<3665:TIHODT>2.0.CO;2.
- Kunkel, KE. 2003. North American trends in extreme precipitation. *Natural Hazards*, 29: 291-305.

- Kunkel, K., Easterling DR, Hubbard K, Redmond K. 2004. Temporal variations in the frost free season in the United States: 1895-2000. *Geophysical Research Letters*, 31(3): L03201.
- Kurz WA, Dymond CC, Stinson G, Rampley GJ, Neilson ET, Carroll AL, Ebata T, Safranyik L. 2008. Mountain pine beetle and forest carbon feedback to climate change. *Nature*, 452(24): 987-990.
- Lapp S, Byrne JM, Kienzle S, Townshend I. 2002. Linking global circulation model synoptic and precipitation for western North America. *International Journal of Climatology*, 22: 1807-1817. DOI: 10.1002/joc.851.
- Lapp S, Byrne J, Townshend I, Kienzle S. 2005. Climate warming impacts on snowpack accumulation in an alpine watershed. *International Journal of Climatology*, 25: 521-536. DOI: 10.1002/joc.1140.
- Larson RP, Byrne, JM, Johnson, DL, Letts MG, Kienzle SW. 2010. Modeling climate change impacts on spring runoff for the Rocky Mountains of Montana and Alberta I: model development, calibration, and historical analysis. *Canadian Water Resources Journal*, 36(1): 17-43.
- Lemke P, Ren J, Alley RB, Allison I, Carrasco J, Flato G, Fujii Y, Kaser G, Mote P, Thomas RH, Zhang T. 2007: Observations: changes in snow, ice and frozen ground. In: *Climate Change 2007: The Physical Science Basis. Contribution of Working Group I to the Fourth Assessment Report of the Intergovernmental Panel on Climate Change*. Cambridge University Press: Cambridge, United Kingdom.
- Liu W, Zhang Z, Wan S. 2009. Predominant role of water in regulating soil and microbial respiration and their responses to climate change in a semiarid grassland. *Global Change Biology* 15: 184-195.
- Luckman BH. 2000. The Little Ice Age in the Canadian Rockies. *Geomorphology* 32: 357-84.
- Luckman BH. 2006. The neoglacial history of Peyto Glacier. In: *Peyto Glacier: One Century of Science*. Demuth, M.N., Munro, D.S., and Young G.J. (eds.). *National Hydrology Research Institute Science Report*, 8: 25-58.
- MacDonald RJ, Byrne JM, and Kienzle SW. 2009. A physically based daily hydrometeorological model for complex mountain terrain. *Journal of Hydrometeorology*, 10: 1430-1446. DOI: 10.1175/2009JHM1093.1.

- MacDonald RJ, Byrne JM, Kienzle SW, Larson RP. 2011. Assessing the potential impacts of climate change on mountainous snowpack in the St Mary River watershed, Montana. *Journal of Hydrometeorology*, 12(2): 262-273. DOI: 10.1175/2010JHM1294.1.
- MacDonald, RJ, Byrne, JM, Kienzle, S, Boon S. 2011. Modeling the potential impacts of climate change on snowpack in the North Saskatchewan River watershed, Alberta. *Water Resources Management*, (In Press).
- Marshall S, White EC. 2010. Alberta glacier inventory and ice volume estimation. *Crowfoot Ice Research and Consulting*: Canmore, Alberta. 55pp.
- Marshall SJ, White EC, Demuth MN, Bolch T, Wheate R, Menounos B, Beedle MJ, Shea JM. 2011. Glacier water resources on the Eastern Slopes of the Canadian Rocky Mountains. *Canadian Water Resources Journal*, 36(2): 109-134.
- Marshall SJ, Losic M. 2011. Temperature lapse rates in glacierized basins. In: *Encyclopedia of Snow, Ice and Glaciers*. Singh VP, Singh P, Haritashya UK. (eds.). 1300pp. *Encyclopedia of Earth Science Series*, Springer: 1145-1150.
- Meehl GA, Tebaldi C, Walton G, Easterling D, McDaniel L. 2009. Relative increase of record high maximum temperatures compared to record low minimum temperatures in the U.S. *Geophysical Research Letters*, 36: L23701. DOI :10.1029/2009GL040736.
- Mekis E, Hogg WD. 1999. Rehabilitation and analysis of Canadian daily precipitation time series. *Atmosphere-Ocean*, 37(1): 53-85.
- Meier MF, Dyurgerov MB, Rick UK, O'Neel S, Pfeffer WT, Anderson RS, Anderson SP, Glazovsky AF. 2007. Glaciers dominate eustatic sea-level rise in the 21st century. *Science*, 317: 1064-1067.
- Menzies J. 1995. Glaciers and ice sheets. In: *Modern glacial environments: processes, dynamics, and sediments*. Menzies, J. (ed.). Butterworth-Heinemann Ltd.: Oxford: 101-138.
- Miller JD, Safford HD, Crimmins MA, Thode AE. 2009. Quantitative evidence for increasing forest fire severity in the Sierra Nevada and Southern Cascade Mountains, California and Nevada, USA. *Ecosystems* 12: 16-32.
- Möller M, Schneider C. 2010. Calibration of glacier volume-area relations from surface extent fluctuations and application to future climate change. *Journal of Glaciology*, 56(195): 33-40.

- Moore RD, Fleming SW, Menounos B, Wheate R, Fountain A, Stahl K, Holm K, Jakob M. 2009. Glacier change in western North America: influences on hydrology, geomorphic hazards and water quality. *Hydrol. Process.* 23: 42-61. DOI: 10.1002/hyp.7162.
- Morris EM. 2006. Techniques for predicting runoff from glacierized areas. In: *Peyto Glacier: One Century of Science*. Demuth, M.N., Munro, D.S., and Young G.J. (eds.). *National Hydrology Research Institute Science Report*, 8: 201-225.
- Munro DS. 2006. Linking the weather to glacier mass balance at Peyto Glacier. In: *Peyto Glacier: One Century of Science*. Demuth, M.N., Munro, D.S., and Young G.J. (eds.). *National Hydrology Research Institute Science Report*, 8: 133-176.
- Nakicenovic N, Alcamo J, Davis G, de Vries B, Fenhann J, Gaffin S, Gregory K, Grübler A, Yong Jung T, Kram T, Lebre La Rovere E, Michaelis L, Mori S, Morita T, Pepper W, Pitcher H, Price L, Riahi K, Roehrl A, Rogner HH, Sankovski A, Schlesinger M, Shukla P, Smith S, Swart R, van Rooijen S, Victor N, Dadi Z. 2000. Special Report on Emissions Scenarios. *IPCC*. Cambridge University Press: Cambridge, United Kingdom. <<http://www.ipcc.ch>>
- Nemeth MW. 2010. Climate change impacts on streamflow in the Upper North Saskatchewan River Basin, Alberta. *University of Lethbridge: Unpublished MSc Thesis*.
- Nemeth MW, Kienzle SW, Byrne JM. 2011. Multi-variable verification of hydrological processes in the upper North Saskatchewan River basin, Alberta, Canada. *Hydrological Sciences Journal (In Press)*. DOI:10.1080/02626667.2011.633917.
- Nogues-Bravo D, Araujo MB, Errea MP, Martinez-Rica JP. 2007. Exposure of global mountain systems to climate warming during the 21st century. *Global Environmental Change*, 17: 420-428.
- Oerlemans J. 1989. On the response of valley glaciers to climate change. In: *Glaciers Fluctuations and Climatic Change*. Oerlemans, J. (ed.). Kluwer Academic Publishers: London. 353-371.
- Oerlemans J, Fortuin, JPF. 1992. Sensitivity of glaciers and small ice caps to greenhouse warming. *Science*, 258(5079): 155-117.
- Oerlemans J. 2005. Extracting a climate signal from 169 glacier records. *Science*, 308(5722): 675-677.
- Østrem G. 2006. History of scientific studies at Peyto Glacier. In: *Peyto Glacier: One Century of Science*. Demuth, M.N., Munro, D.S., and Young G.J. (eds.). *National Hydrology Research Institute Science Report*, 8: 1-23.

- Pederson GT, Gray ST, Woodhouse CA, Betancourt JL, Fagre DB, Littell JS, Watson E, Luckman BH, Graumlich LJ. 2011. The unusual nature of recent snowpack decline in the North American Cordillera. *Science* 333(6040): 332-335. DOI: 10.1126/science.1201570.
- Peel MC, Finlayson BL, and McMahon TL. 2007. Updated world map of the Köppen Geiger climate classification. *Hyrol. Earth Syst. Sci.*, 11: 1633-1644.
- Peterson TC. 2005. Climate change indices. *World Meteorological Organization Bulletin*, 54(2): 83-86.
- Pigeon KE, Jiskoot H. 2008. Meteorological controls on snowpack formation and dynamics in the southern Canadian Rocky Mountains. *Arctic, Antarctic, and Alpine Research* 40(4): 716-730. DOI: 10.1657/1523-0430(07-054)[PIGEON]2.0.CO;2.
- Portman RW, Solomon S, Hegerl GC. 2009. Spatial and seasonal patterns in climate change, temperatures, and precipitation across the United States. *Proceedings of the National Academy of Sciences of the United States of America*: 106(18): 7324-7329.
- Pryor SC, Howe JA, Kunkel KE. 2009. How spatially coherent and statistically robust are temporal changes in extreme precipitation in the contiguous USA? *International Journal of Climatology* 29: 31-45.
- Purkey DR, Joyce B, Vicuna S, Hanemann MW, Dale LL, Yates D, Dracup JA. 2008. Robust analysis of future climate change impacts on water for agriculture and other sectors: a case study in the Sacramento Valley. *Climatic Change* 87(Suppl 1): 109-122. DOI: 10.1007/s10584-007-9375-8.
- Rajagopalan B, Nowak K, Prairie J, Hoerling M, Harding B, Barsugli J, Ray A, Udall B. 2009. Water supply risk on the Colorado River: Can management mitigate? *Water Resources Research* 45: W08201. DOI: 10.1029/2008WR007652.
- Rolland C. 2003. Spatial and seasonal variations of air temperature lapse rates in alpine regions. *Journal of Climate*, 16: 1032-1046.
- Running SW. 2006. Is global warming causing more larger wildfires? *Science*, 313: 927-928.

- Seager R, Ting M, Held I, Kushnir Y, Lu J, Vecchi G, Huang HP, Harnik N, Leetmaa A, Lau NC, Li C, Velez J, Naik N. 2007. Model projections of an imminent transition to a more arid climate in southwestern North America. *Science*, 316: 1181-1184.
- Seager R, Vecchi, GA. 2010. Greenhouse warming and the 21st century hydroclimate of southwestern North America. *Proceedings of the National Academy of Sciences of the United States of America*, 107(50): 21277-21282. DOI: 10.1073/pnas.0910856107.
- Shea JM, Marshall SJ, Anslow FS. 2005. Hydrometeorological relationships on Haig Glacier, Alberta, Canada. *Annals of Glaciology* 40: 52-60. DOI: 10.3189/172756405781813465
- Shea JM, Moore DR, Stahl K. 2009. Derivation of melt factors from glacier mass balance records in western Canada. *Journal of Glaciology*, 55(189): 123-129.
- Shea JM and Moore DR. 2010. Prediction of spatially distributed regional-scale fields of air temperature and vapour pressure over mountain glaciers. *Journal of Geophysical Research – Atmosphere* (115): D23107. DOI:10.1029/2010JD014351
- Sheppard DL. 1996. Modeling the spatial characteristics of hydrometeorology in the upper Oldman River basin, Alberta. *University of Lethbridge: Unpublished MSc Thesis*.
- Solomon S, Qin D, Manning M, Chen Z, Marquis M, Averyt KB, Tignor M, Miller HL. 2007. Contribution of Working Group I to the Fourth Assessment Report of the Intergovernmental Panel on Climate Change, 2007. Cambridge University Press: Cambridge, United Kingdom.
- Stahl K, Moore RD, Shea JM, Hutchinson D, Cannon AJ. 2008. Coupled modeling of glacier and streamflow response to future climate scenarios. *Water Resources Research*, 44: W02422: 1-13. DOI: 10.1029/2007WR005956.
- Stewart IS, Cayan DR, Dettinger MD. 2004. Changes in snowmelt runoff timing in western North America under a ‘business as usual’ climate change scenario. *Climatic Change*, 62: 217-232.
- St. Jacques JM, Sauchyn DJ, Zhao Y. 2010. Northern Rocky Mountain streamflow records: Global warming trends, human impacts or natural variability? *Geophysical Research Letters*, 37: L06407. DOI: 10.1029/2009GL042045.
- Quick MC, Pipes A. 1977. U.B.C. watershed model. *Hydrological Sciences Bulletin*, XX11 (1): 153-161.

- Van Der Veen CJ. 1999. *Fundamentals of Glacier Dynamics*. A.A. Balkema: Rotterdam, Netherlands.
- Ye B, Ding Y, Liu F, Liu C. 2003. Responses of various-sized alpine glaciers and runoff to climatic change. *Journal of Glaciology*, 49(164): 1-7.
- Vincent LA, Mekis E. 2006. Changes in daily and extreme temperature and precipitation indices for Canada over the twentieth century. *Atmosphere-Ocean*, 44(2): 177-193.
- Vicuna S, Leonardson R, Hanemann MW, Dale LL, Dracup JA. 2008. Climate change impacts on high elevation hydropower generation in California's Sierra Nevada: a case study in the Upper American River. *Climatic Change*, 87(Suppl 1): 123-137. doi: 10.1007/s10584-007-9365-x.
- Wei Y, Tandong Y, Baiqing X, Hang Z. 2010. Influence of supraglacial debris on summer ablation and mass balance in the 24K Glacier, Southeast Tibetan Plateau. *Geografiska Annaler*, 92A(3): 353-360.
- Westerling AL, Hidalgo HG, Cayan DR, Swetnam TW. 2006. Warming and earlier spring increase western U.S. forest wildfire activity. *Science*, 313: 940-943.
- Westerling AL, Bryant BP. 2008. Climate change and wildfire in California. *Climatic Change*, 87 (Suppl 1): 231-249. DOI: 10.1007/s10584-007-9363-z.
- Wilcox BP. 2010. Transformative ecosystem change and ecohydrology: ushering in a new era for watershed management. *Ecohydrology* 3: 126-130. DOI: 10.1002/eco.104.
- Williams CN, Menne MJ, Vose RS, Easterling DR. 2006. United States Historical Climatology Network Daily Temperature, Precipitation, and Snow Data. *USHCN ORNL/CDIAC-118 NDP-070*. <http://cdiac.ornl.gov/epubs/ndp/ushcn/ndp070.html>
- Zemp M, Roer I, Kaab A, Hoelzle M, Paul F, Haeberli W. 2008. *Global glacier changes: facts and figures*. UNEP World Glacier Monitoring Service: Zurich, 88 pp.
- Zhang X, Vincent LA, Hogg WD, Nitsoo A. 2000. Temperature and precipitation trends in Canada during the 20th century. *Atmosphere-Ocean* 38(3), 395-429.
- Zhang X, Hogg WD, Mekis E. 2001. Spatial and temporal characteristics of heavy precipitation events over Canada. *Journal of Climate*, 14: 1923-1936.
- Zhang X, Yang F. 2004. RClimDex (1.0) User's Manual. *Climate Research Branch Environment Canada*. <http://cccma.seos.uvic.ca/ETCCDMI/software.shtml>